NASA Contractor Report 187448

DEVELOPMENT AND APPLICATION OF A TECHNIQUE FOR REDUCING AIRFRAME FINITE ELEMENT MODELS FOR DYNAMICS ANALYSIS

M. Hashemi-Kia and M. Toossi

MCDONNELL DOUGLAS HELICOPTER COMPANY
Mesa, Arizona

Contract NAS1-17498
October 1990

National Aeronautics and Space Administration

Langley Research Center
Hampton, Virginia 23665-5225

FOREWORD

McDonnell Douglas Helicopter Company (MDHC) has been conducting a study of finite element modeling of helicopter airframes to predict vibration. This work is being performed under U.S. Government Contract NAS1-17498. The contract is monitored by the NASA Langley Research Center, Structures Directorate.

This report presents the results of an effort spent on the development and application of a computational procedure for reduction of large finite element models of airframe type structures for efficient dynamic analysis. This procedure was applied to the airframe finite element model of AH-64A Attack Helicopter and is presented in this report. Key NASA and MDHC personnel are listed below:

NASA LANGLEY	MCDONNELL DOUGLAS HELICOPTR COMPANY
Panice H. Clark, Contracting Officer	Mostafa Toossi, Project Engineer
Joseph W. Owens, Contract Specialist	Robert J. King, Project Manager
John H. Cline, Technical Representative	Mostafa Hashemi-kia, Cognizant Engineer
Raymond G. Kvaternik, Leader, Rotorcraft Structural Dynamics Group	

TABLE OF CONTENTS

1.0 INTRODUCTION

INTRODUCTION

The NASA Langley Research Center is sponsoring a rotorcraft structural dynamics program with the overall objective to establish in the United States a superior capability to utilize finite element analysis models for calculations to support industrial design of helicopter airframe structures. Viewed as a whole, the program is planned to include efforts by NASA, Universities, and the U.S. Helicopter Industry. In the initial phase of the program, teams from major manufacturers of helicopter airframes will apply extant finite element analysis methods to calculate static internal loads and vibrations of helicopter airframes of both metal and composite construction, conduct laboratory measurements of the structural behavior of these airframes, and perform correlations between analysis and measurements to build up a basis upon which to evaluate the results of the applications. To maintain the necessary scientific observation and control, emphasis throughout these activities will be on advance planning, documentation of methods and procedures, and through discussion of results and experiences, all with industry wide critique to allow maximum technology transfer between companies. The finite element models formed in this phase will then serve as the basis for the development, application, and evaluation of both improved modeling techniques and advanced analytical and computational techniques, all aimed at strengthening and enhancing the technology base which supports industrial design of helicopter airframe structures. Here again, procedures for mutual critique have been established, and these procedures call for a thorough discussion among the program participants of each method prior to the applications and of the results and experiences after the applications. The aformentioned rotorcraft structural dynamics program has been given the acronym DAMVIBS (Design Analysis Methods for VIBrationS).

As a major helicopter manufacturer, McDonnell Douglas Helicopter Company is participating in this program. As a part of this effort, this report presents the work done on development and application of a computational procedure which can be used to condense large airframe finite element models for efficient dynamics analysis. This procedure is applied to full dynamic finite element model of the AH-64A Attack Helicopter. The reduced model is then validated by application in a vibration reduction study.

2.0 MODEL REDUCTION METHODOLOGY

COMMENTS ON MODEL REDUCTION PHILOSOPHY

The major goals in the development of this model reduction procedure were twofold. First, to preserve the global dynamic characteristics of the full model while providing a substantial reduction in the size. Second, to retain the relationship between the physical characteristics of the reduced and full models by generating a reduced model which resembles the conventional stick model. This latter item proved to be beneficial by; a) providing sufficient information for performing efficient vibration reduction studies, and b) providing sufficient guidlines for performing optimization studies.

Altough there are already several reduction techniques available in literature (Refs. 1-5), there are still certain shortcomings associated with each of them. For example, in the case of Guyan Reduction (Ref. 1), the accuracy of the reduced mass matrix depends strongly on the judment of analyst. In other cases (Refs. 1,4, and 5) the reduced mass matrix does not reveal any direct information about the physical characteristics of the actual mass distribution. Such characteristic is sometime beneficial where by examination of the terms of the reduced mass matrix, some insight can be gained about the mass distribution of the actual structure. A similar argument also applies in the case of the reduced stiffness matrix wherein use of the Generalized Dynamic Reduction procedure (Ref. 5) leads to a reduced stiffness matrix which can not be related to the physical characteristics of the actual structure.

The objective of this effort is not to dispute the accuracy or efficiency of the existing reduction techniques but to provide an alternative which emphasizes a reduced model that provides better insight into the physical characteristics of the actual structure. An important feature of this procedure is its modularity because it can be applied to individual substructures as well as to the whole model. This feature is important for optimization applications where it is often desirable to keep the portion of the structure to be optimized as a full model while reducing the remaining part of the overall FEM to a managable size.

COMMENTS ON MODEL REDUCTION PHILOSOPHY

- DEVELOPING A REDUCTION PROCEDURE WHICH:
  - PRESERVES THE GLOBAL CHARACTERISTICS OF THE FULL MODEL WHILE SUBSTANTIALLY REDUCING THE SIZE
  - RETAINS A RELATION BETWEEN THE PHYSICAL CHARACTERISTICS OF THE REDUCED AND FULL MODELS
  - IS MODULAR

STRUCTURAL INFLUENCE COEFFICIENTS

The principal of superposition which is used in the analyses of linearly elastic structures is utilized here. This principal states that the total linear or angular deflection of any point of the structure is the sum of the deflections or rotations produced by the individual forces and moments. The same principal also applies to the situation where the net force or moment generated at a point is equal to the sum of the forces or moments produced through application of individual displacements or rotations. In mathematical form, this principal is stated as follows:

$$\left\{\begin{array}{c} Y_1 \\ Y_2 \\ \cdot \\ \cdot \\ \cdot \\ Y_N \\ \hline M_1 \\ M_2 \\ \cdot \\ \cdot \\ \cdot \\ M_N \end{array}\right\} = \left[\begin{array}{cccc|cccc} K_{11}^{\nu\nu} & K_{12}^{\nu\nu} & \cdots & K_{1N}^{\nu\nu} & K_{11}^{\nu\theta} & K_{12}^{\nu\theta} & \cdots & K_{1N}^{\nu\theta} \\ K_{21}^{\nu\nu} & K_{22}^{\nu\nu} & \cdots & K_{2N}^{\nu\nu} & K_{21}^{\nu\theta} & K_{22}^{\nu\theta} & \cdots & K_{2N}^{\nu\theta} \\ \cdot & \cdot & \cdots & \cdot & \cdot & \cdot & \cdots & \cdot \\ \cdot & \cdot & \cdots & \cdot & \cdot & \cdot & \cdots & \cdot \\ \cdot & \cdot & \cdots & \cdot & \cdot & \cdot & \cdots & \cdot \\ K_{N1}^{\nu\nu} & K_{N2}^{\nu\nu} & \cdots & K_{NN}^{\nu\nu} & K_{N1}^{\nu\theta} & K_{N2}^{\nu\theta} & \cdots & K_{NN}^{\nu\theta} \\ \hline K_{11}^{\theta\nu} & K_{12}^{\theta\nu} & \cdots & K_{1N}^{\theta\nu} & K_{11}^{\theta\theta} & K_{12}^{\theta\theta} & \cdots & K_{1N}^{\theta\theta} \\ K_{21}^{\theta\nu} & K_{22}^{\theta\nu} & \cdots & K_{2N}^{\theta\nu} & K_{21}^{\theta\theta} & K_{22}^{\theta\theta} & \cdots & K_{2N}^{\theta\theta} \\ \cdot & \cdot & \cdots & \cdot & \cdot & \cdot & \cdots & \cdot \\ \cdot & \cdot & \cdots & \cdot & \cdot & \cdot & \cdots & \cdot \\ \cdot & \cdot & \cdots & \cdot & \cdot & \cdot & \cdots & \cdot \\ K_{N1}^{\theta\nu} & K_{N2}^{\theta\nu} & \cdots & K_{NN}^{\theta\nu} & K_{N1}^{\theta\theta} & K_{N2}^{\theta\theta} & \cdots & K_{NN}^{\theta\theta} \end{array}\right] \left\{\begin{array}{c} \nu_1 \\ \nu_2 \\ \cdot \\ \cdot \\ \cdot \\ \nu_N \\ \hline \theta_1 \\ \theta_2 \\ \cdot \\ \cdot \\ \cdot \\ \theta_N \end{array}\right\} \tag{1}$$

where the stiffness influence coefficient, $K_{ij}^{\alpha\beta}$, represents the load at the node i in the α direction due to unit applied displacement at node j in the β direction.

STRUCTURAL INFLUENCE COEFFICIENTS

$$\left\{\begin{array}{c} Y \\ \hline M \end{array}\right\} = \left[\begin{array}{c|c} K_{ij}{}^{\nu\nu} & K_{ij}{}^{\nu\theta} \\ \hline K_{ij}{}^{\theta\nu} & K_{ij}{}^{\theta\theta} \end{array}\right] \left\{\begin{array}{c} \nu \\ \hline \theta \end{array}\right\}$$

$$K_{ij}{}^{\alpha\beta} = F_i{}^{\alpha} / X_j{}^{\beta}$$

STRUCTURAL INFLUENCE COEFFICIENTS (continued)

Using the above definition of the stiffness influence coefficients, a "simulation" process similar to the procedure used during the experimental measurement of the actual structure influence coefficients is developed. In this "simulation," the full analytical model resembles the actual structure whose elastic characteristics are defined in terms of the stiffness matrix. Once this matrix is defined, it is used to correctly take into the account the contributions of other elements to the elastic coupling effects between each pair of selected points (i.e., points to be included in the reduced model). Similar to the experimental measurement process, only the selected points of the structure will be constrained and other points of the structure will be allowed to move freely and contribute to the elastic deformation of the structure under unit enforced displacement. The model is constrained at all the selected points initially and a systematic procedure is devised to "unlock" the appropriate degree-of-freedom (DOF) while keeping other DOFs locked during the application of displacements (will be discussed in more detail in the implementation section). Subsequently, the reaction forces are calculated only at the selected points and are used to assemble different columns of the reduced stiffness matrix. This procedure, which provides results similar to those obtained from the usual static condensation technique, offers certain advantages which will be discussed in the application section.

This process is illustrated for a simple planar beam model, shown below. The stiffness coefficients of the reduced model are calculated by applying unit displacement or rotation at each of the selected grid points while holding all other selected grid points fixed and then calculating the resulting reaction loads of all DOF of all the selected points. This process is repeated for all the other selected points and, as a result, a set of stiffness coefficients representing the reduced model stiffness matrix are obtained. As can be seen from this figure, frames 1-6 show the application of unit displacement at each of the selected grid points while frames 7-12 show the application of a unit rotation. The center frame indicates the type of reaction forces which result from the application of a unit displacement. It should be pointed out that the calculated reaction forces represent the "equivalent" elastic contributions of all the structural elements connecting the selected grid point to its surronding selected grid points.

STRUCTURAL INFLUENCE COEFFICIENTS
(Continued)

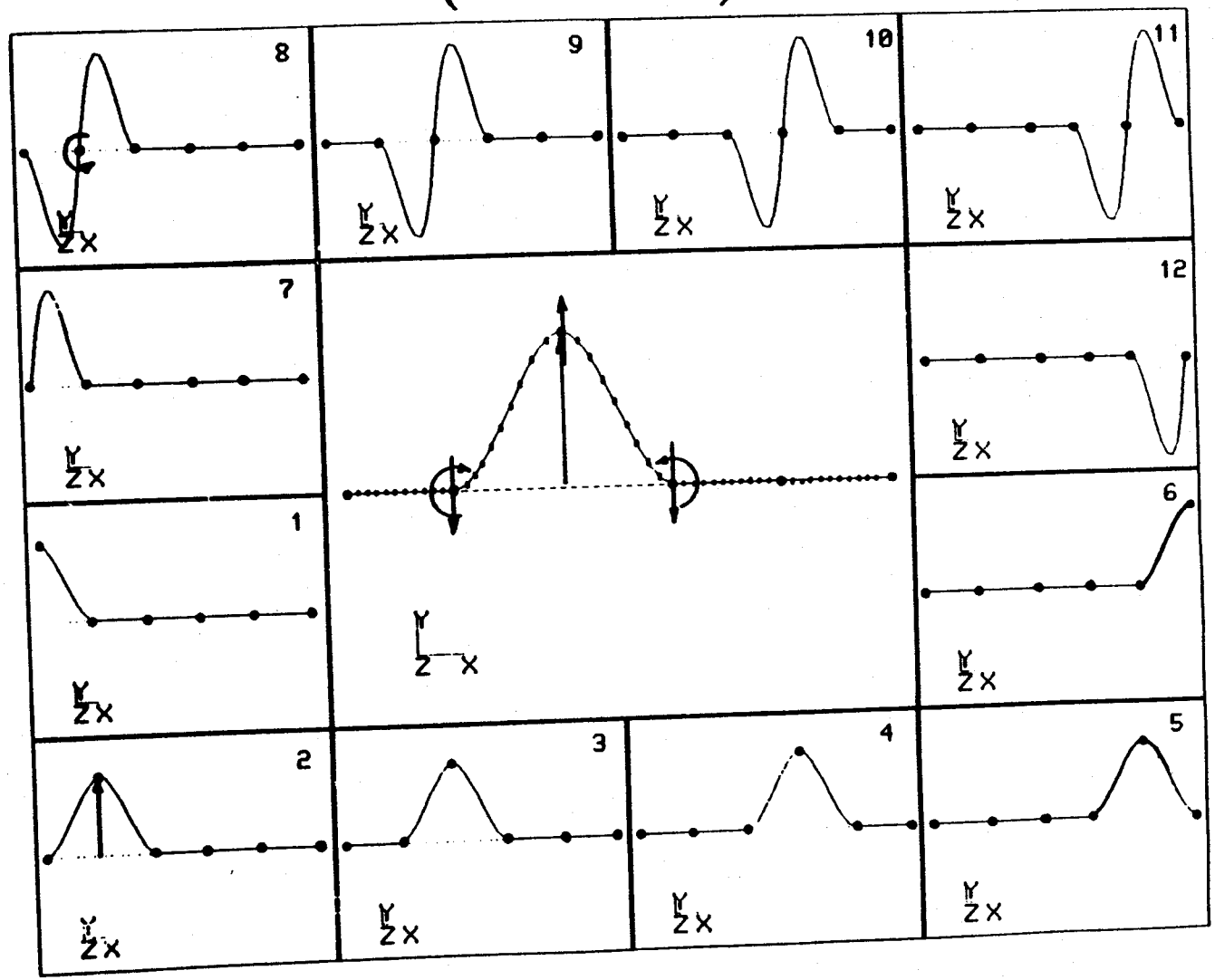

CALCULATION OF FORCES OF CONSTRAINT

As stated earlier, subsequent to enforcement of a unit displacement or rotation on a selected grid point, a set of reaction forces are obtained which are used in the assembly of the reduced stiffness matrix. Thus, the key factor in obtaining an accurate reduced stiffness matrix is the correct calculation of these reaction forces. For this purpose, steps are taken in the "simulation" process to correctly take into account the "equivalent" elastic effects of all the structural elements connecting the selected grid point of interest to its immediate surrounding selected grid points. As a part of the requirements, it was stated that due to the definition of the stiffness influence coefficient, while applying the unit displacement at each of the selected grid points, it is necessary to constrain all of the other grid points. As a result, once a unit displacement is applied to the constrained model, the resulting reaction forces at each of the selected constrained points correspond to the forces of constraint.

In MSC/NASTRAN, these forces are calculated by solving the following equation.

$$\left[\begin{array}{c|c} K_{ff} & K_{fs} \\ \hline K_{sf} & K_{ss} \end{array}\right] \left\{\begin{array}{c} U_f \\ \hline U_s \end{array}\right\} = \left\{\begin{array}{c} P_f \\ \hline P_s \end{array}\right\} + \left\{\begin{array}{c} 0 \\ \hline Q_s \end{array}\right\} \tag{1}$$

where Q_s represents the vector of forces of constraint. Again, the resulting assembled reduced stiffness matrix will be similar to one obtained from the usual static condensation technique. However, study of each of the individual set of calculated reaction forces reveal certain information about the elastic behavior of corresponding section of the full model which prove to be beneficial in a better understanding of the structure. More discussion will be presented in the application section.

CALCULATION OF FORCES OF CONSTRAINT

$[K]$	Stiffness matrix
U	Displacement vector
P	Applied load vector
Q	Reaction force at the boundary nodes

Subscripts:

f	Set containing (free) structural points
s	Set containing points eliminated by SPCs

$$\left[\begin{array}{c|c} K_{ff} & K_{fs} \\ \hline K_{sf} & K_{ss} \end{array}\right] \left\{\begin{array}{c} U_f \\ \hline U_s \end{array}\right\} = \left\{\begin{array}{c} P_f \\ \hline P_s \end{array}\right\} + \left\{\begin{array}{c} 0 \\ \hline Q_s \end{array}\right\}$$

$$\{Q_s\} = \left[[K_{ss}] - [K_{sf}]\,[K_{ff}]^{-1}\,[K_{fs}]\right]\{U_s\} + [K_{sf}]\,[K_{ff}]^{-1}\,\{P_f\} - \{P_s\}$$

MASS CONDENSATION

For the mass matrix condensation, the primary objective is to use a technique that results in a reduced mass matrix which provides a better insight into the mass distribution of the actual structure. As stated earlier, such a characteristic can be beneficial for situations where rapid vibration reduction studies are desirable and it is necessary for the analyst to have a better understanding of the mass distribution of the areas of interest. Consequently, an in-house mass lumping procedure is used which will be discussed in detail in the implementation section.

MASS CONDENSATION

- GENERATING A REDUCED MASS MATRIX THAT PROVIDES DIRECT INSIGHT INTO ACTUAL MASS DISTRIBUTION OF FULL MODEL

- AN IN-HOUSE MASS LUMPING ALGORITHM USED

3.0 NASTRAN IMPLEMENTATION

STIFFNESS CONDENSATION

Condensation of the full model stiffness matrix is performed by a set of MSC/NASTRAN DMAP alters (shown below) using the static rigid format (SOL-24). As a part of the reduction process, all the selected grid points of the full model (i.e., points to be included in the reduced model) are initially constrained by imposing permanent single-point constraints (in all six directions) on the GRID cards corresponding to these selected grid points. Next, a set of SPCD cards together with equal number of FORCE (or MOMENT) cards are defined in the Bulk Data Deck to simulate the applied unit displacements or rotations. As indicated below, the total number of pairs of SPCD and FORCE (or MOMENT) cards is equal to n where n is the total number of degrees-of-freedom of the reduced model. For calculating the reaction forces, n number of SUBCASEs are defined in the Case Control Deck where each SUBCASE referrs to one pair of SPCD and FORCE cards. For example, the first SUBCASE corresponds to application of a unit displacement to the first selected grid point along the basic coordinate, X-axis. The resulting single-point forces of constraint of all DOF of all the selected grid points are then printed out. Similarly, a unit displacement or rotation is applied along different axes to the same selected grid points. This process is repeated for other selected grid points. For the example shown below, the enforced displacements are applied to the selected grid points of the full model only along the X-axis. Appropriate changes need to be made to the SPCD and FORCE cards when different displacements or rotations are applied. Once all the forces of constraints are obtained, they are assembled together through a FORTRAN program to form a set of DMIG cards, representing the reduced stiffness matrix.

STIFFNESS CONDENSATION

SOL 24
SET SID = (SELECTED GRID POINT ID'S OF THE FULL MODEL)
SPCFORCE = SID
SUBCASE 1
LOAD = 1
SUBCASE 2
LOAD = 2
. . .
SUBCASE n
LOAD = n

BEGIN BULK
SPCD,1,G_1,1,1.0
FORCE,1,G_1,,0.0,1.0,0.0,0.0
SPCD,2,G_2,1,1.0
FORCE,2,G_2,,0.0,1.0,0.0,0.0
. . .
SPCD,n,G_n,1,1.0
FORCE,n,G_n,,0.0,1.0,0.0,0.0
. . .
ENDDATA

STIFFNESS CONDENSATION (continued)

Subsequent to application of displacements or rotations, the resulting SPCFORCEs are used in assembling the reduced stiffness matrix. For this purpose, a FORTRAN program which reads the MSC/NASTRAN output (i.e., SPCFORCEs) is used to position the resulting SPCFORCEs in the appropriate columns of the reduced stiffness matrix. The following figure shows the general form of the resulting reduced stiffness matrix. The first column represents the SPCFORCEs obtained from the application of a unit displacement along the X-axis of the first selected grid point while the tenth column is the result of the application of a unit moment about the X-axis for the second selected grid point. Subsequent to assembly of the reduced stiffness matrix, a set of MSC/NASTRAN DMIG cards are generated which can be used for different follow-up analyses. It should pointed out that the matrix shown below contains all six degrees-of-freedom of the selected grid points for the reduced model. However, the reduction procedure also applies to situations where only translational degrees-of-freedom for the reduced model are of interest.

STIFFNESS CONDENSATION (continued)

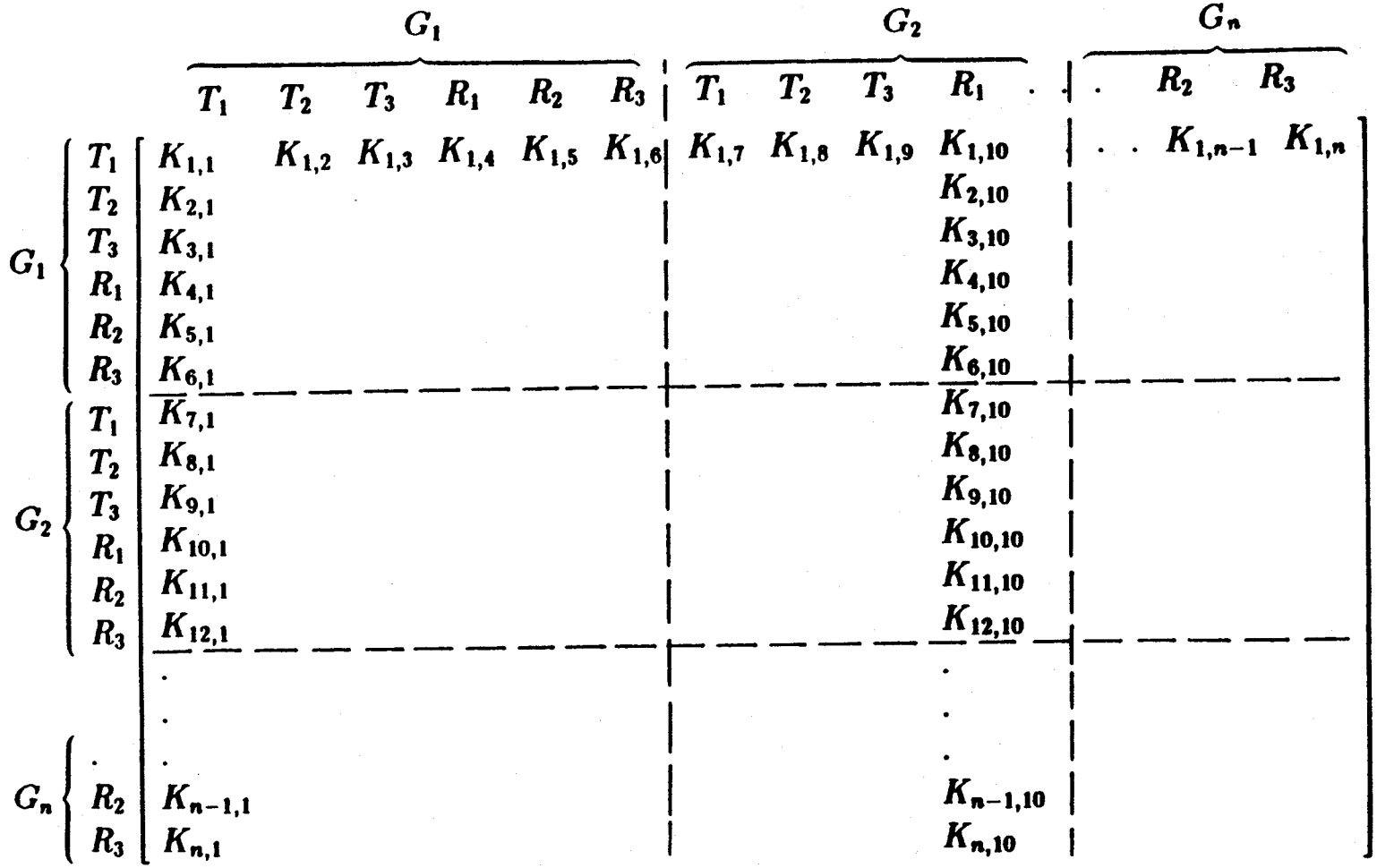

MASS CONDENSATION

As stated earlier, the primary objective is to use a technique that results in a reduced mass matrix which provides a better insight into the mass distribution of the actual structure. For this purpose, an in-house computer program was used which systematically distributes the full model mass data to the reduced model grid points. The resulting reduced model mass distribution were then presented in the form of a set of MSC/NASTRAN CONM2 cards for the reduced model.

Distribution of the full model mass data is based on the algorithm shown below. In this equation, $WTMASS$ represents the portion of mass item M which is distributed to a selected grid point (i.e, one of the reduced model grid point) located at a distance D from the mass item.

$$WTMASS = \frac{M/D}{\sum_{i=1}^{N} \frac{1}{D_i}} \tag{2}$$

For the mass lumping process, the lumping program requires two sets of information, namely, the full model mass data records (e.g., consistent with the MIL-STD1374A) and the location of the selected grid points of the full model (i.e., points which make up the reduced model). Starting with the first full model mass item, the program internally generates an imaginary volume (i.e., lumping volume) around the mass item. Next, by searching through the selected grid points, it identifies those grids which are confined within this volume and then assigns a different portion of the mass item to each of the selected grid points using the above equation. Then, in case where there are still some remaining portions, the program increases the size of the lumping volume and starts assigning portions of the remaining mass item to the new set of grids which may now be within the confinement of the increased volume. This process is repeated until the mass item is completely distributed to the surrounding grids.

This process will be repeated for each of the full model mass items. However, proper care is taken within the program for avoiding the relumping of the mass of those items which have already been accounted for. Also, additional options are also made available in the program for the manual distribution of large mass items.

MASS CONDENSATION

- GENERATING A REDUCED MASS MATRIX THAT PROVIDES DIRECT INSIGHT INTO ACTUAL MASS DISTRIBUTION OF FULL MODEL

- METHODOLOGY:

  - REDISTRIBUTING MASS OF EACH ITEM BASED ON THE FOLLOWING:

$$WTMASS = \frac{M/D}{\Sigma_{i=1}^{N} \frac{1}{D_i}}$$

  - WTMASS - Portion of mass of item assigned to a grid point
  - M - Mass of the full model item
  - D - Distance between mass item C.G. and the reduced model grid point

4.0 APPLICATION

AH-64A VEHICLE DESCRIPTION

The AH-64A Apache is a twin-engine, four-bladed rotary-wing aircraft operated by a tandem seated crew of two. It is intended for use by Army attack helicopter units. The airframe is a redundant semi-monocoque construction representing a fail-safe, damage tolerant design. The aircraft is equipped with main and tail landing gears which are functional for both normal landings and crash attenuation. Provisions are made for a nose mounted weapon system and for the carriage of wing mounted external stores.

The T700-GE-701 engines on the Apache are mounted high on the outside of the airframe. The engines are widely separated to reduce the risk of both engines sustaining combat damage. The rotor blades consist of multiple fiberglass spar tubes and stainless steel outer skin. This construction results in a ballistically survivable blade. The main rotor hub is fully articulated with redundant lead-lag dampers on each blade. An M230 30mm chain gun is mounted on the bottom of the airframe between the crew stations. Hellfire missiles and/or 2.75 in. FFAR rockets can be carried on the wing mounted pylons. The sighting for the weapon system is performed by the Target Acquisition and Designation System (TADS) and the Pilot Night Vision System (PNVS) located in the front of the airframe.

The photograph below shows an AH-64A in its primary mission configuration with 8 Hellfire missiles, 38 FFAR rockets, and 600 rounds of 30mm ammunition.

AH-64A VEHICLE DESCRIPTION

AH-64A OVERALL DIMENSIONS

The accompanying three view drawing shows the overall dimensions for the AH-64A aircraft.

General Data:

Primary Mission Gross Weight	14,694 lb.
Basic Structural Design Gross Weight	14,660
Maximum Alternate Mission Gross Weight	17,650
Ferry Mission Gross Weight	21,000
Main Rotor RPM	289
Tail Rotor RPM	1,403
V_{ne}	204 kn
V_h	164
V_{lat}	45
V_{aft}	45
Flight Maneuver Limits	+3.5g to -0.5g

AH-64A OVERALL DIMENSIONS

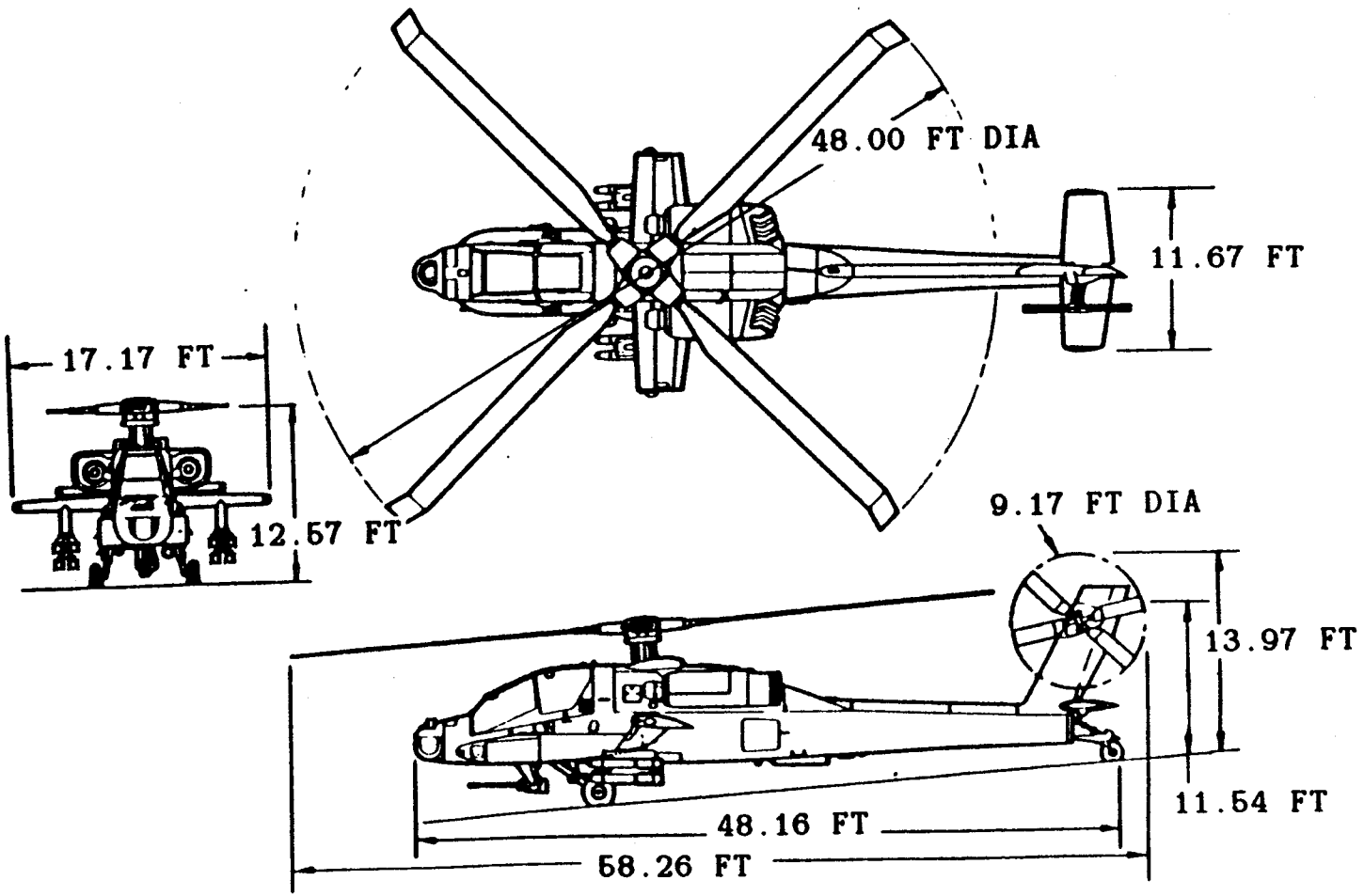

DESCRIPTION OF AH-64A FULL NASTRAN FINITE ELEMENT MODEL

The full analytical model used for this work is the dynamic MSC/NASTRAN finite element model of the AH-64A airframe which is shown in the following figure. This model, which contains a total number of 5100 degrees-of-freedom (DOF), was used for both the model reduction process and vibration reduction studies. It should be pointed out that this model represents a modified version of the MSC/NASTRAN model which was developed earlier under this contract in a separate task. These modifications were made to provide a more detailed treatment of local effects and include refinements of the model in the forward avionics bays, the engine support structure and the engine nacelle.

DESCRIPTION OF AH-64A FULL NASTRAN FINITE ELEMENT MODEL

Degrees-Of-Freedom	5097
Grid Points	2610
Mass Elements	1641
Structural Elements	6728

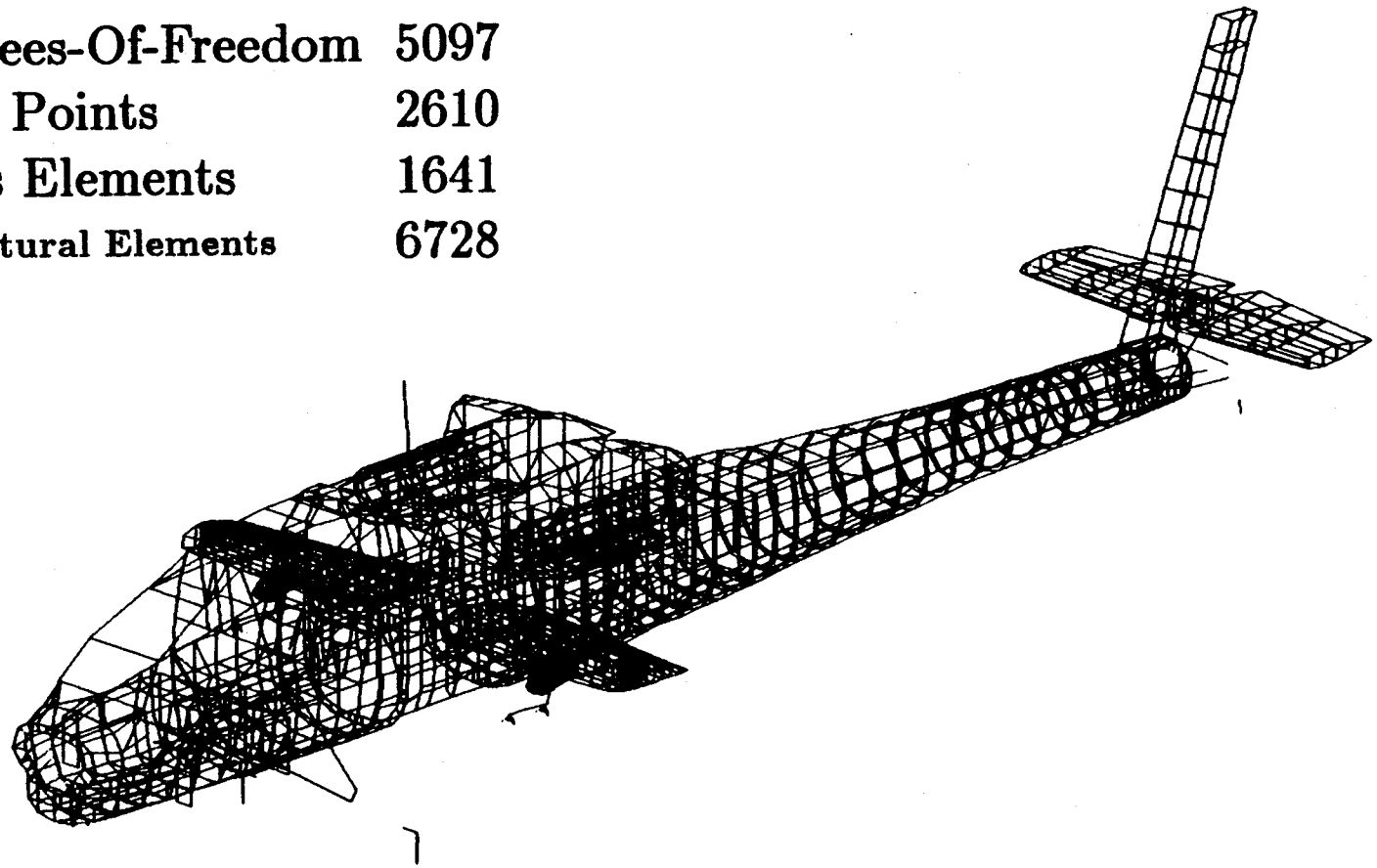

DESCRIPTION OF AH-64A FULL NASTRAN FINITE ELEMENT MODEL (Continued)

Prior to performing the reduction process, certain modifications were made to the full model in order to provide for an easier adaptation of the reduction procedure and a more accurate representation of the global behavior of each transverse section of the full FEM.

These changes included the addition of a set of RBE2 rigid elements at each fuselage frame which resulted in a set of grid points located near the centers of the frames. Subsequently, these grid points, together with some of the existing full model grid points, were used to define the grid point locations of the reduced model. Further explanation as to the consequences of the use of these rigid elements will be discussed in the following sections.

DESCRIPTION OF AH-64A FULL NASTRAN FINITE ELEMENT MODEL (Continued)

- ADDITION OF RBE2 ELEMENTS TO THE FULL MODEL FOR:
  - EASIER ADAPTATION OF THE REDUCTION PROCEDURE
  - BETTER REPRESENTATION OF GLOBAL BEHAVIOR OF EACH TRANSVERSE SECTION

MODAL CHARACTERISTICS OF FULL MODEL

Prior to the development and application of the reduction procedure, a study was performed to determine the dynamic characteristics of the full model. For this purpose, the natural frequencies and mode shapes of the full model were calculated over the frequency range of $(0 - 25)$ Hz. Frequencies of all the modes in this range are listed in the table below. Of the modes calculated, only those which represent global modes of the airframe will be used in the correlation studies. These eight particular modes are shown in the following figures. It should be pointed out that the addition of the RBE2 elements resulted in slight changes in the frequencies and modes of the original full model which are reflected in the following results. However, these changes did not impose any restrictions on the reduction process since the modified full model will be used in the reduction process.

MODAL CHARACTERISTICS OF FULL MODEL
NATURAL FREQUENCIES

Mode Number	Frequency (Hz)
1	2.167
2	2.169
3	2.197
4	2.218
5	4.333
6	4.416
* 7	5.452
* 8	6.001
9	6.972
* 10	10.697
11	11.302
* 12	11.443
* 13	11.967
* 14	13.406

Mode Number	Frequency (Hz)
* 15	14.158
16	16.751
17	17.012
18	17.483
19	17.713
20	17.947
21	18.477
22	18.508
23	18.652
* 24	20.626
25	21.530
26	22.115
27	23.080
28	24.258

* Modes which are used in correlation studies.

MODAL CHARACTERISTICS OF FULL MODEL
TAILBOOM TORSION (5.45 Hz)

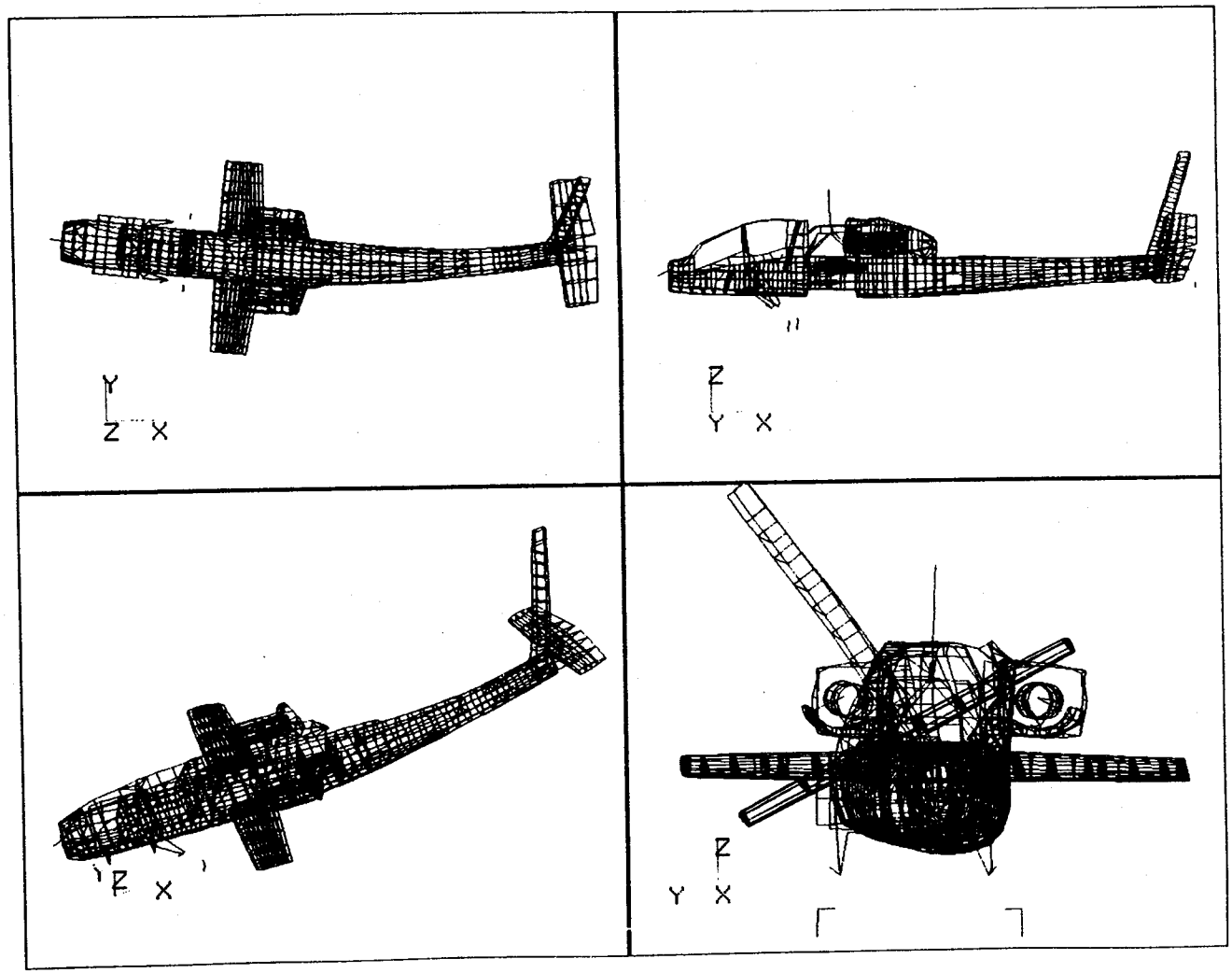

MODAL CHARACTERISTICS OF FULL MODEL
FIRST VERTICAL BENDING (6.00 Hz)

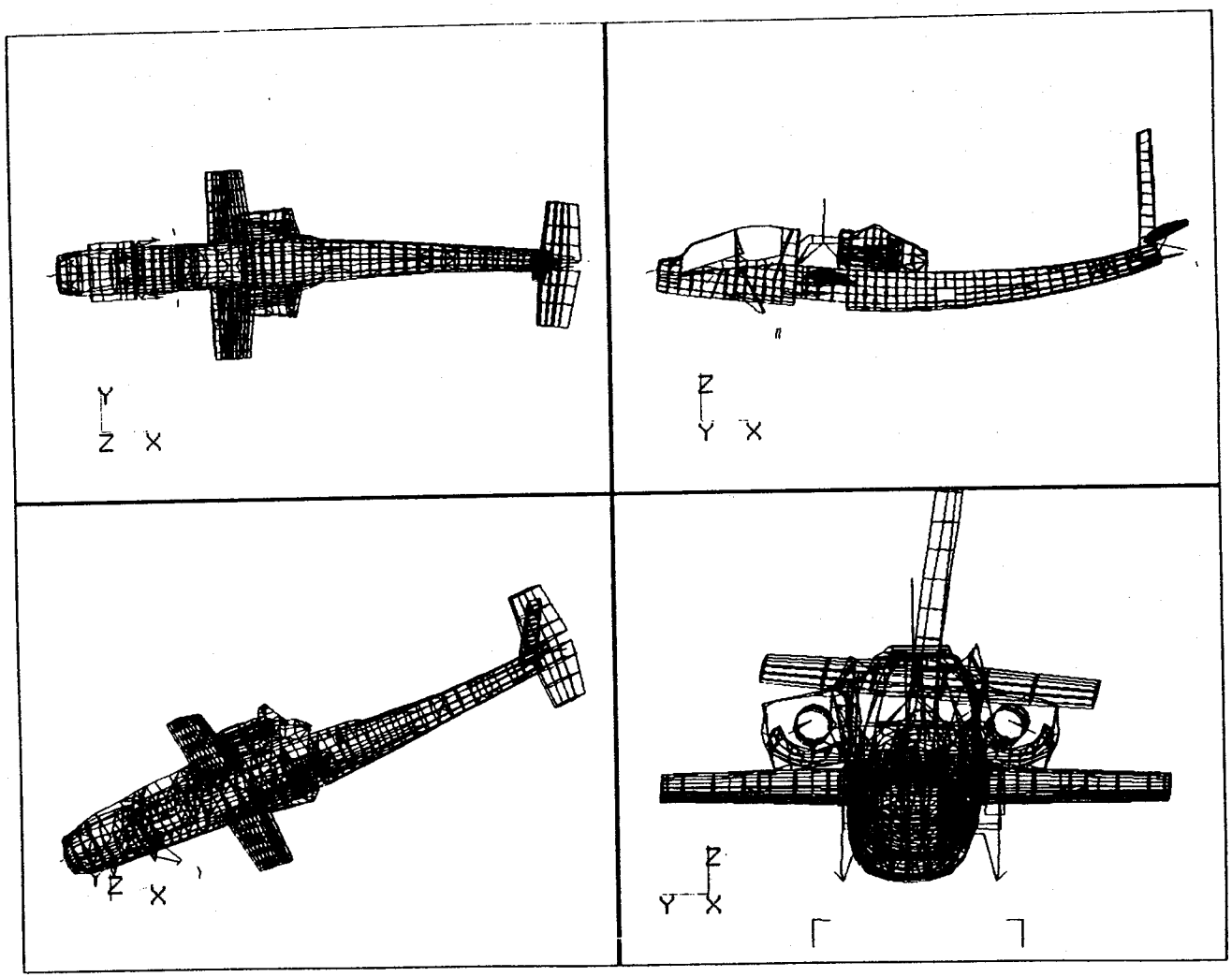

MODAL CHARACTERISTICS OF FULL MODEL
FIRST LATERAL BENDING (10.70 Hz)

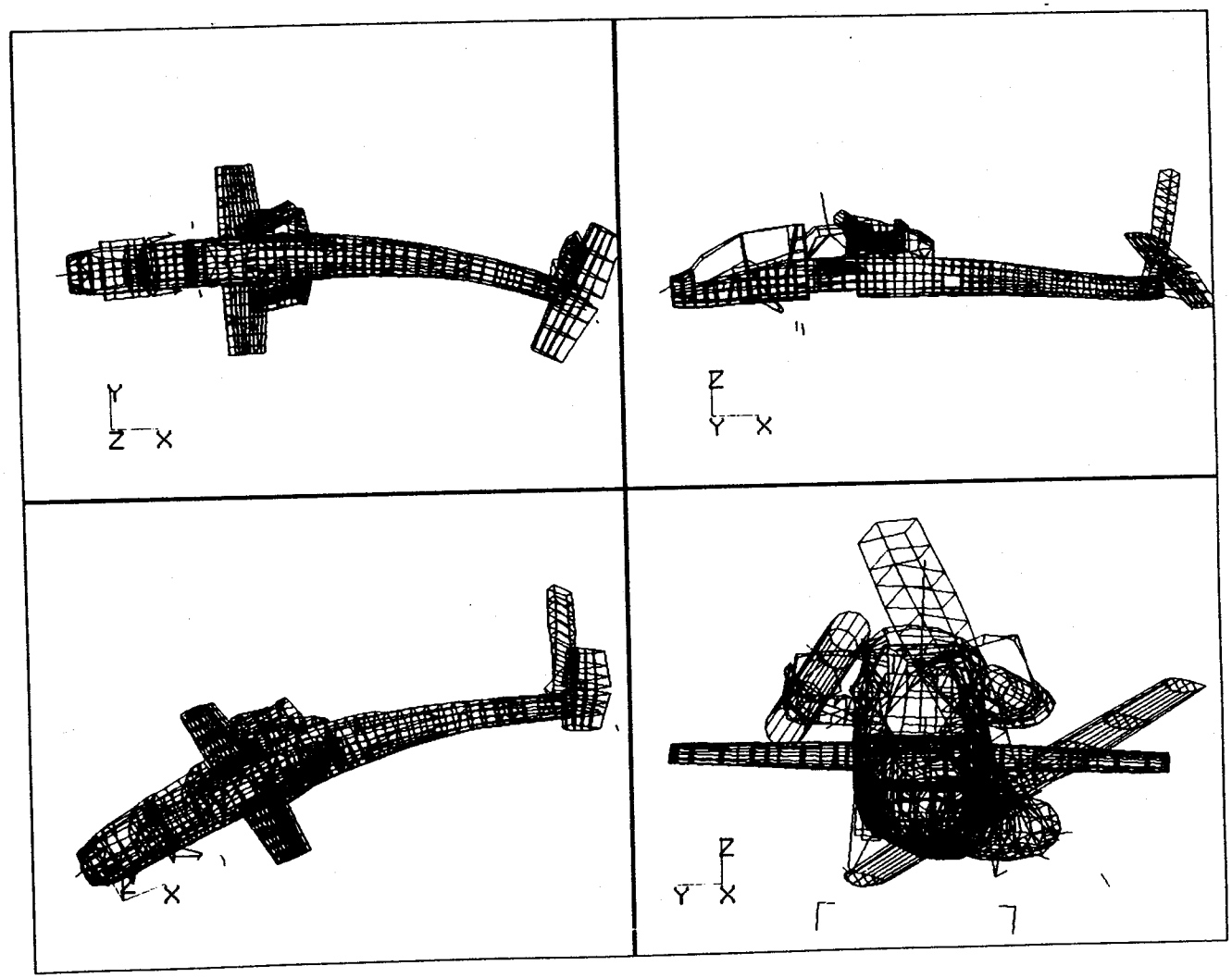

MODAL CHARACTERISTICS OF FULL MODEL
SYMMETRIC ENGINE YAW AND PITCH (11.44 Hz)

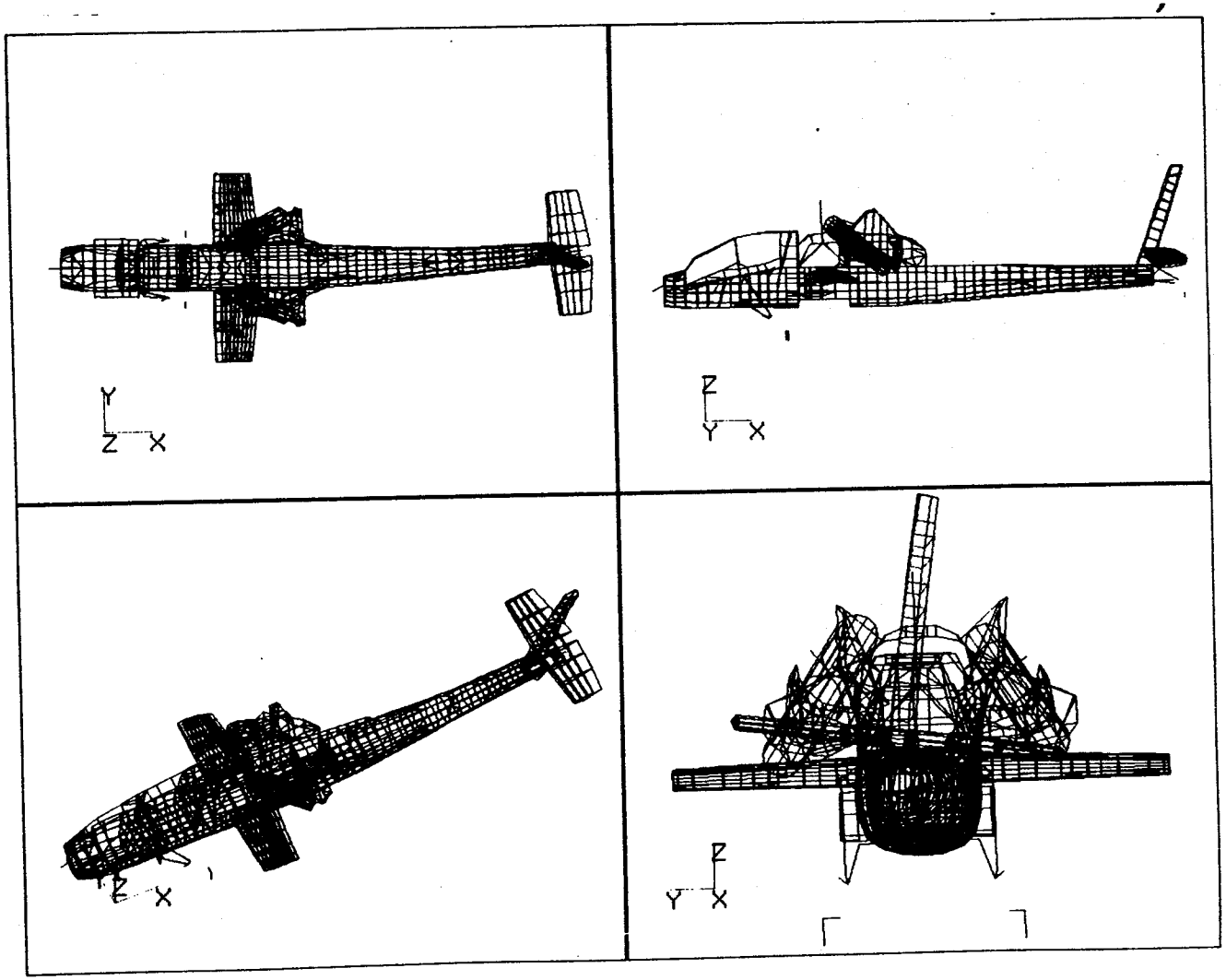

MODAL CHARACTERISTICS OF FULL MODEL
VERTICAL TAIL LONGITUDINAL BENDING (11.97 Hz)

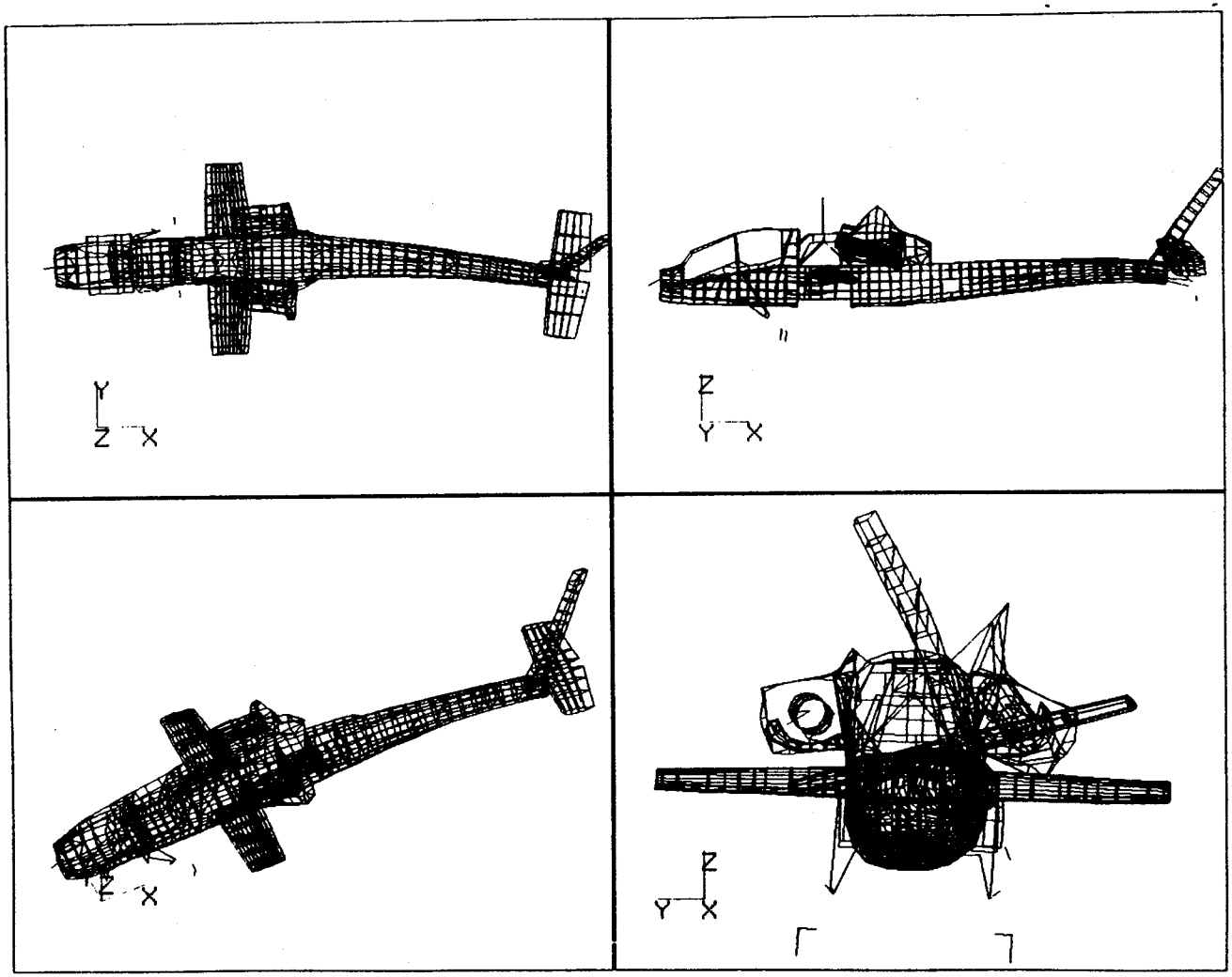

MODAL CHARACTERISTICS OF FULL MODEL
MAST LONGITUDINAL BENDING (13.41 Hz)

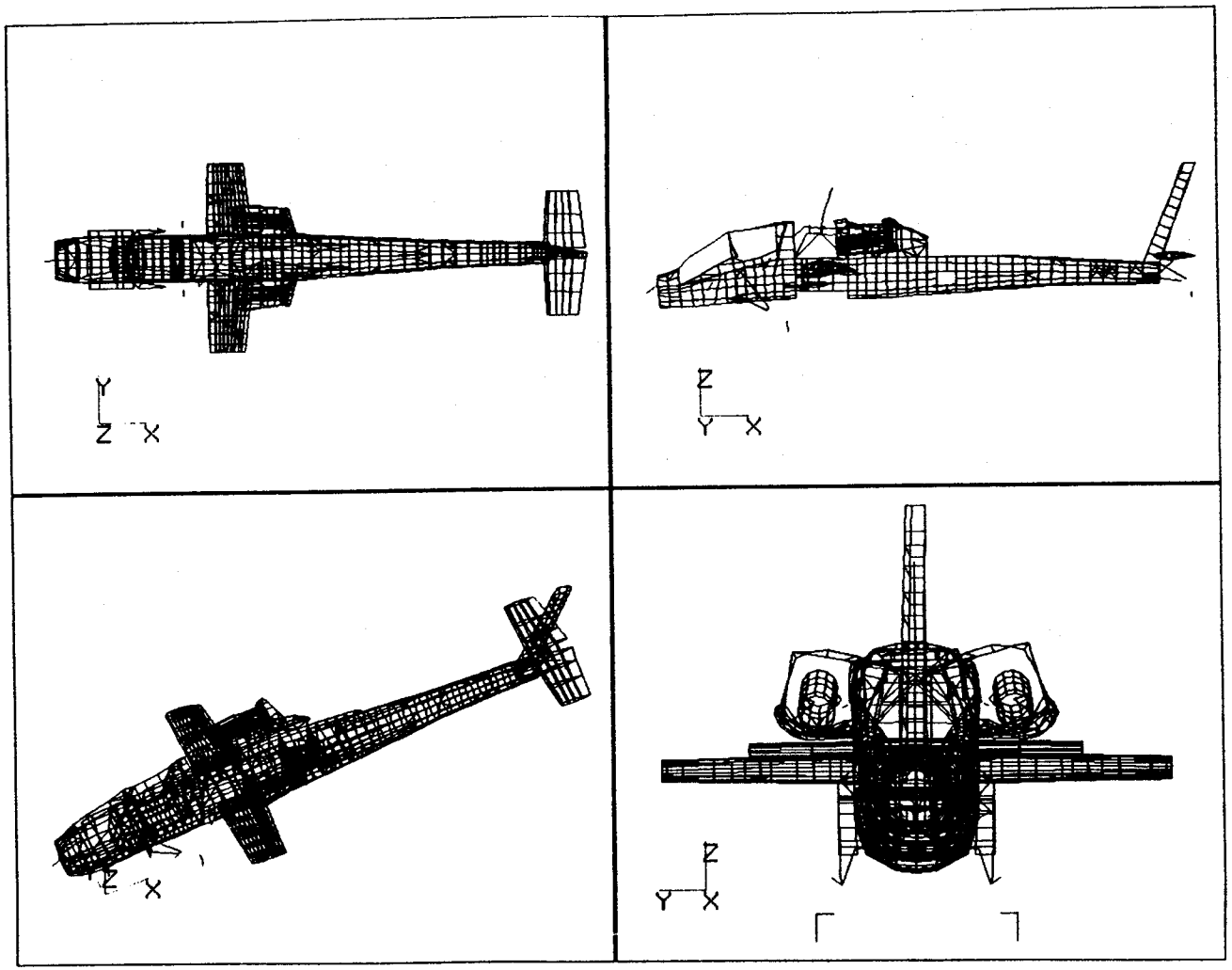

MODAL CHARACTERISTICS OF FULL MODEL
ANTISYMMETRIC ENGINE YAW (14.16 Hz)

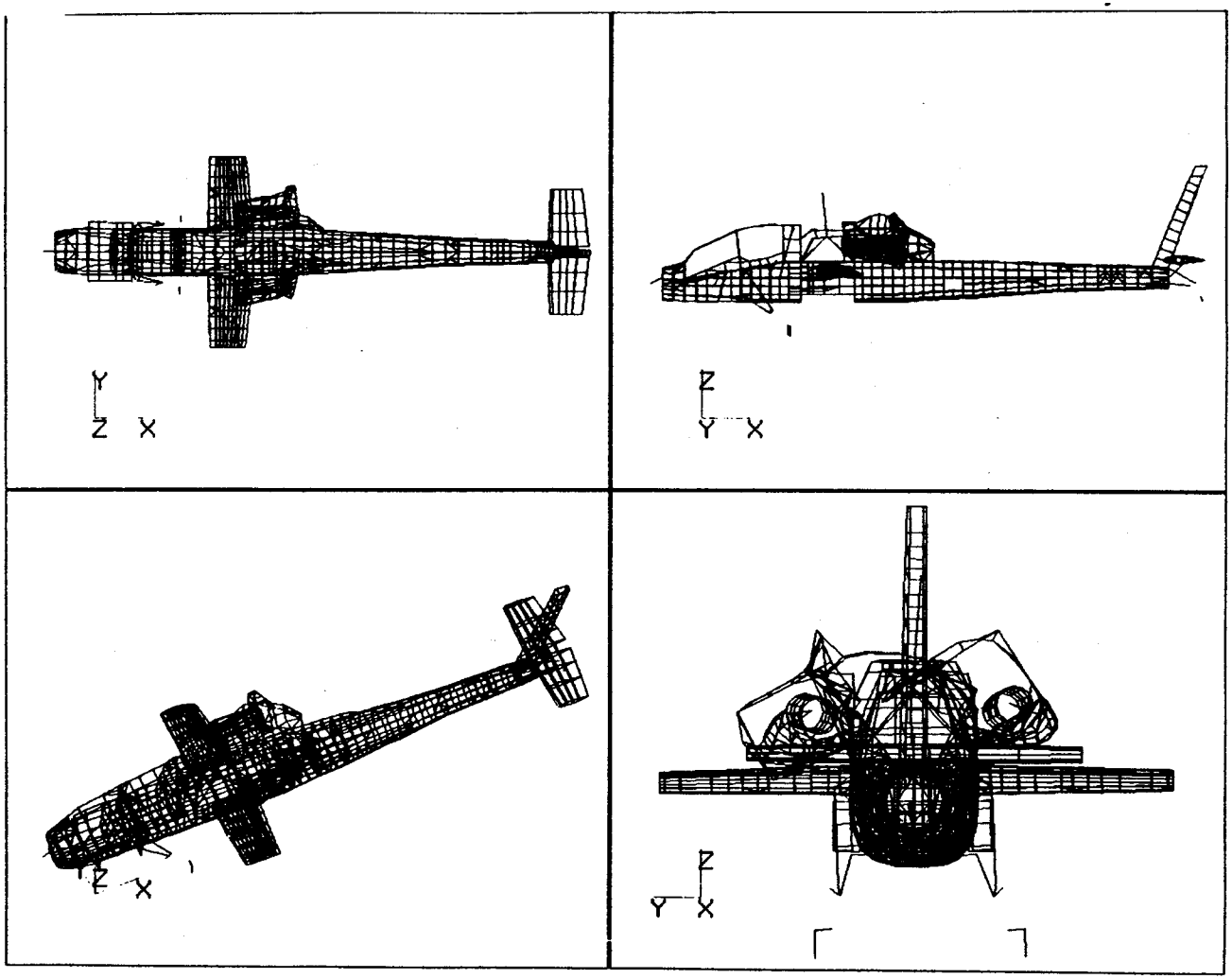

MODAL CHARACTERISTICS OF FULL MODEL
STABILATOR YAW (20.63 Hz)

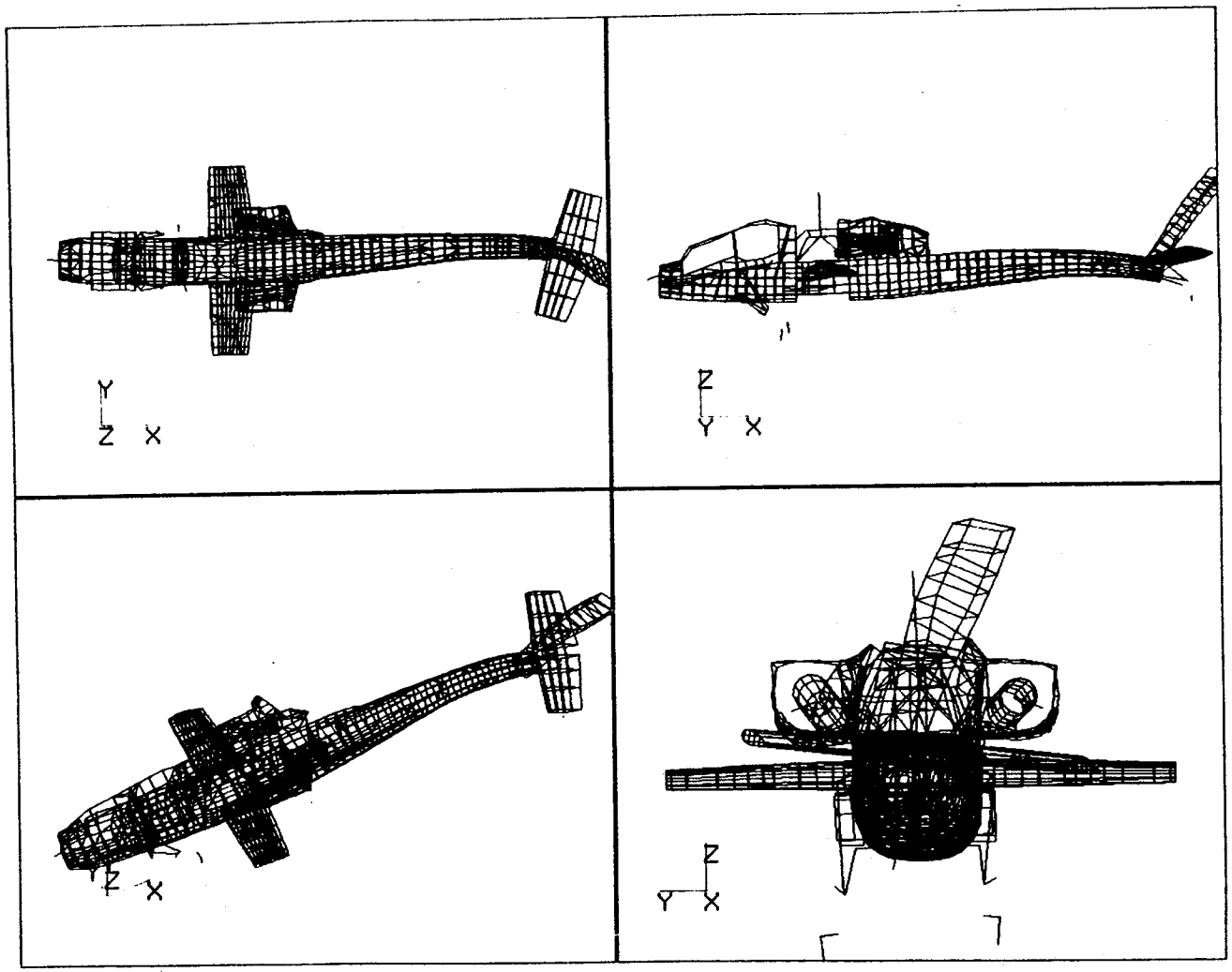

THE REDUCED MODEL

Following the application of the reduction procedure to the full AH-64A airframe dynamic finite element model, the reduced model shown in the following figure was obtained. This model, which has 83 grid points and a total of 498 DOF, is only a mathematical representation of the reduced (stick) model (i.e., the elastic properties are defined in terms of stiffness matrix rather than physical elements such as bar, beam, etc.). Obviously, it is desirable and beneficial to carry this mathematical reduced model one step further and develop an equivalent "physical" reduced model. However, this process was not pursued at this time. Instead, the "mathematical" reduced model was adapted for sensitivity analysis study which will be discussed in a later section.

As stated earlier, the resulting reduced stiffness matrix is the same as the one obtained from static condensation for this particular application. However, in other applications where the points near the center of each frame are dependent on the surrounding points on frames (i.e., RBE3 is used to represent the motion of the center point as a function of surrounding points on frame), static condensation (i.e., ASET) can not be used whereas this procedure can be used to obtain the reduced stiffness matrix. Another desirable feature of this reduction procedure is that due to the "simulation" procedure used, the elastic couplings which take place between each pair of selected grid points can be easily identified from forces of constraint during application of each individual unit displacement or rotation. This usually provides a better understanding of the behavior of each particular location of the structure. Finally, the reduction process can be performed with an arbitrary number of degrees-of-freedom at each grid location. For example, in situations where the rotational effects are of no interest, only the three translational DOFs can be included in the reduced model. This is simply done through imposing only translational unit displacements during the stiffness condensation process.

THE REDUCED MODEL

Degrees-Of-Freedom 498
Grid Points 83

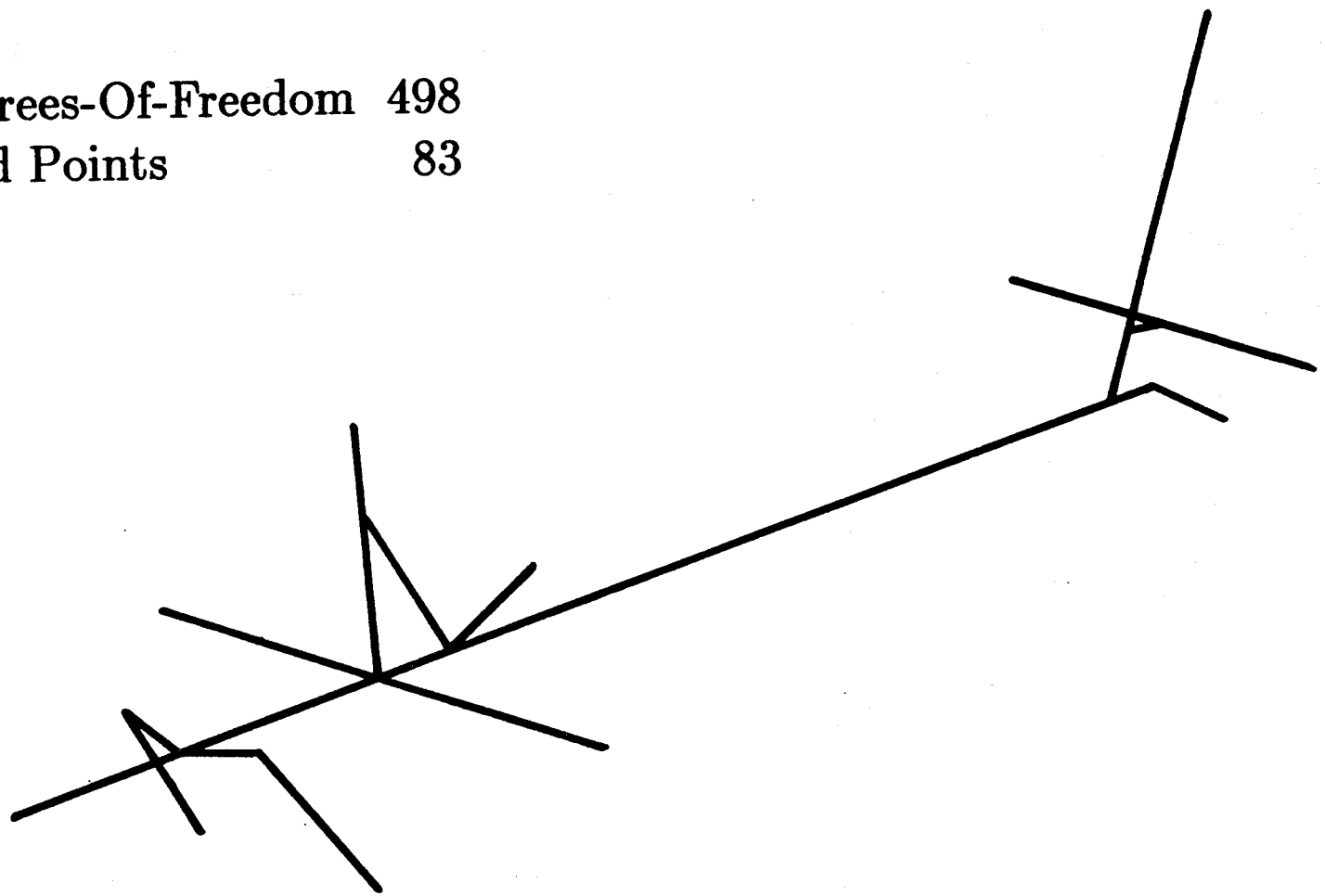

MODAL CHARACTERISTICS OF REDUCED MODEL

To determine the dynamic characteristics of the reduced model, a set of DMIG cards (generated from stiffness condensation process) together with a set of CONM2 cards (obtained from mass lumping program) were used in a normal mode analysis (SOL 3). The table below shows all the natural frequencies calculated through 25 Hz. Those frequencies which are used for the correlation studies are flagged. Corresponding mode shapes are shown in the figures which follow the table.

MODAL CHARACTERISTICS OF REDUCED MODEL
NATURAL FREQUENCIES

Mode Number	Frequency (Hz)
* 1	5.623
* 2	6.153
* 3	9.764
4	11.417
* 5	11.668
* 6	12.308
* 7	14.326
* 8	16.433
9	17.268
10	18.420
* 11	19.603
12	21.001
13	21.145
14	21.990
15	22.226
16	23.344

* Modes which are used in correlation studies.

MODAL CHARACTERISTICS OF REDUCED MODEL
TAILBOOM TORSION MODE (5.62 HZ)

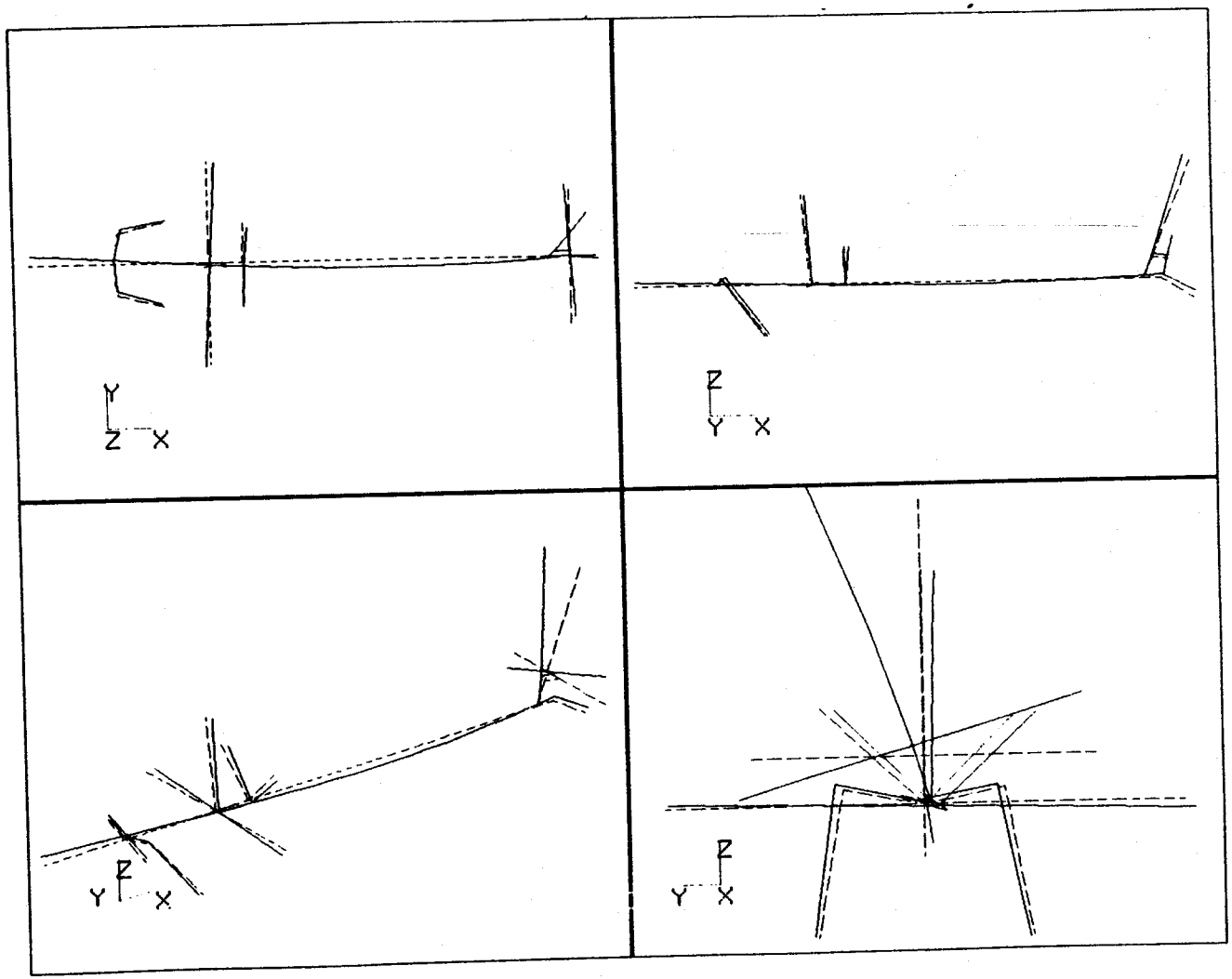

MODAL CHARACTERISTICS OF REDUCED MODEL
FIRST VERTICAL BENDING MODE (6.15 Hz)

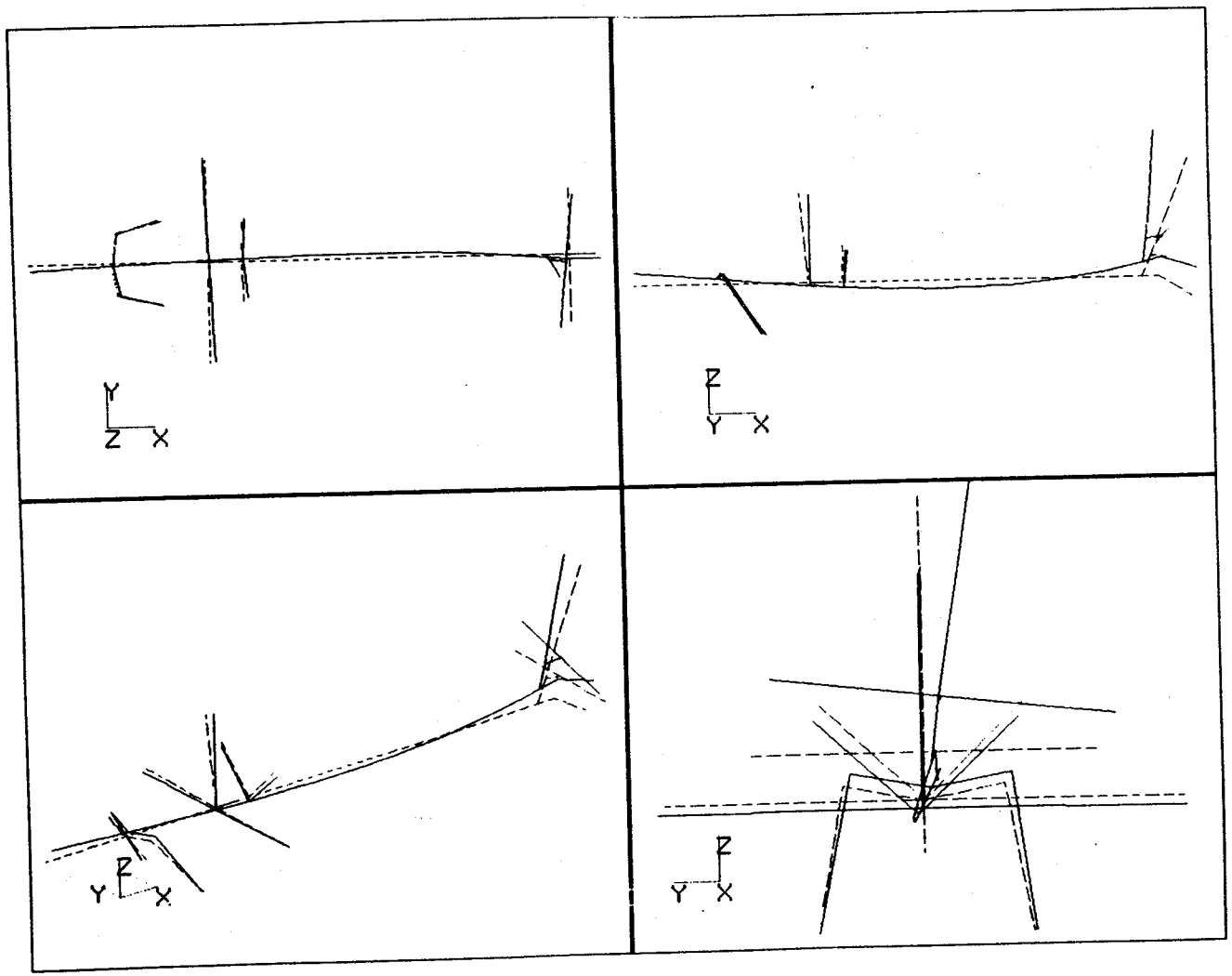

MODAL CHARACTERISTICS OF REDUCED MODEL
FIRST LATERAL BENDING MODE (9.76 Hz)

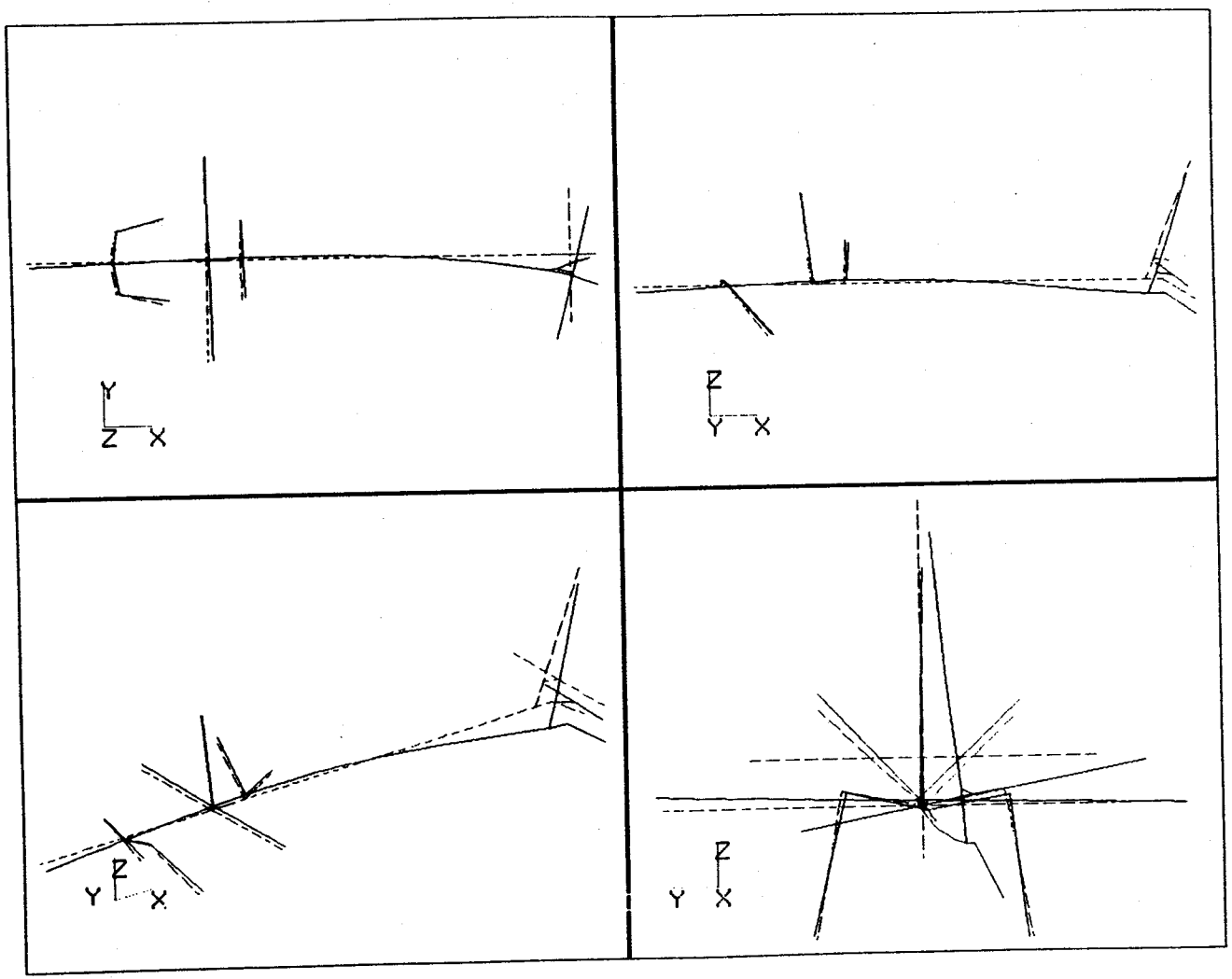

MODAL CHARACTERISTICS OF REDUCED MODEL
SYMMETRIC ENGINE YAW AND PITCH MODE (11.67 Hz)

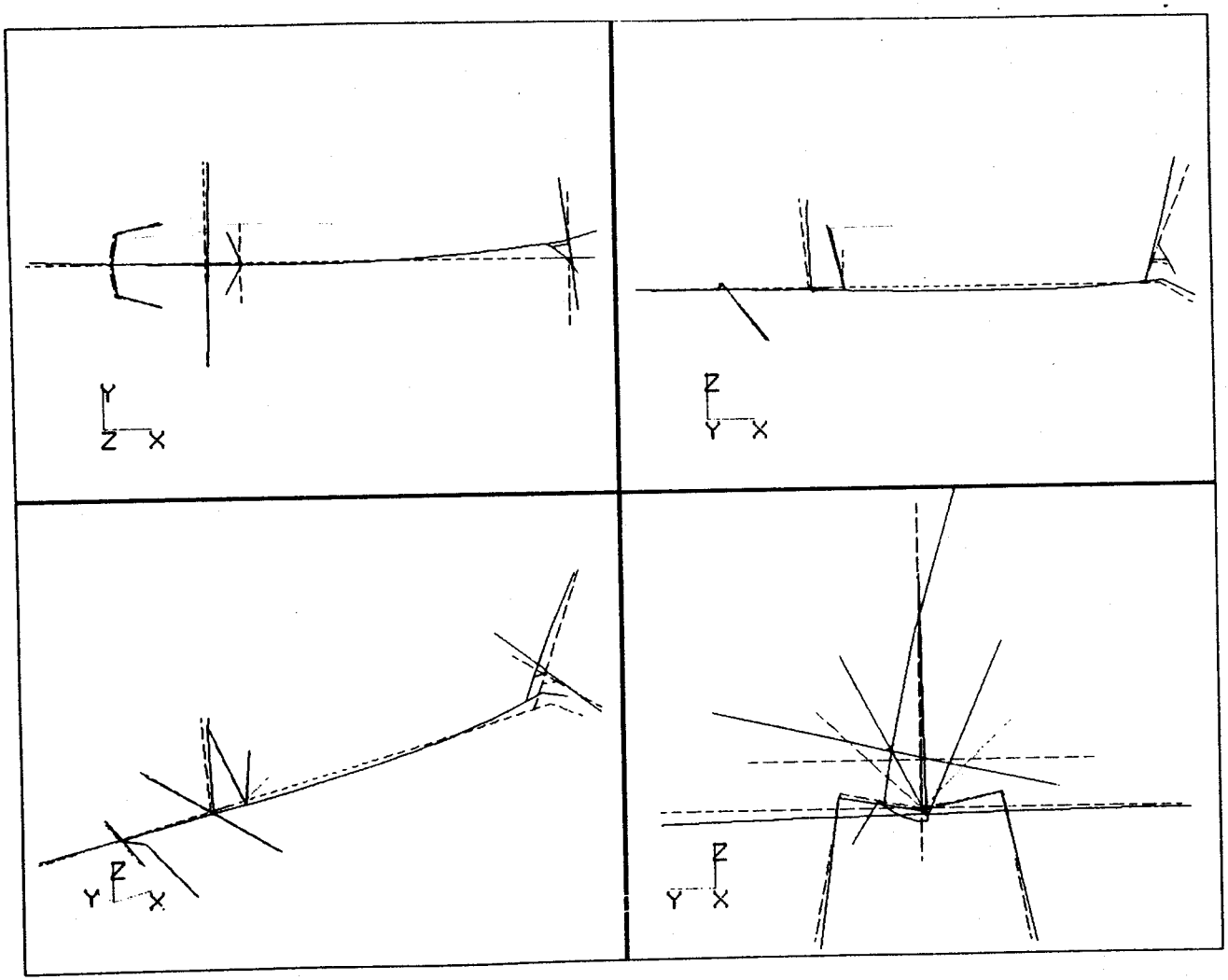

MODAL CHARACTERISTICS OF REDUCED MODEL
VERTICAL TAIL LONGITUDINAL BENDING MODE (12.31 Hz)

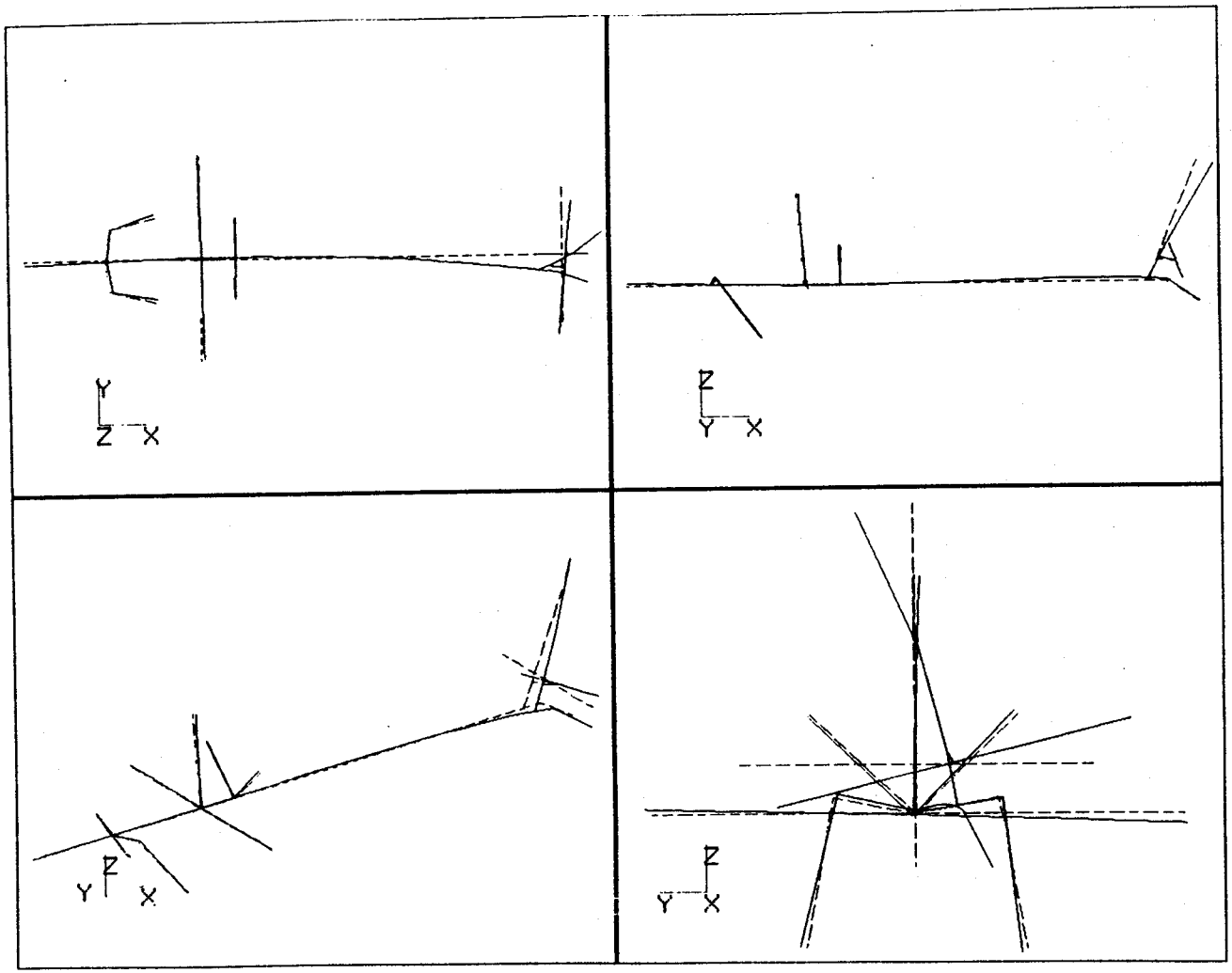

MODAL CHARACTERISTICS OF REDUCED MODEL
MAST LONGITUDINAL BENDING MODE (14.33 Hz)

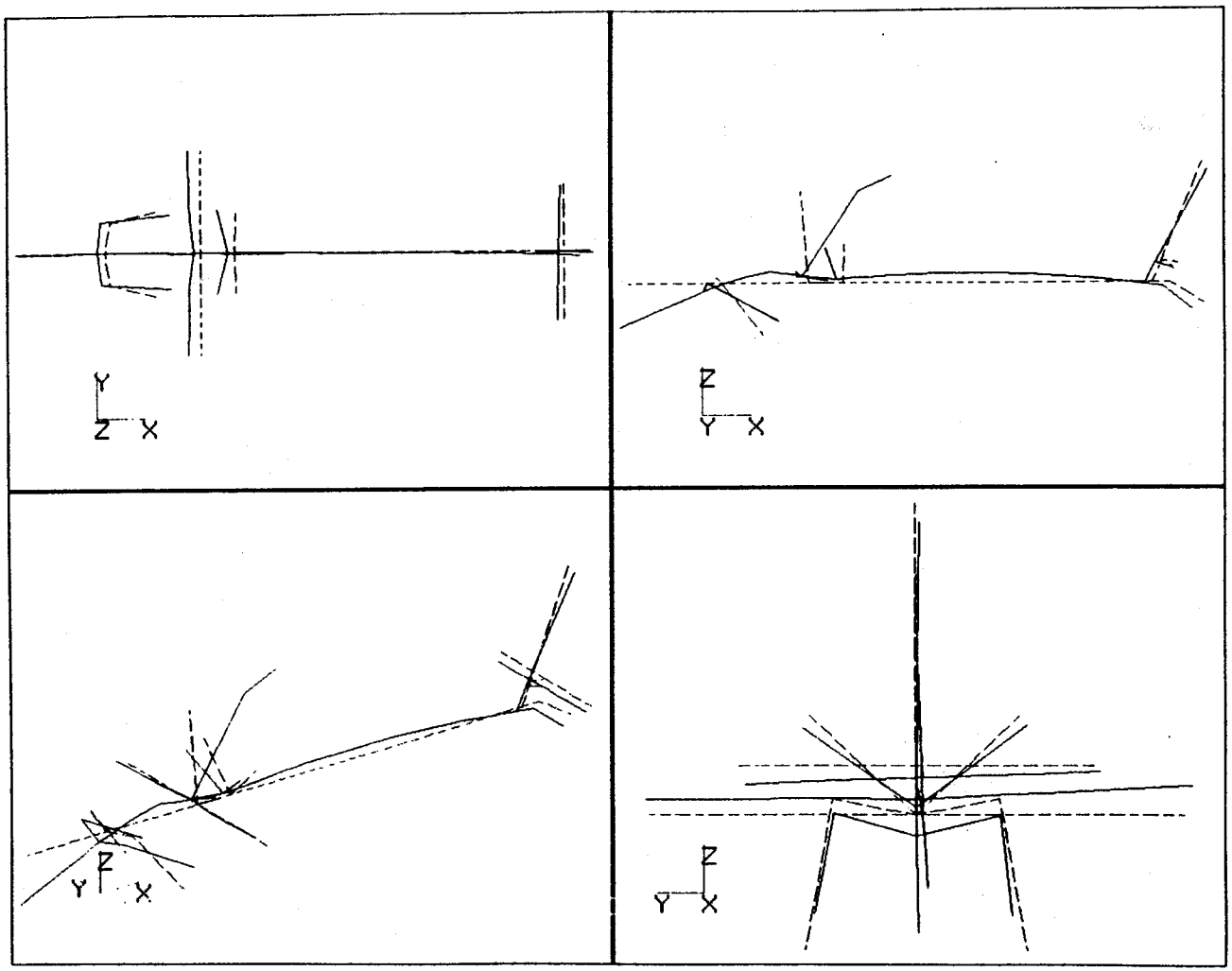

MODAL CHARACTERISTICS OF REDUCED MODEL
ANTISYMMETRIC ENGINE YAW MODE (16.43 Hz)

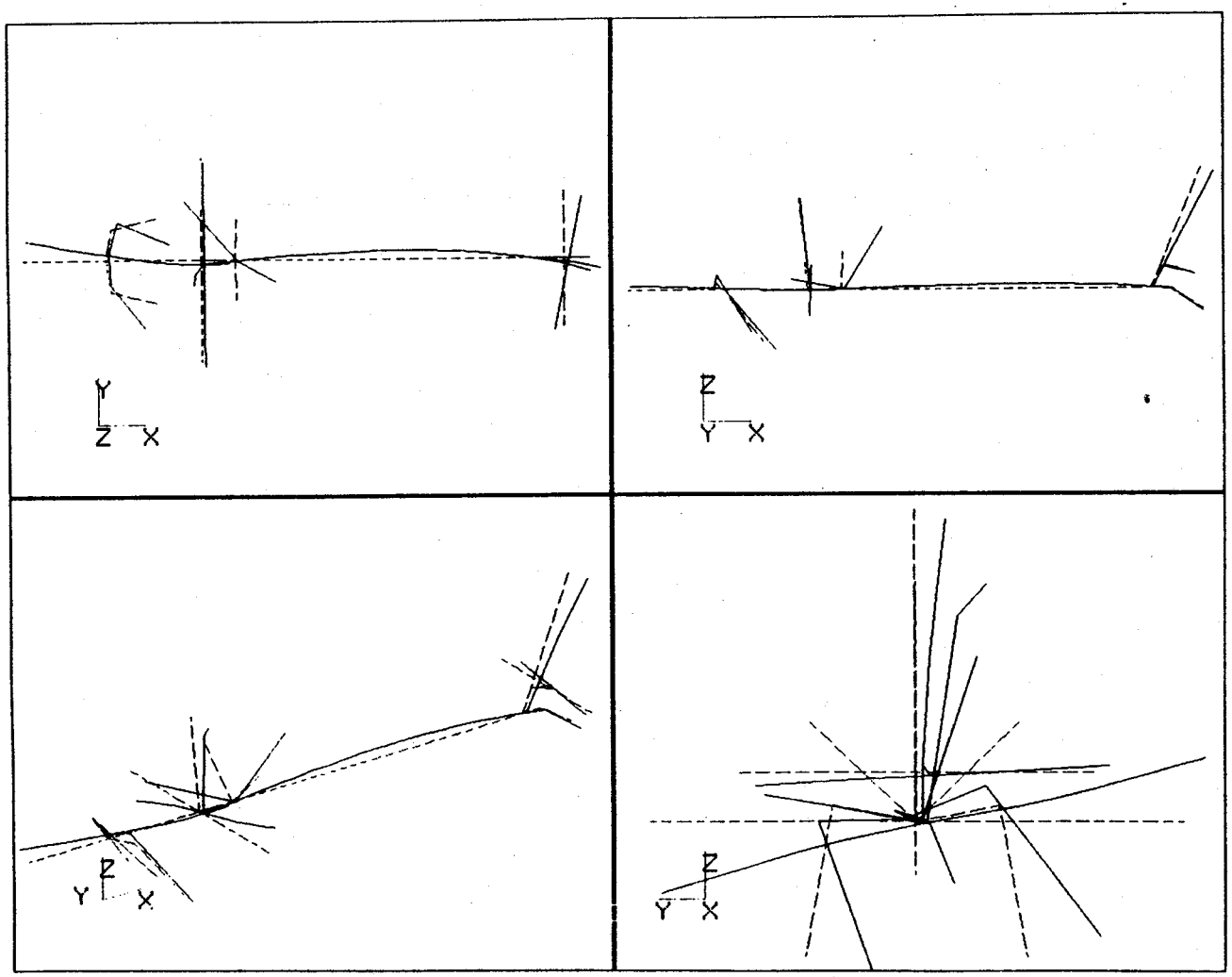

MODAL CHARACTERISTICS OF REDUCED MODEL
STABILATOR YAW MODE (19.6 Hz)

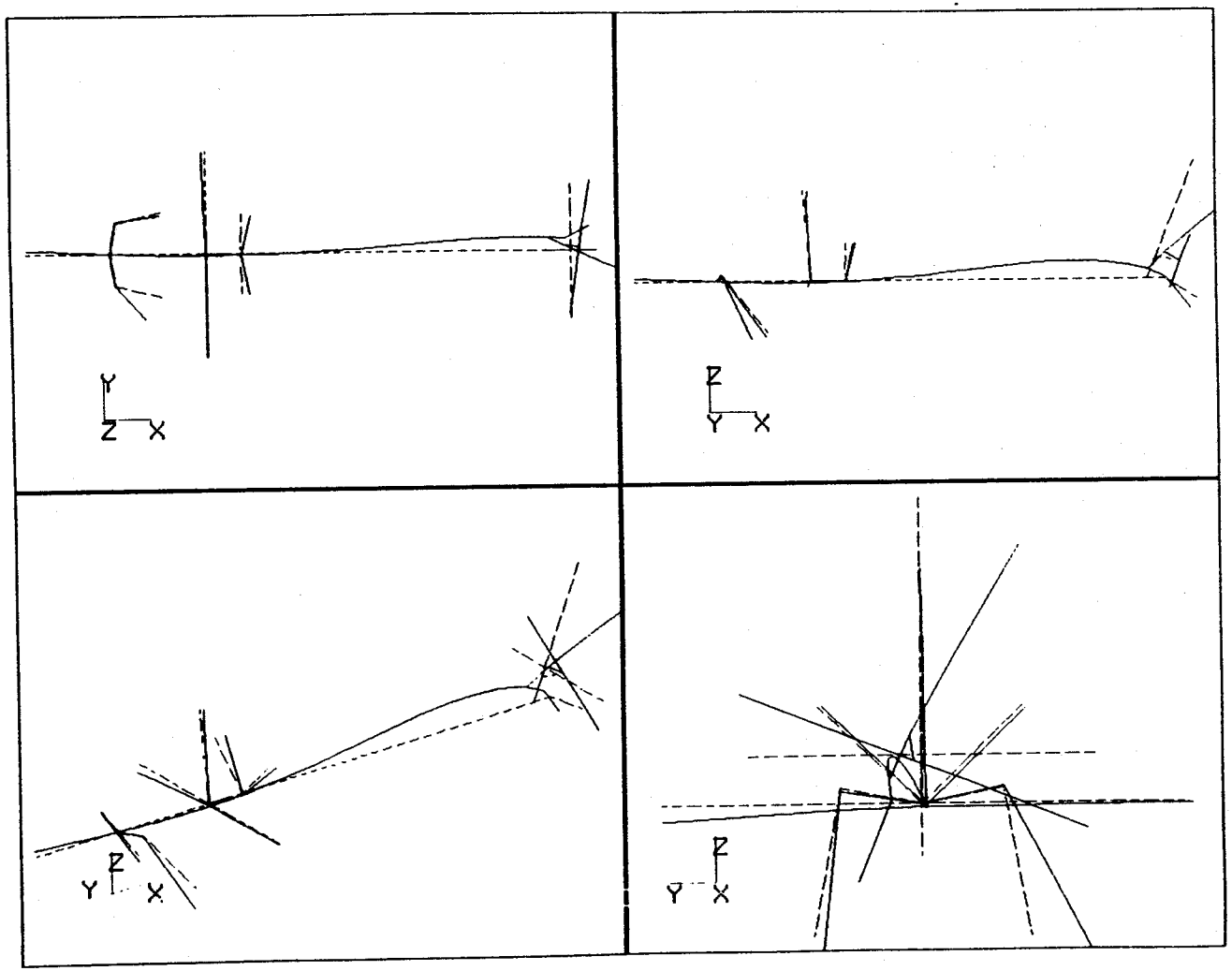

5.0 CORRELATION STUDIES

CORRELATION OF STATIC DEFORMATIONS

Prior to performing the correlation study, a set of grid points (i.e., all the reduced model grid points together with their corresponding full model counterparts) were selected. These grid points were then grouped together in such a manner that the starting grid number corresponds to the nose of the aircraft while the last grid number is representative of the tip of the tail landing gear. The following table shows the arrangements used between the grid points (shown on the following figures) and different areas of the airframe model. Subsequently, both the full and reduced models were constrained at the nose of the aircraft (i.e., grid point 1) in all six directions. A set of separate concentrated static forces and moments were applied at the tip of vertical tail (i.e., grid point 83) in each direction and the resulting translational deflections were calculated for each loading condition. The following figures show the resulting translational deformation patterns between the two models for all six cases. These results indicate excellent agreement in deflections, which in turn is indicative of good agreement between the two stiffness matrices.

CORRELATION OF STATIC DEFORMATIONS

Grid Locations	Areas of the Aircraft
1 - 8	Forward Fuselage section
9 - 12	Main Landing Gear
13 - 21	Front Area of Mid Fuselage Section
22 - 23	Main Rotor Mast Section
24 - 31	Right Wing Section
32 - 39	Left Wing Section
40 - 42	Middle Area of Mid Fuselage Section
43 - 44	Engine Locations
45 - 56	Aft Area of Mid Fuselage Section
57 - 69	Tailboom Section
70 - 71	Lower Portion of Vertical Tail
72 - 79	Horizontal Stabilator
80 - 81	Upper Portion of Vertical Tail
82 - 83	Tail Landing Gear Locations

CORRELATION OF STATIC DEFORMATIONS

(Fx APPLIED AT GRID LOCATION 83)

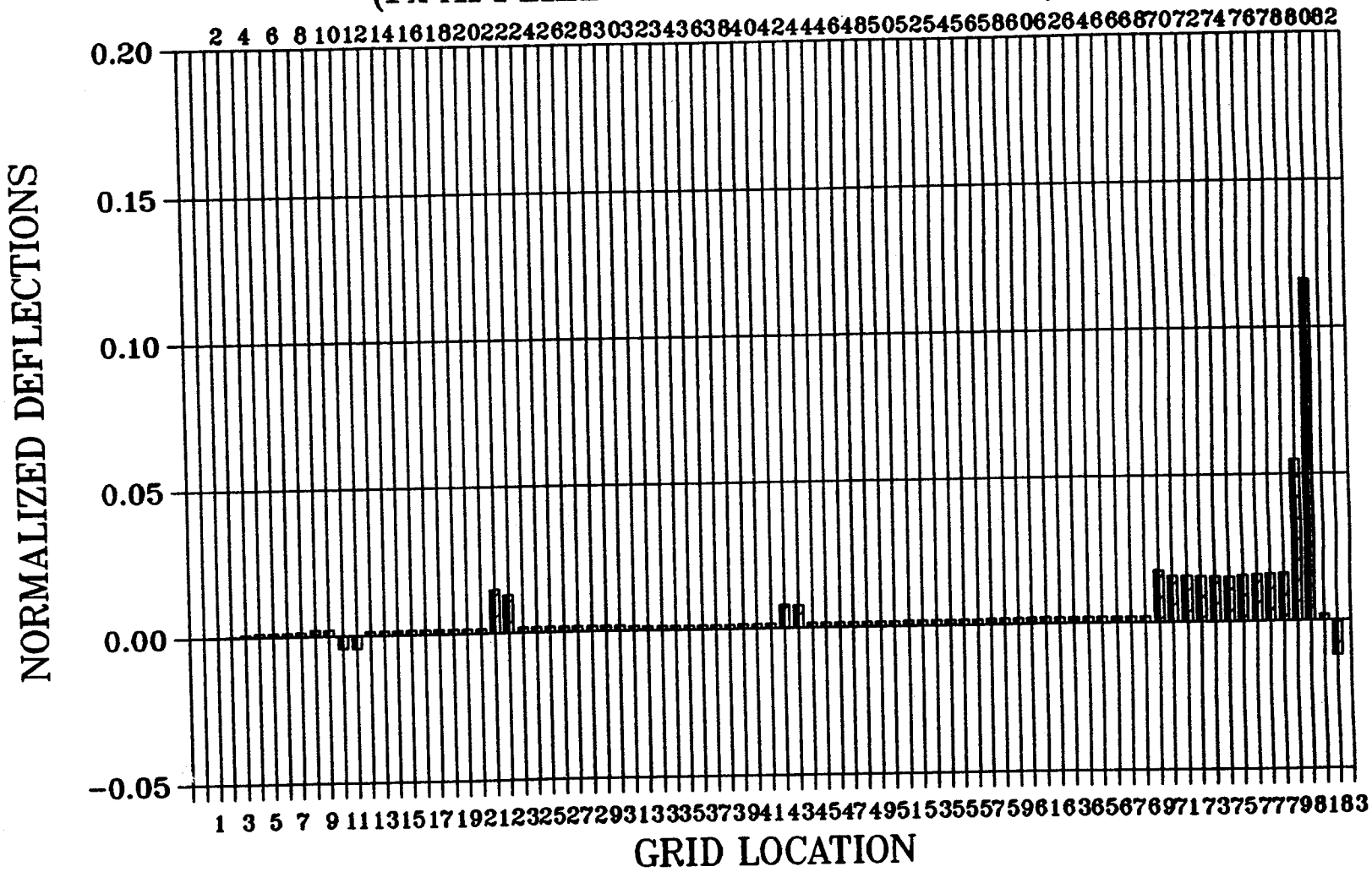

FULL MODEL, X-COMP.
STICK MODEL, X-COMP.

CORRELATION OF STATIC DEFORMATIONS

(Fx APPLIED AT GRID LOCATION 83)

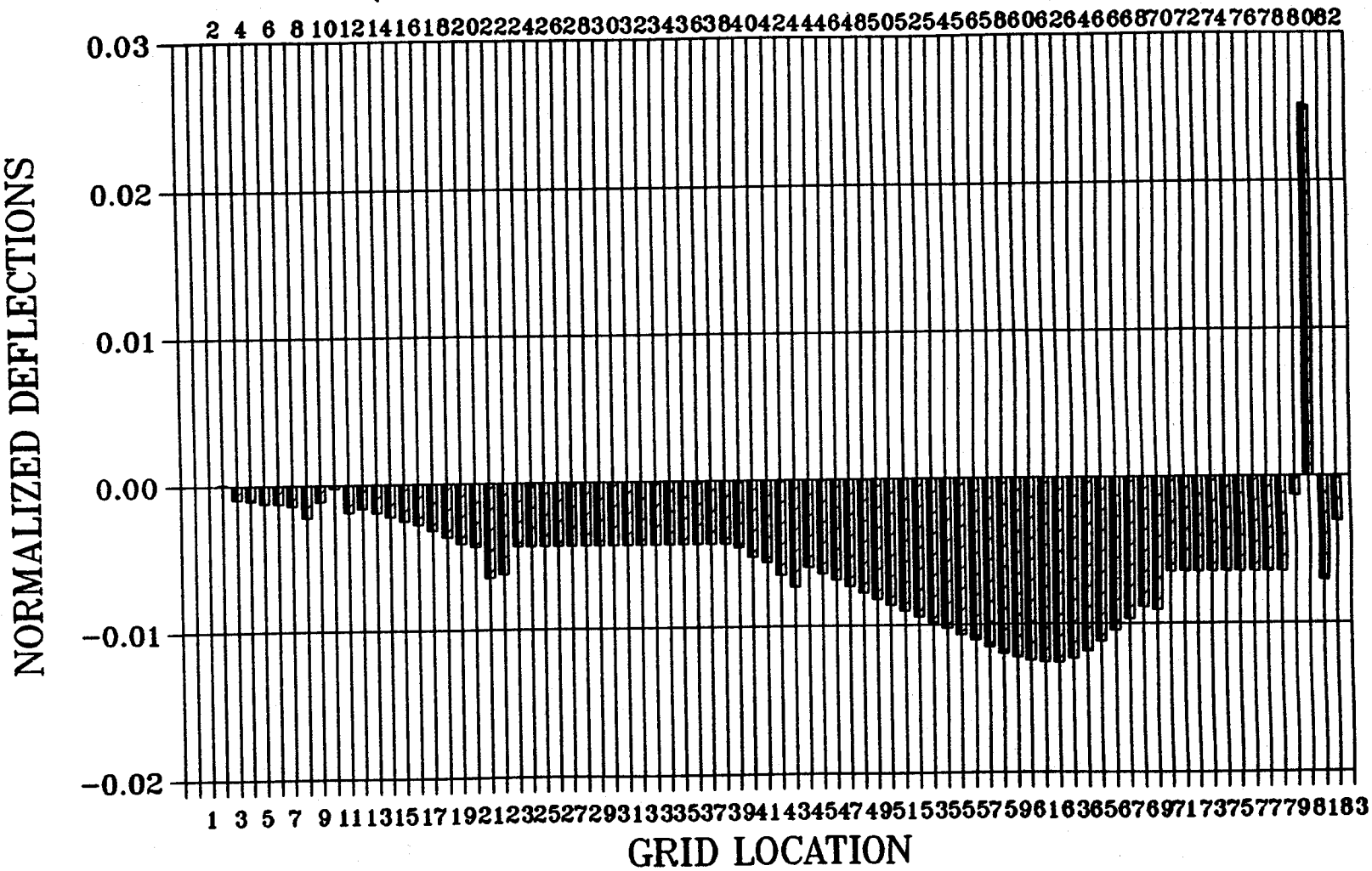

FULL MODEL, Y-COMP.

STICK MODEL, Y-COMP.

CORRELATION OF STATIC DEFORMATIONS

(Fx APPLIED AT GRID LOCATION 83)

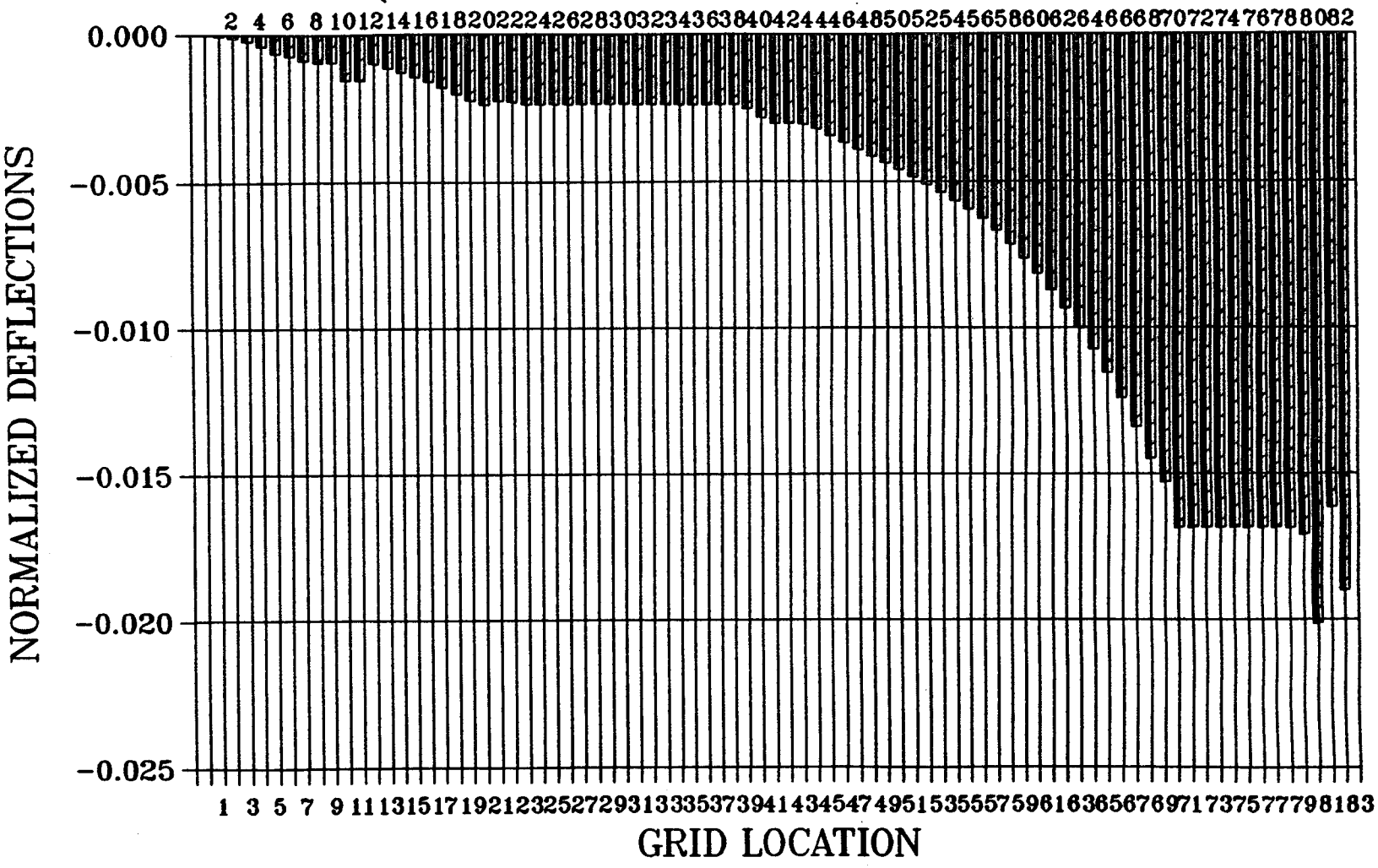

FULL MODEL, Z-COMP.
STICK MODEL, Z-COMP.

CORRELATION OF STATIC DEFORMATIONS

(Fy APPLIED AT GRID LOCATION 83)

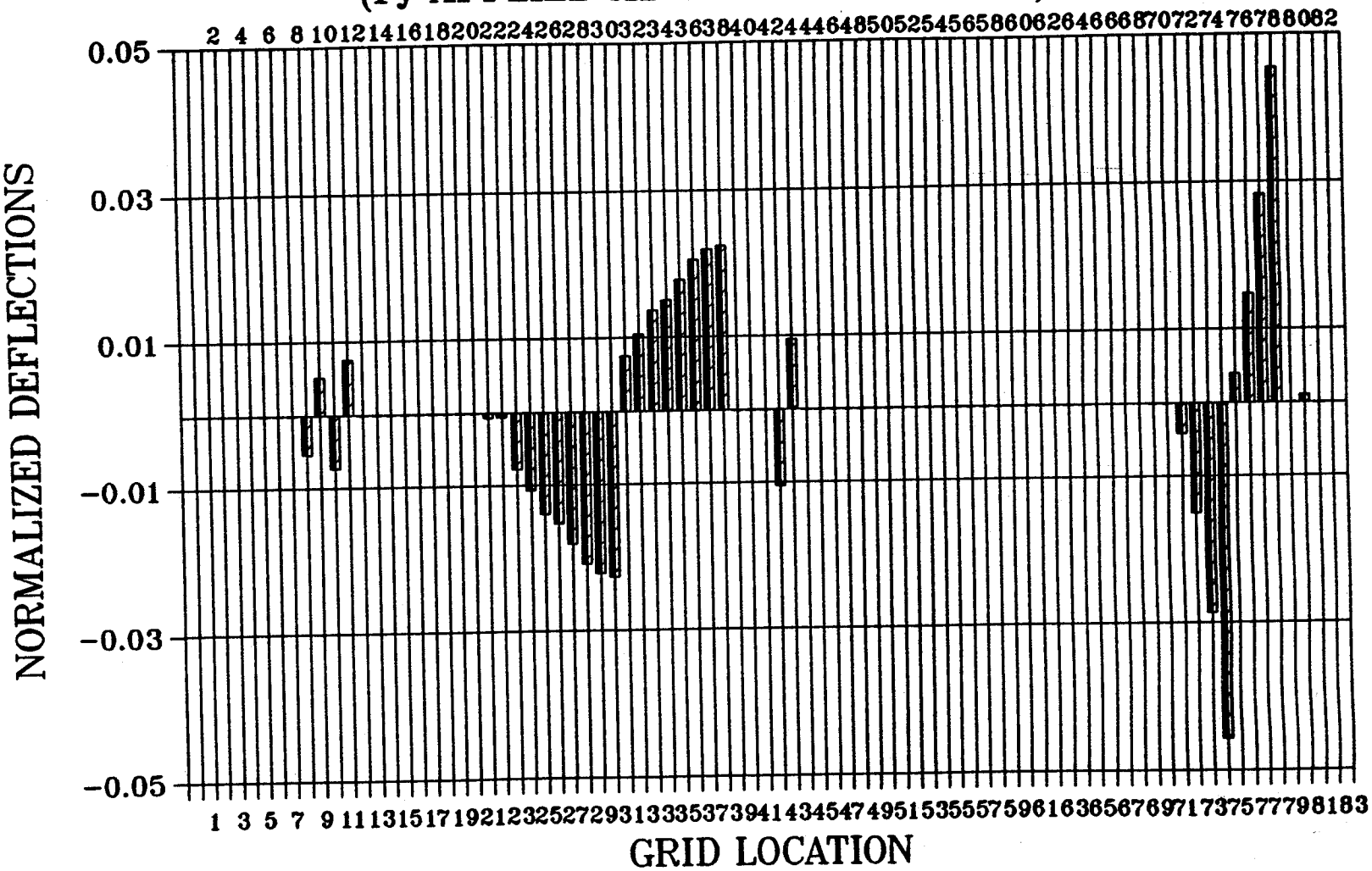

FULL MODEL, X–COMP.
STICK MODEL, X–COMP.

CORRELATION OF STATIC DEFORMATIONS

(Fy APPLIED AT GRID LOCATION 83)

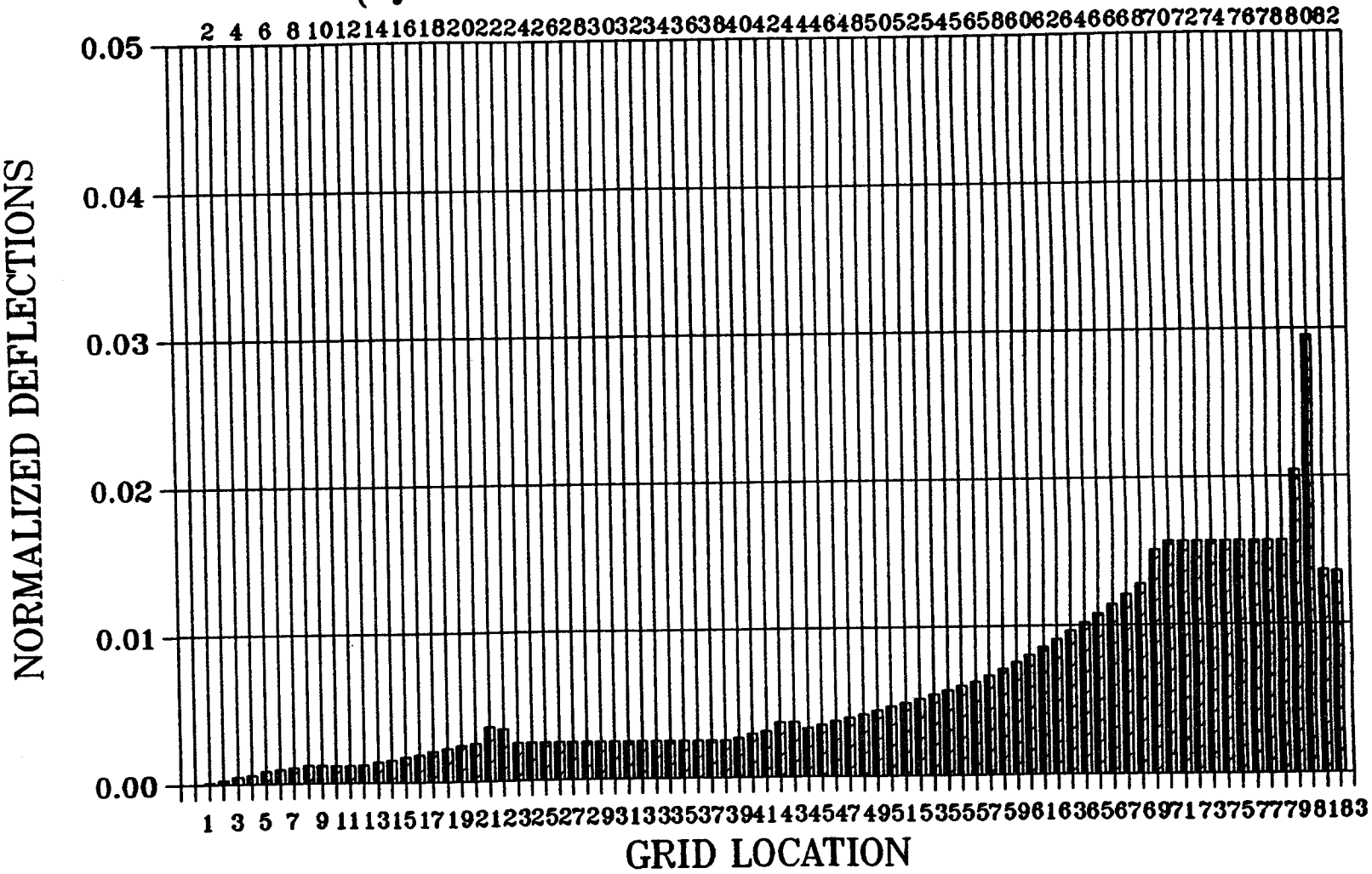

CORRELATION OF STATIC DEFORMATIONS

(Fy APPLIED AT GRID LOCATION 83)

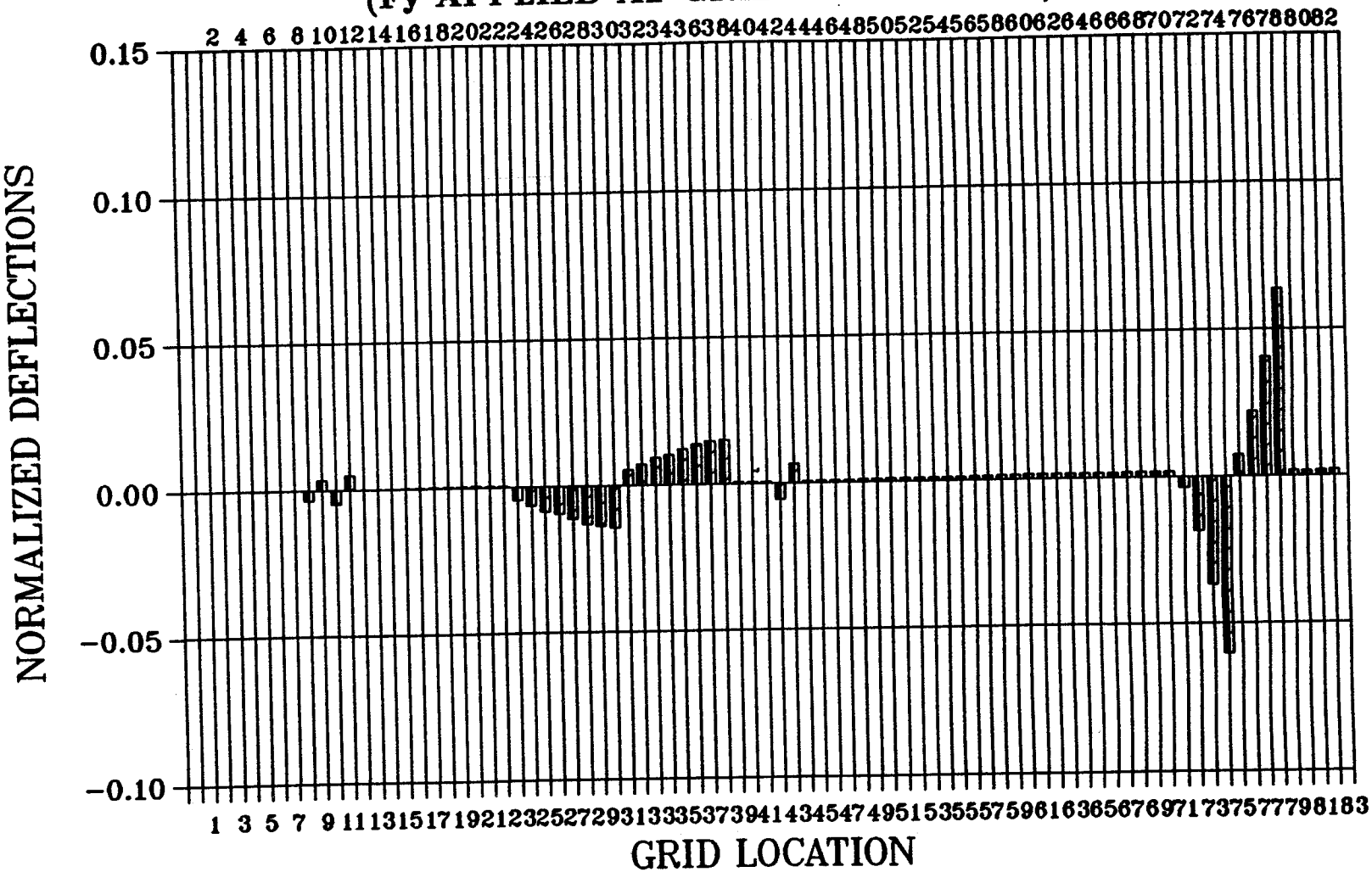

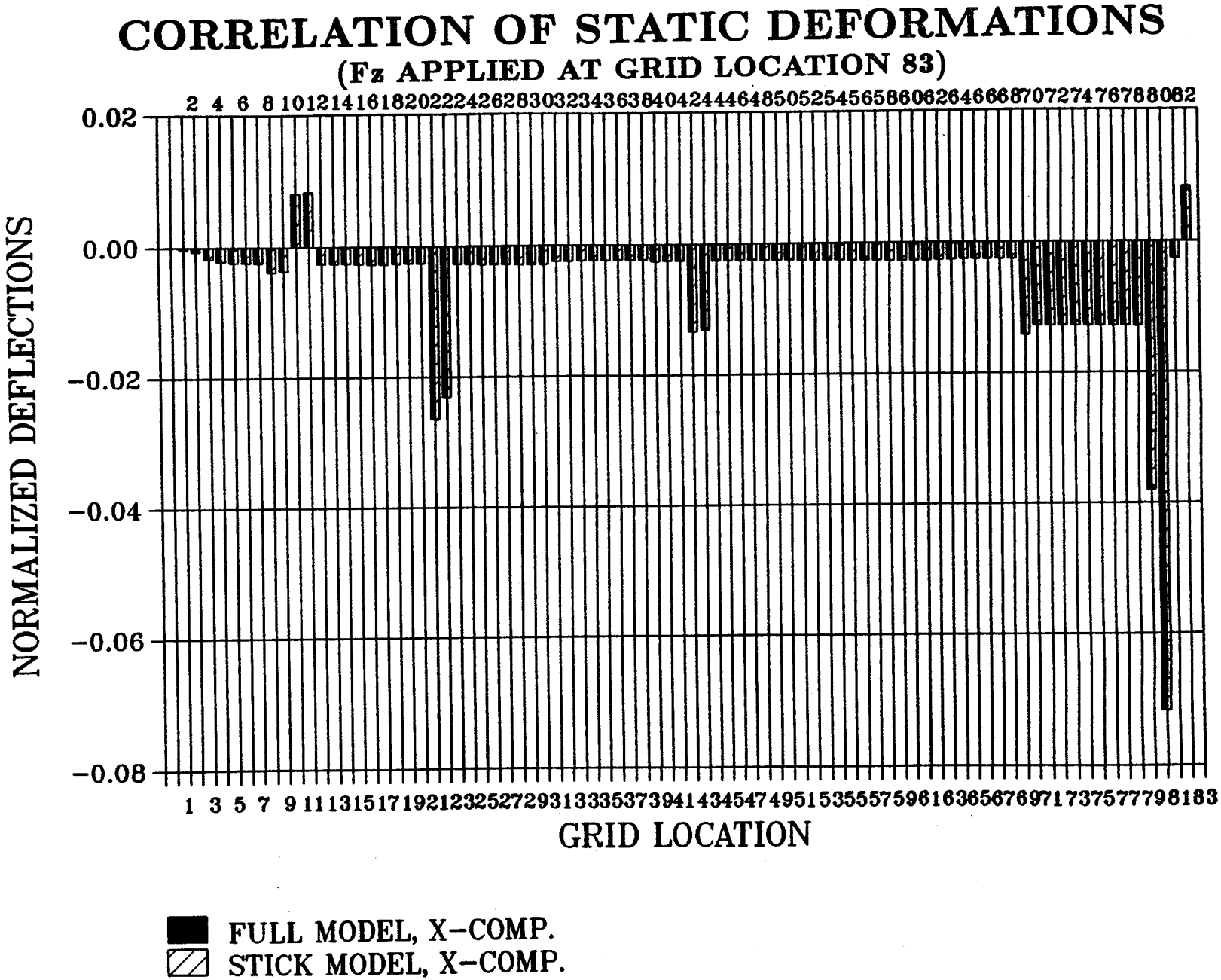
CORRELATION OF STATIC DEFORMATIONS
(Fz APPLIED AT GRID LOCATION 83)
NORMALIZED DEFLECTIONS
0.02
0.00
-0.02
-0.04
-0.06
-0.08
GRID LOCATION
FULL MODEL, X-COMP.
STICK MODEL, X-COMP.

CORRELATION OF STATIC DEFORMATIONS

(Fz APPLIED AT GRID LOCATION 83)

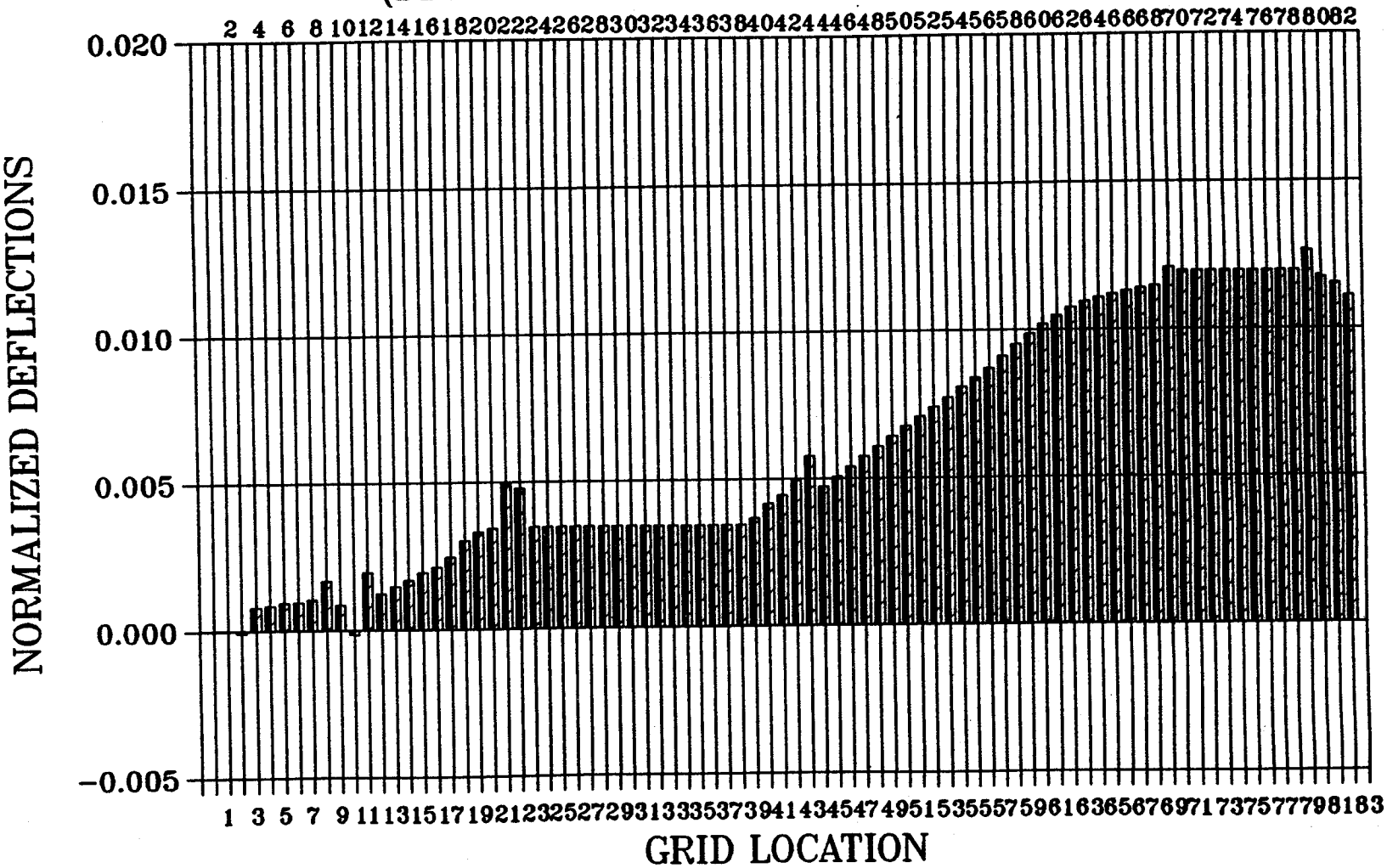

CORRELATION OF STATIC DEFORMATIONS

(Fz APPLIED AT GRID LOCATION 83)

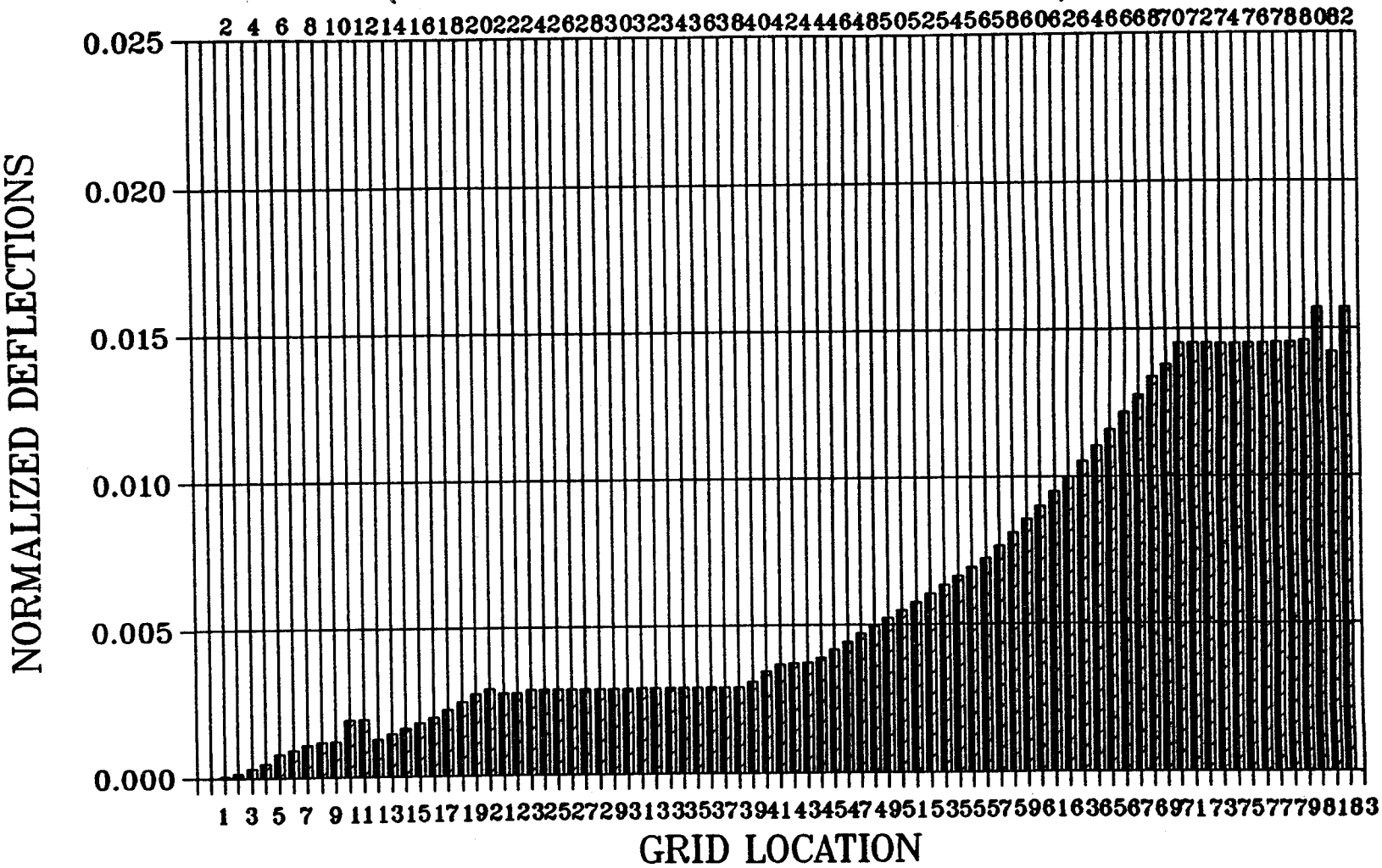

FULL MODEL, Z-COMP.
STICK MODEL, Z-COMP.

CORRELATION OF STATIC DEFORMATIONS

(Mx APPLIED AT GRID LOCATION 83)

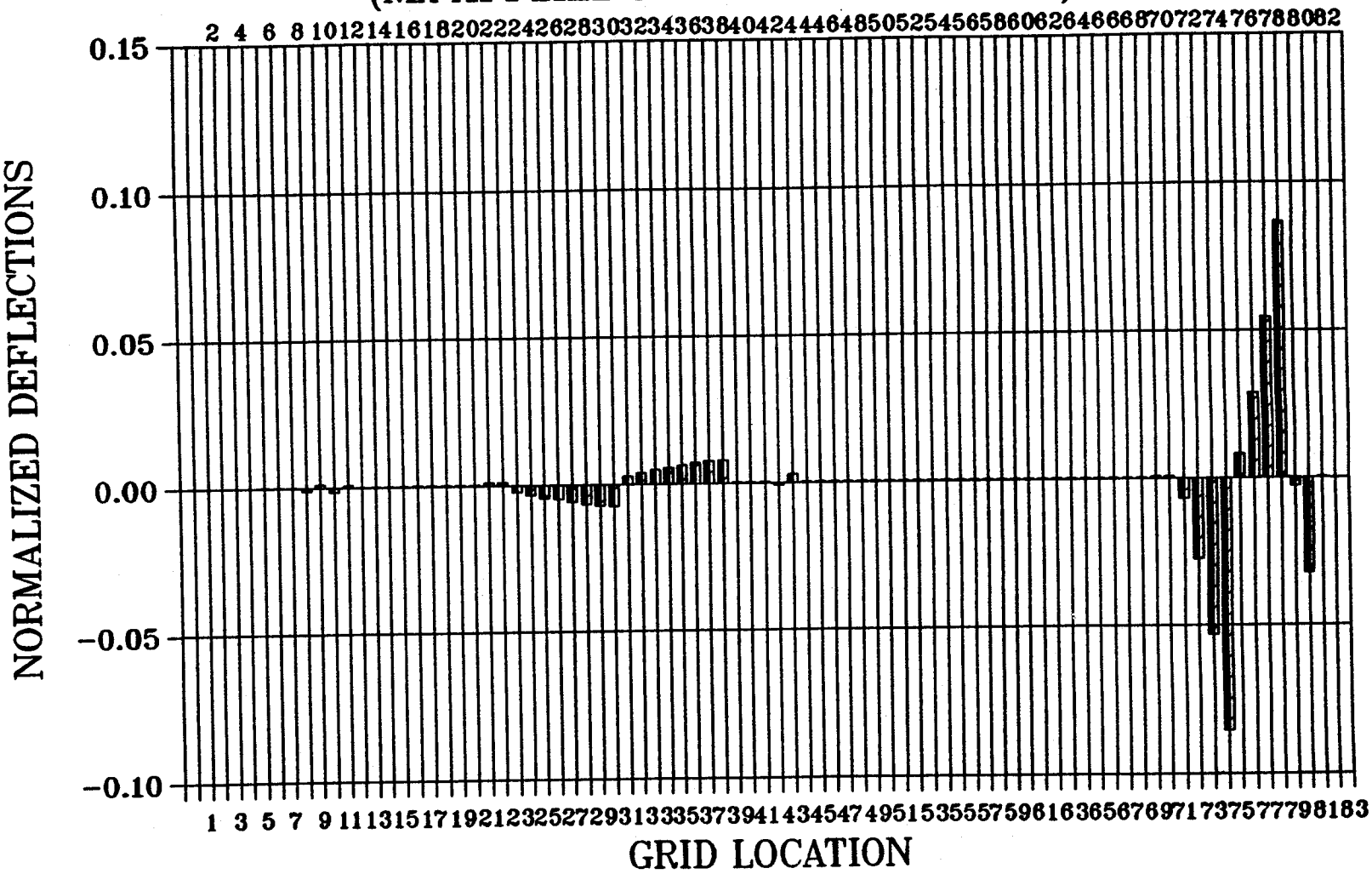

FULL MODEL, X–COMP.
STICK MODEL, X–COMP.

CORRELATION OF STATIC DEFORMATIONS

(Mx APPLIED AT GRID LOCATION 83)

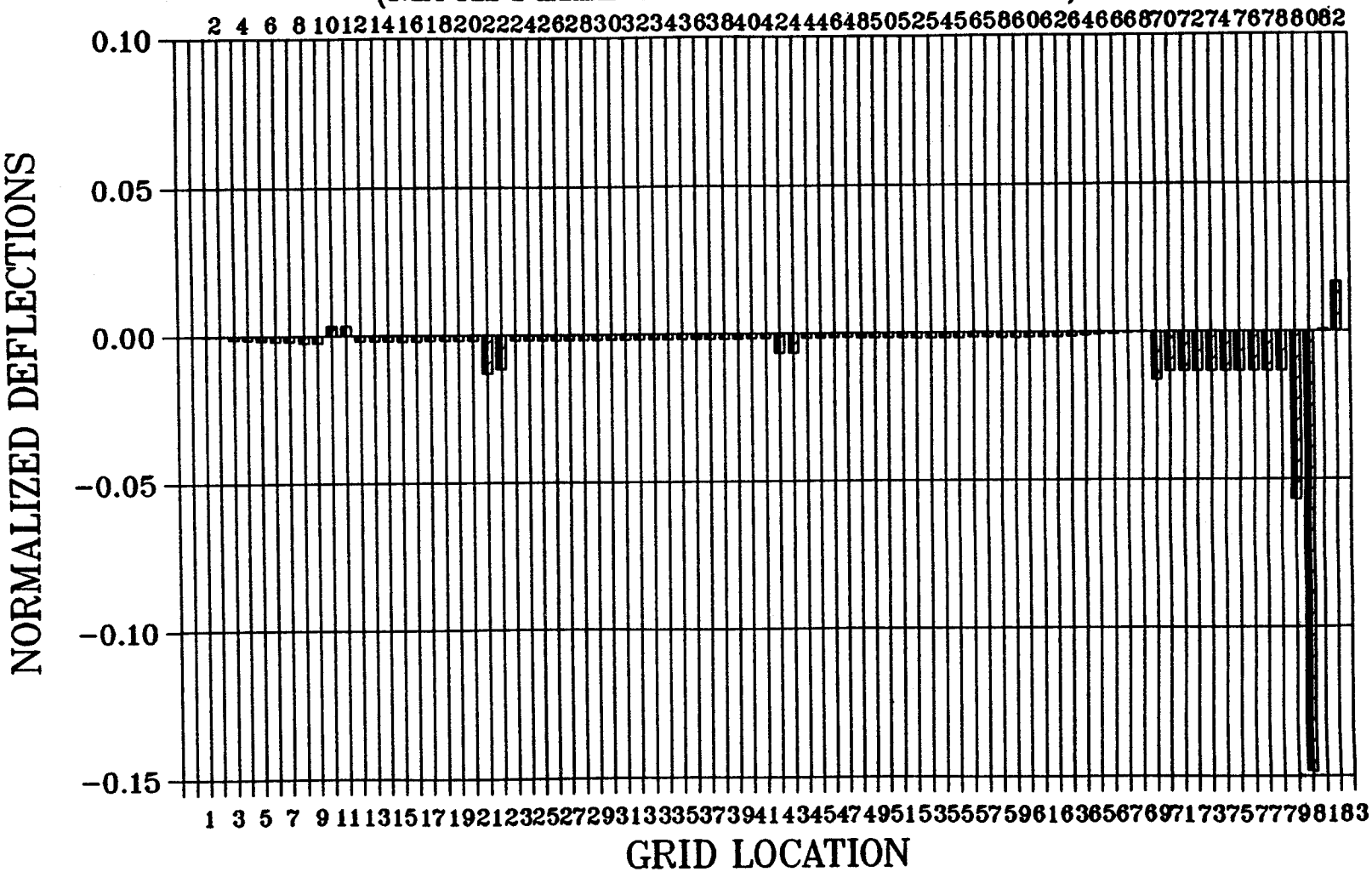

FULL MODEL, Y−COMP.
STICK MODEL, Y−COMP.

CORRELATION OF STATIC DEFORMATIONS

(Mx APPLIED AT GRID LOCATION 83)

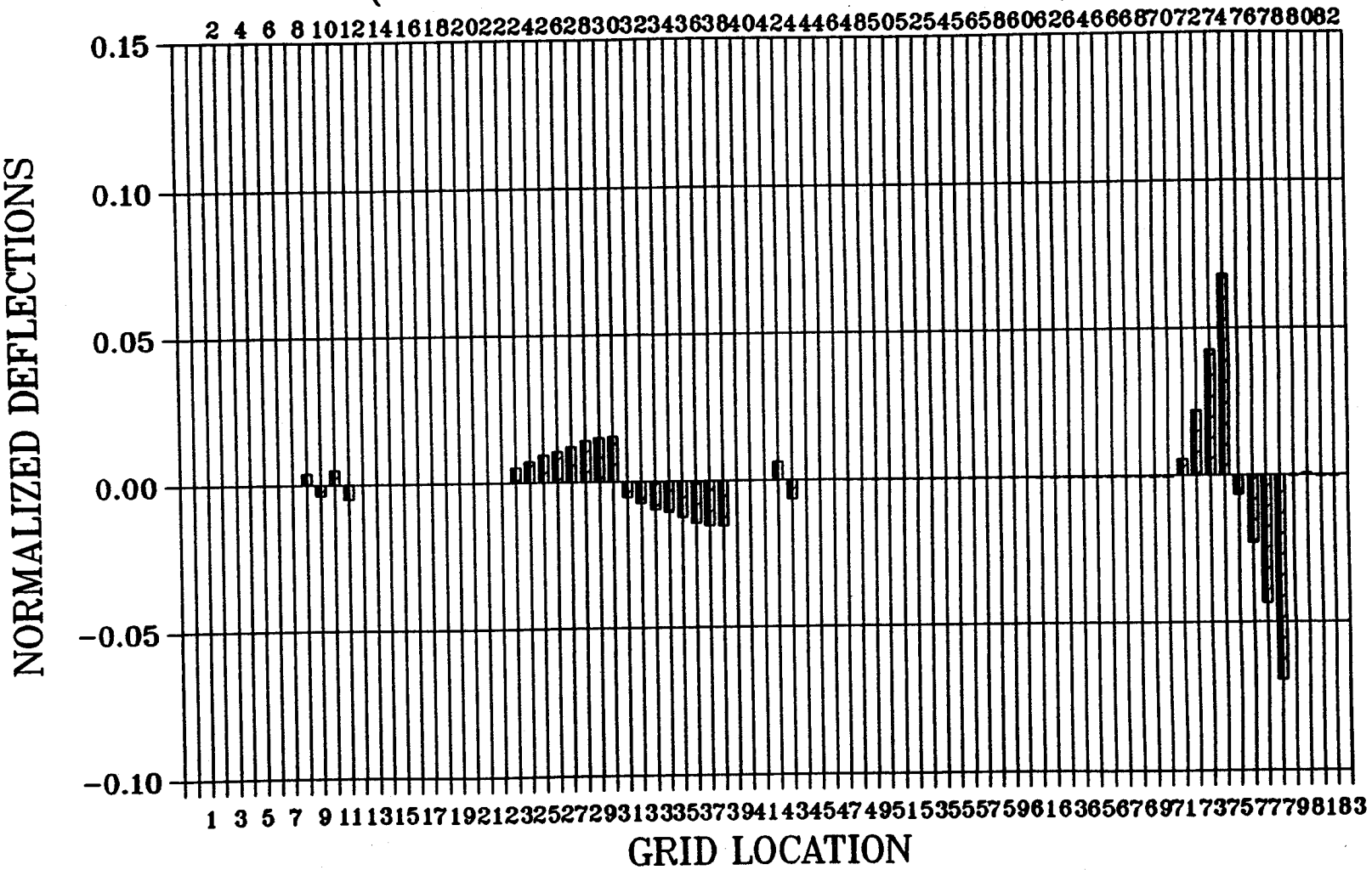

FULL MODEL, Z−COMP.
STICK MODEL, Z−COMP.

CORRELATION OF STATIC DEFORMATIONS

(My APPLIED AT GRID LOCATION 83)

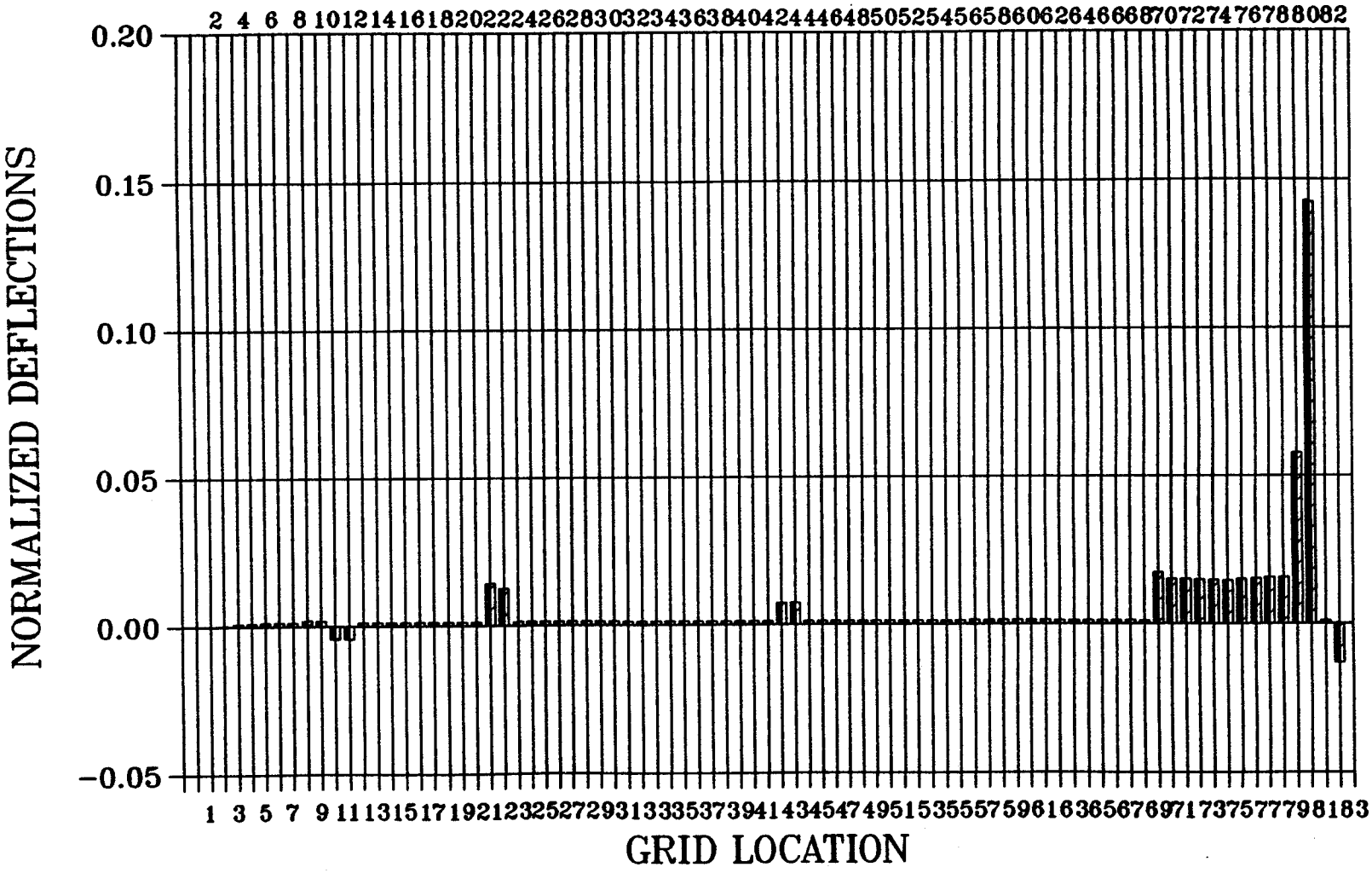

FULL MODEL, X−COMP.

STICK MODEL, X−COMP.

CORRELATION OF STATIC DEFORMATIONS

(My APPLIED AT GRID LOCATION 83)

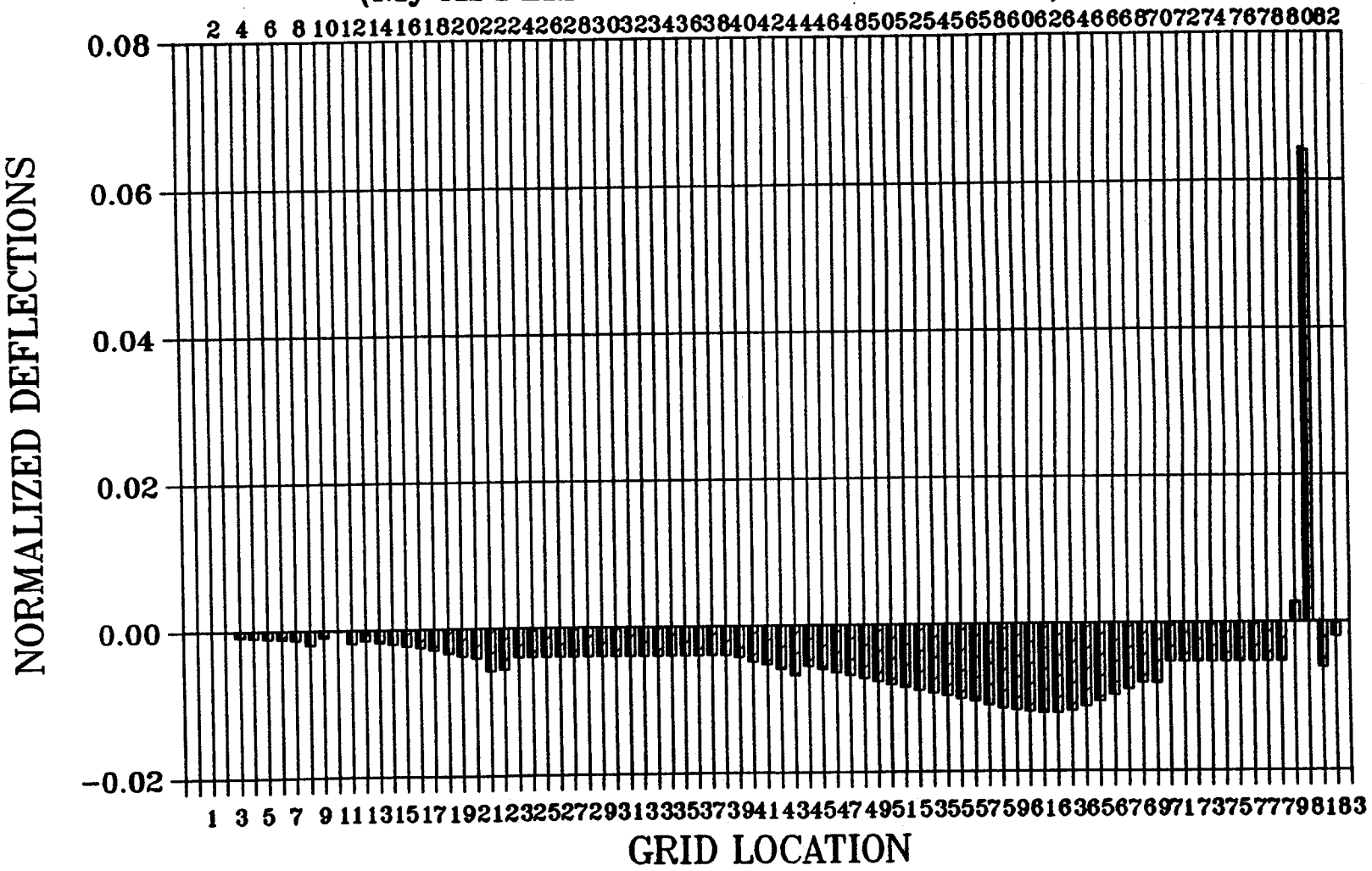

FULL MODEL, Y-COMP.
STICK MODEL, Y-COMP.

CORRELATION OF STATIC DEFORMATIONS

(My APPLIED AT GRID LOCATION 83)

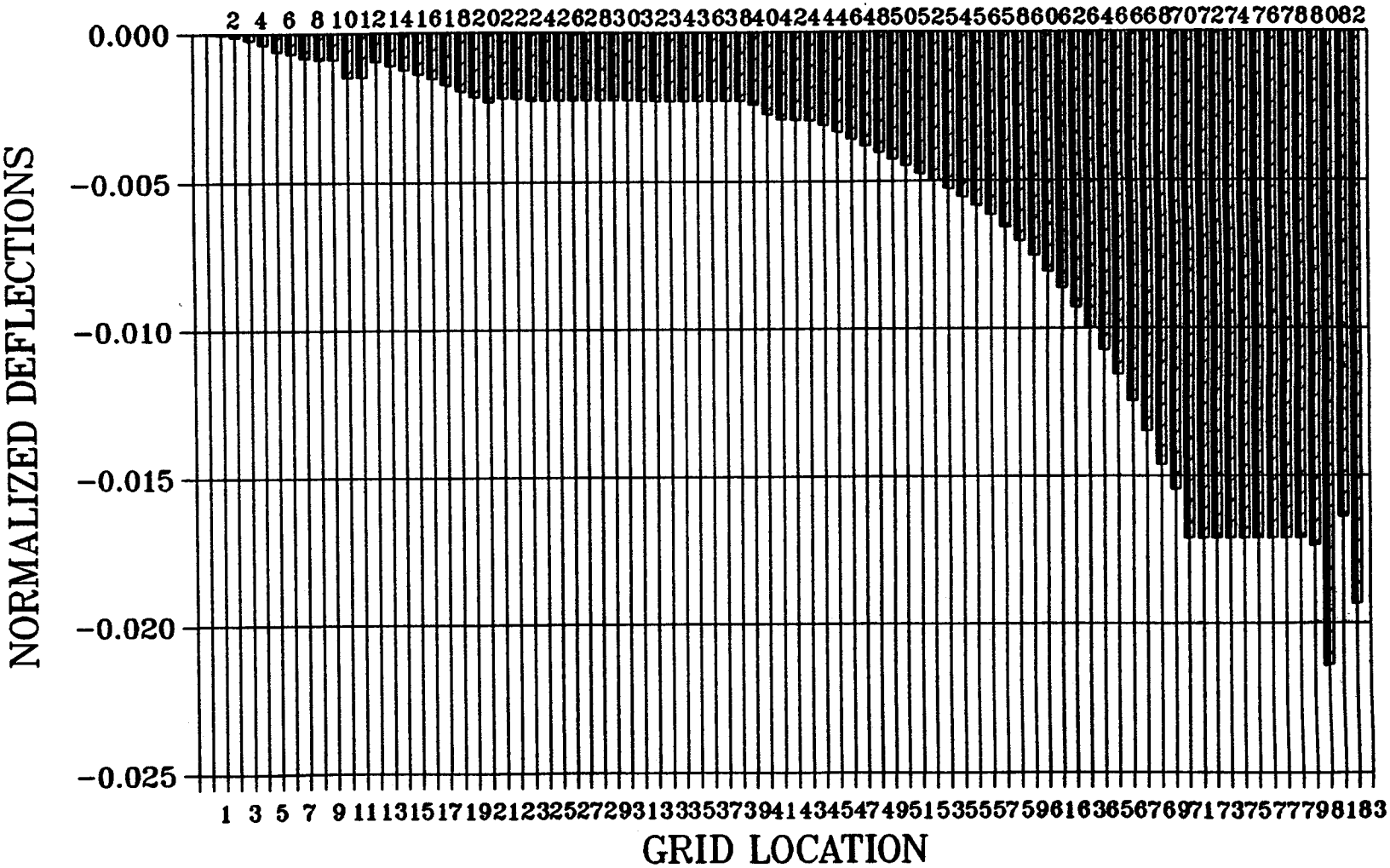

CORRELATION OF STATIC DEFORMATIONS

(Mz APPLIED AT GRID LOCATION 83)

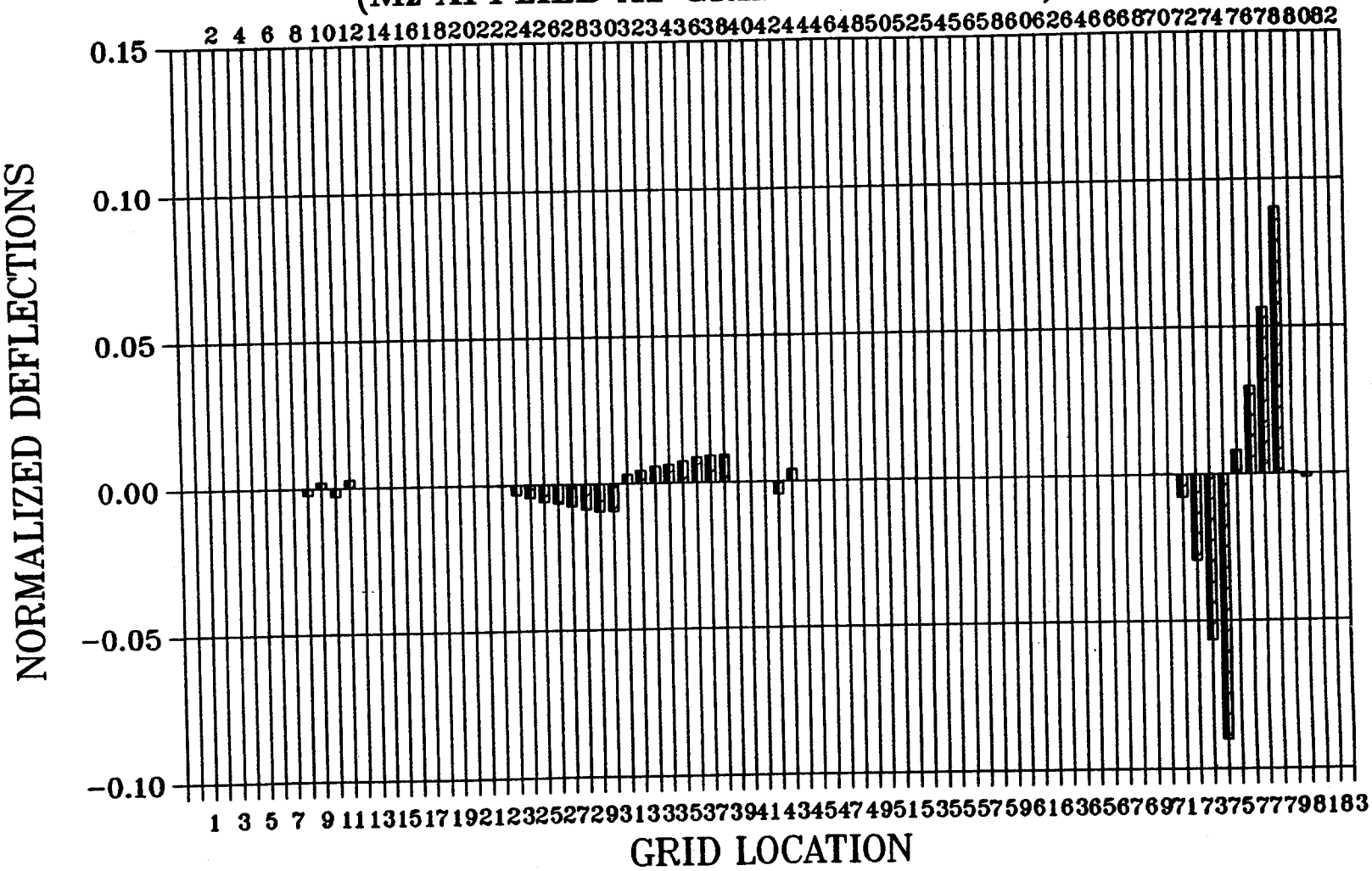

FULL MODEL, X−COMP.

STICK MODEL, X−COMP.

CORRELATION OF STATIC DEFORMATIONS

(Mz APPLIED AT GRID LOCATION 83)

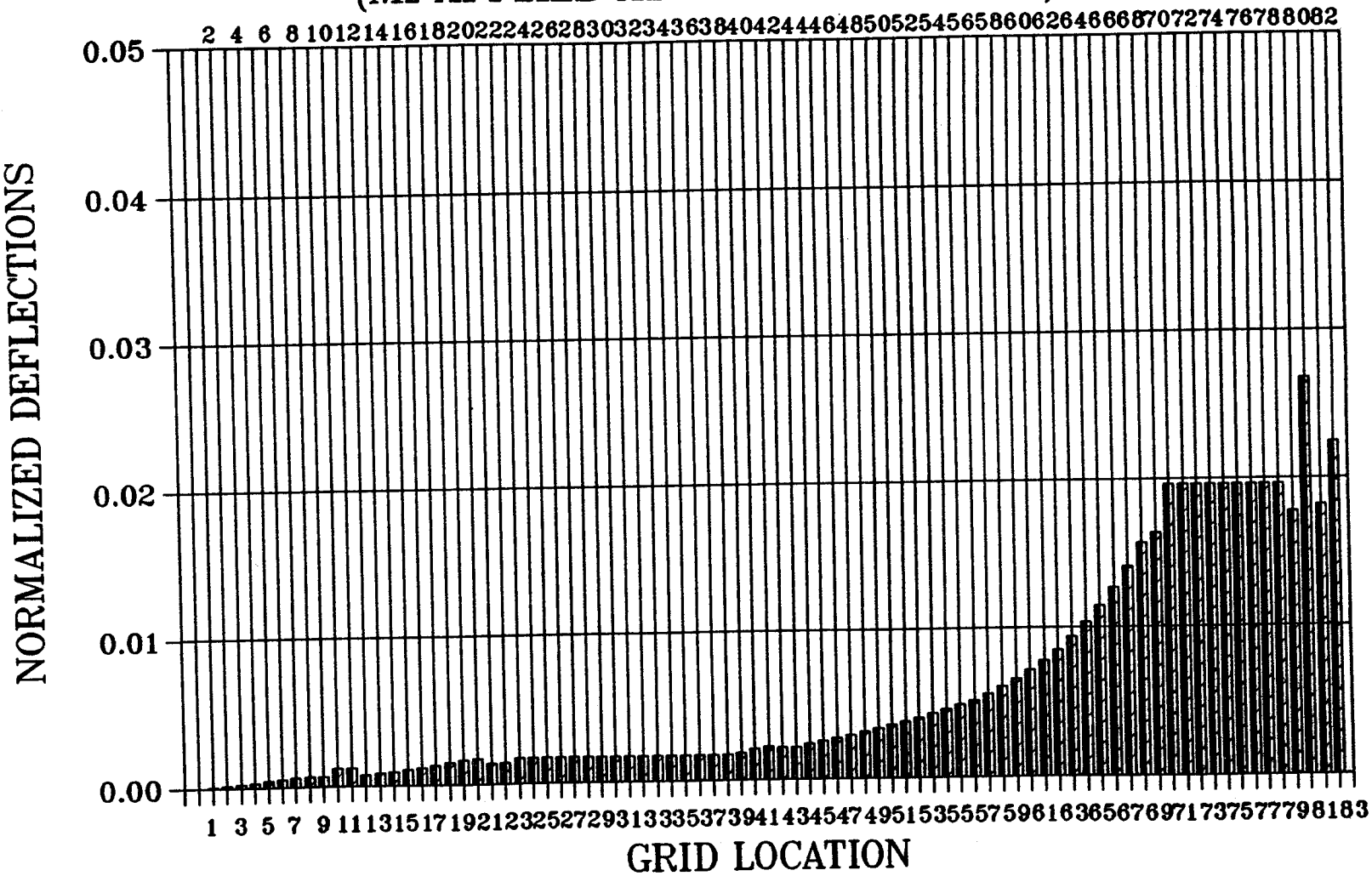

FULL MODEL, Y–COMP.

STICK MODEL, Y–COMP.

CORRELATION OF STATIC DEFORMATIONS

(Mz APPLIED AT GRID LOCATION 83)

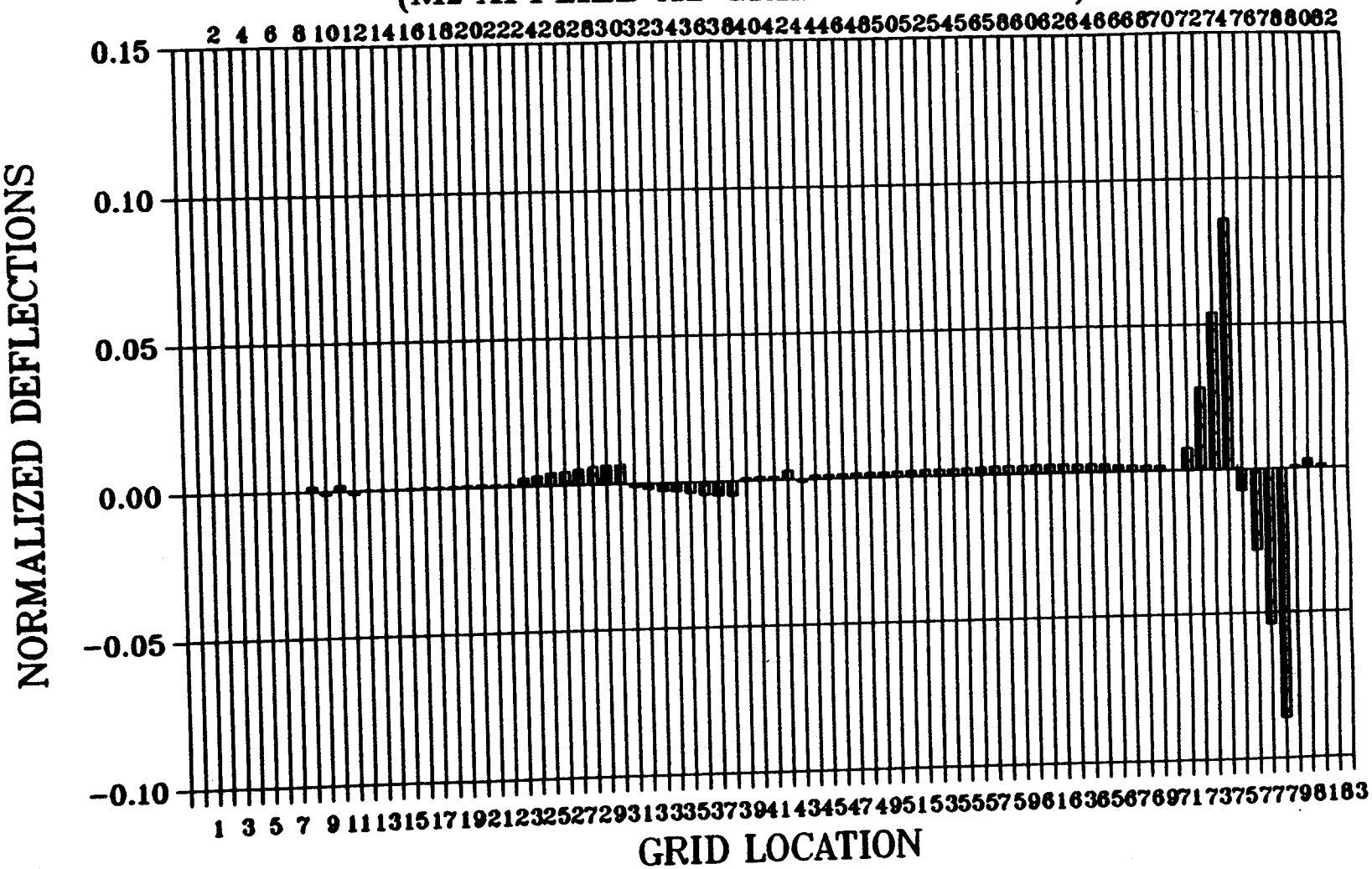

CORRELATION OF MODAL DATA

The next step of the correlation process was to check the accuracy of the modal data which in turn reflects on the accuracy of the reduced mass matrix. For this purpose, an in-house computer program which provided a systematic way of checking the degree of correlation between frequencies, mode shapes or a combination of the two, was used. The criteria used for the correlation process were based on selecting modes which have both closest natural frequencies and best correspondence between the mode shapes. Prior to the calculation of these correlation factors, each model's mode shapes were normalized to mathematically provide a value of one (e.g., for correlation factors) for the best correlation and zero for the worst case. In this equation the resulting Φ_{ij}

$$\Phi_{ij} = \frac{\phi_{ij}}{2\left[\sum_{m=1}^{N} |\phi_{mj}|\right]} \tag{1}$$

represents the jth normalized modal amplitude at the ith location. Subsequent to normalizing the modes, three correlation factors were used together in deciding which two modes correspond best to each other. The first factor, FC_{ij}, uses frequency information between the ith mode of one model against the jth mode of the other model. The parameters T and A refer to the full and reduced model, respectively. The second factor, $CORR_{ij}$, referred to as the shape factor, uses the mode shape information only. Finally, the combined factor, CC_{ij}, which uses both mode shapes and frequencies, is given by the third equation.

$$FC_{ij} = 1.0 - \left[\frac{|TF_i - AF_j|}{TF_i}\right] \tag{2}$$

$$CORR_{ij} = \max\left\{\sum_{m=1}^{N} |T\Phi_{mi} - A\Phi_{mj}|, \sum_{m=1}^{N} |T\Phi_{mi} + A\Phi_{mj}|\right\} - \min\left\{\sum_{m=1}^{N} |T\Phi_{mi} - A\Phi_{mj}|, \sum_{m=1}^{N} |T\Phi_{mi} + A\Phi_{mj}|\right\} - \tag{3}$$

$$CC_{ij} = \sqrt{(CORR_{ij})(FC_{ij}{}^2)} \tag{4}$$

In the above equation, N represents the number of grid points used in the reduced model. Also, it should be mentioned that, based on past experience, it was found that an exponent value of 2, used in the last equation, usually results in a better indication of correlation between two modes.

CORRELATION OF MODAL DATA

- FREQUENCY CORRELATION:

$$FC_{ij} = 1.0 - \left[\frac{|TF_i - AF_j|}{TF_i}\right]$$

- MODE SHAPE CORRELATION:

$$CORR_{ij} = \max\left\{\sum_{m=1}^{N} |T\Phi_{mi} - A\Phi_{mj}|, \sum_{m=1}^{N} |T\Phi_{mi} + A\Phi_{mj}|\right\} - \min\left\{\sum_{m=1}^{N} |T\Phi_{mi} - A\Phi_{mj}|, \sum_{m=1}^{N} |T\Phi_{mi} + A\Phi_{mj}|\right\}$$

- COMBINED MODE AND FREQUENCY CORRELATION:

$$CC_{ij} = \sqrt{(CORR_{ij})(FC_{ij}{}^2)}$$

CORRELATION OF MODAL DATA (Continued)

After applying the above correlation criteria to the modal data obtained from the full and reduced (i.e., stick) models, a set of correlation factors (CC_{ij}) were obtained which indicated the degree of correlation between each pair of modes. After careful examination of these factors and their corresponding modes, the modes indicated in the following table were selected. As can be seen from the table, a high degree of correlation exists between these selected modes. As was expected, most of the local modes of the full model were no longer present in the reduced model. This was because local areas were not included in the reduced model grid locations. For example, the first four modes of the full model represent the pilot and copilot seat modes whose definitions are not included in the reduced model. Thus, these modes were not seen in the reduced model. In addition, the mode shapes were visually examined to confirm that most of the reduced model mode shapes were global airframe modes. For qualitative comparison of the degree of correlation between each pair of modes, they were superimposed on each other which are shown in the figures following the table. In these figures the reduced model is referred to as a "stick" model. Similar to the procedure used in the static case, a set of bar charts are presented which provide a quantitative assessment of the degree of correlation between the corresponding modes. In these bar charts, the normalized mode shape of the full model RBE2 rigid elements (i.e., the independent degree-of-freedom) located near the center of each frame is plotted against its reduced (stick) model counterpart.

CORRELATION OF MODAL DATA
STICK VS. FULL MODEL

MODE	FREQUENCY (HZ) FULL	STICK	MODE SHAPE CORRELATION*
TAILBOOM TORSION	5.45	5.62	0.92
1ST VERT. BENDING	6.00	6.15	0.93
1ST LATERAL BENDING	10.70	9.76	0.84
SYM. ENGINE YAW AND PITCH	11.44	11.67	0.90
VERT. TAIL LONG. BENDING	11.97	12.31	0.91
MAST LONG. BENDING	13.41	14.33	0.87
ANTISYM. ENGINE YAW	14.16	16.43	0.70
STABILATOR YAW	20.63	19.60	0.81

* 1.00 = PERFECT CORRELATION
  0.00 = NO CORRELATION

CORRELATION OF MODAL DATA

STICK VS. FULL MODEL

TAILBOOM TORSION MODE

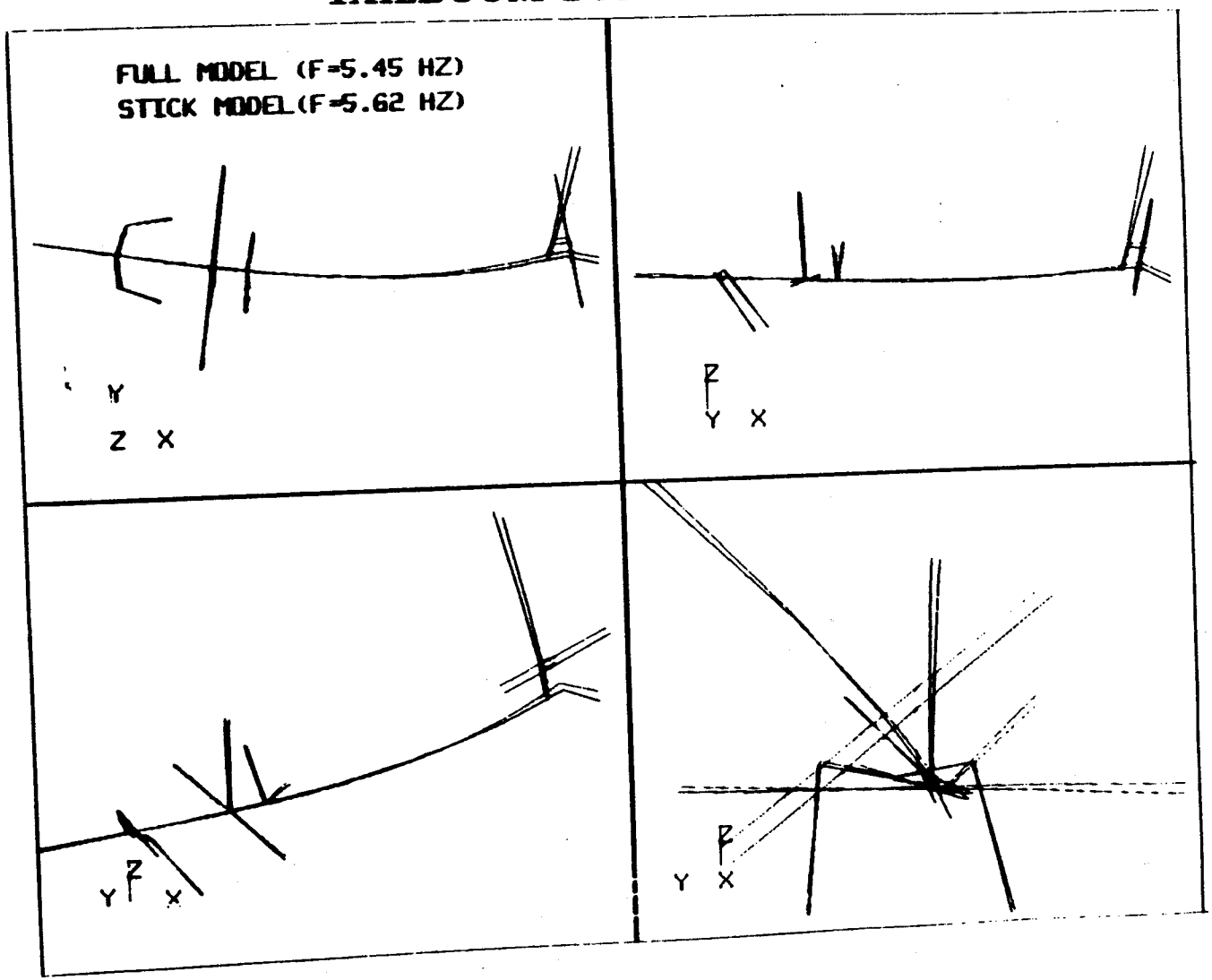

CORRELATION OF MODAL DATA
STICK VS. FULL MODEL
FIRST VERTICAL BENDING MODE

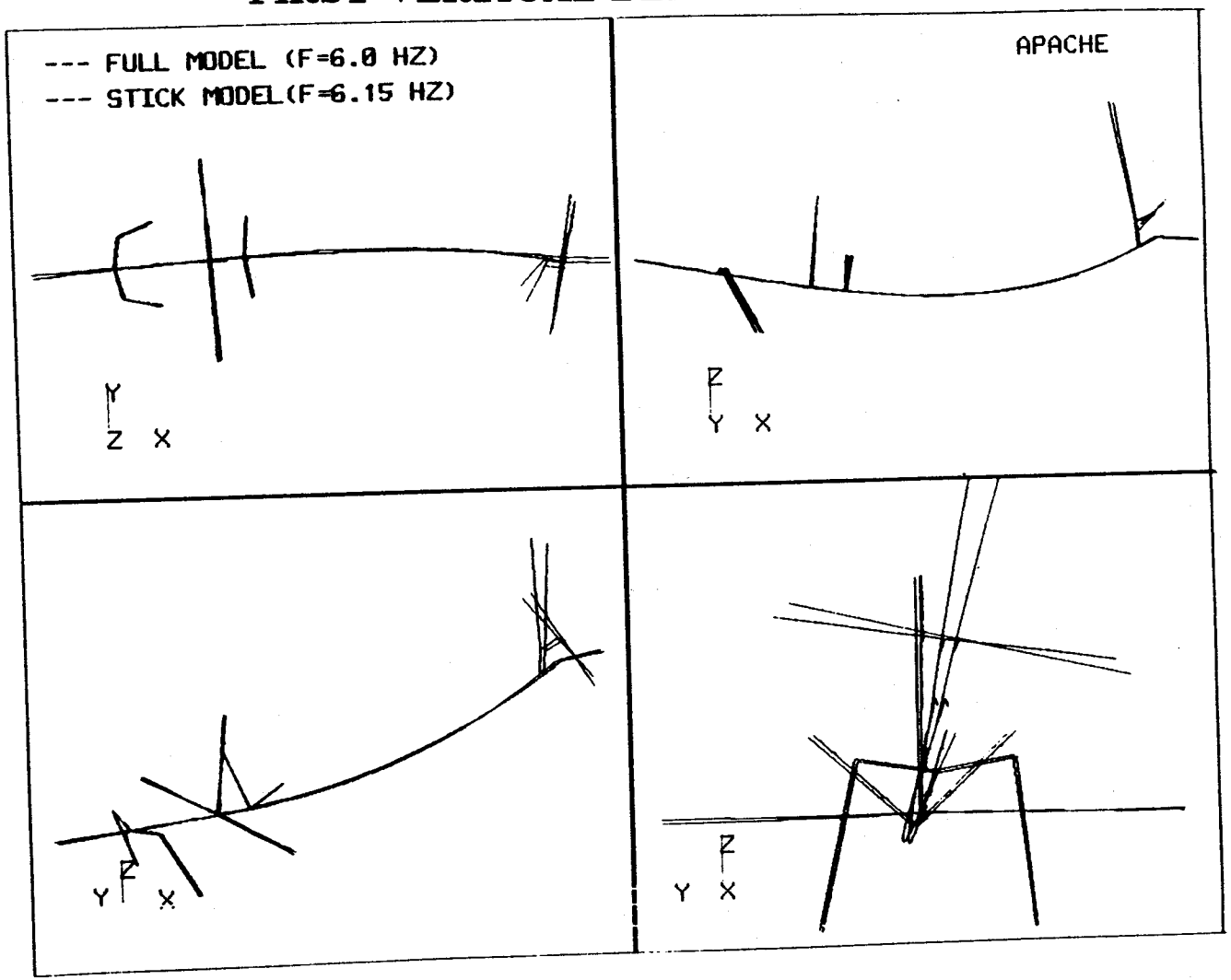

CORRELATION OF MODAL DATA

STICK VS. FULL MODEL

FIRST LATERAL BENDING MODE

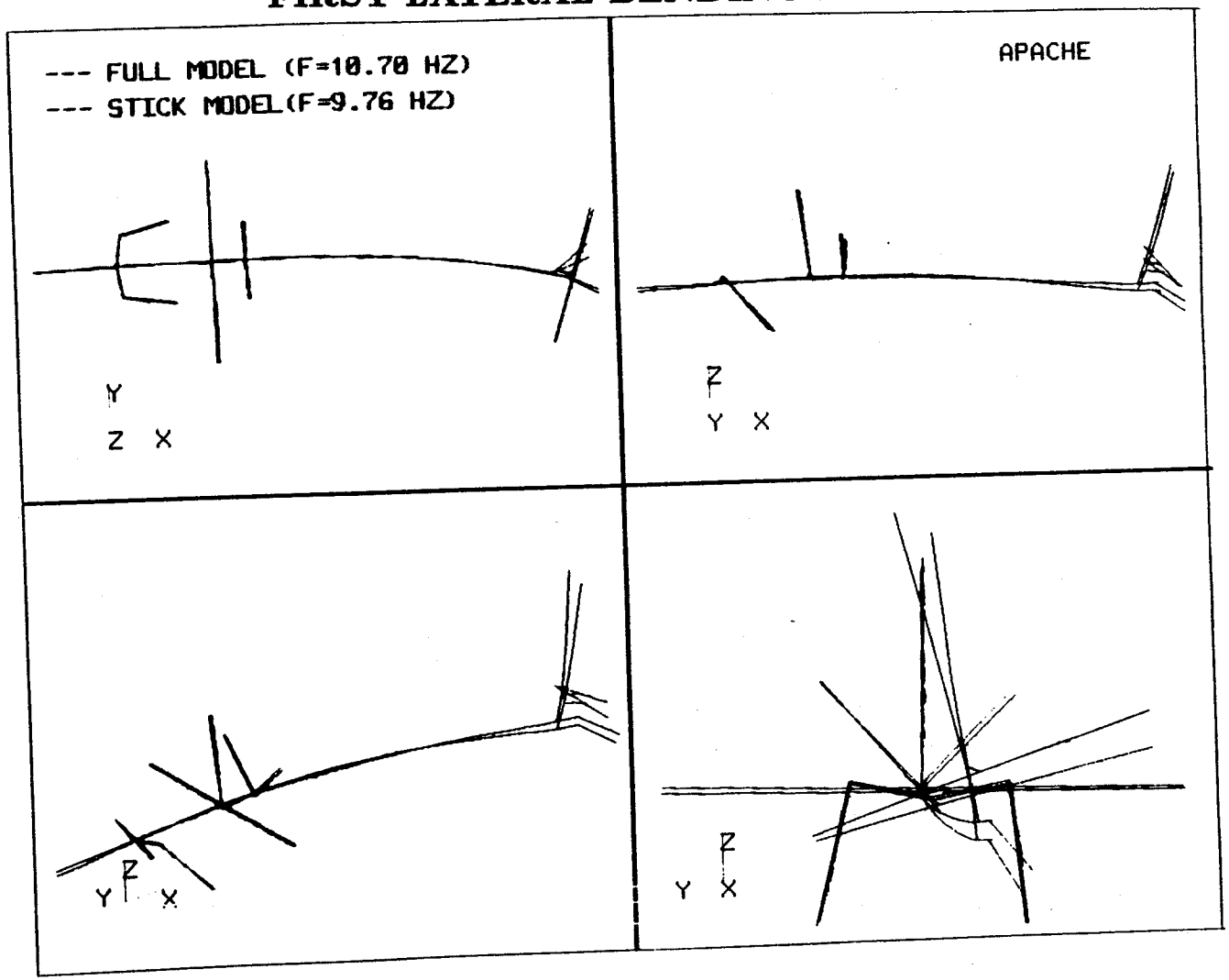

CORRELATION OF MODAL DATA

STICK VS. FULL MODEL

SYMMETRIC ENGINE YAW AND PITCH MODE

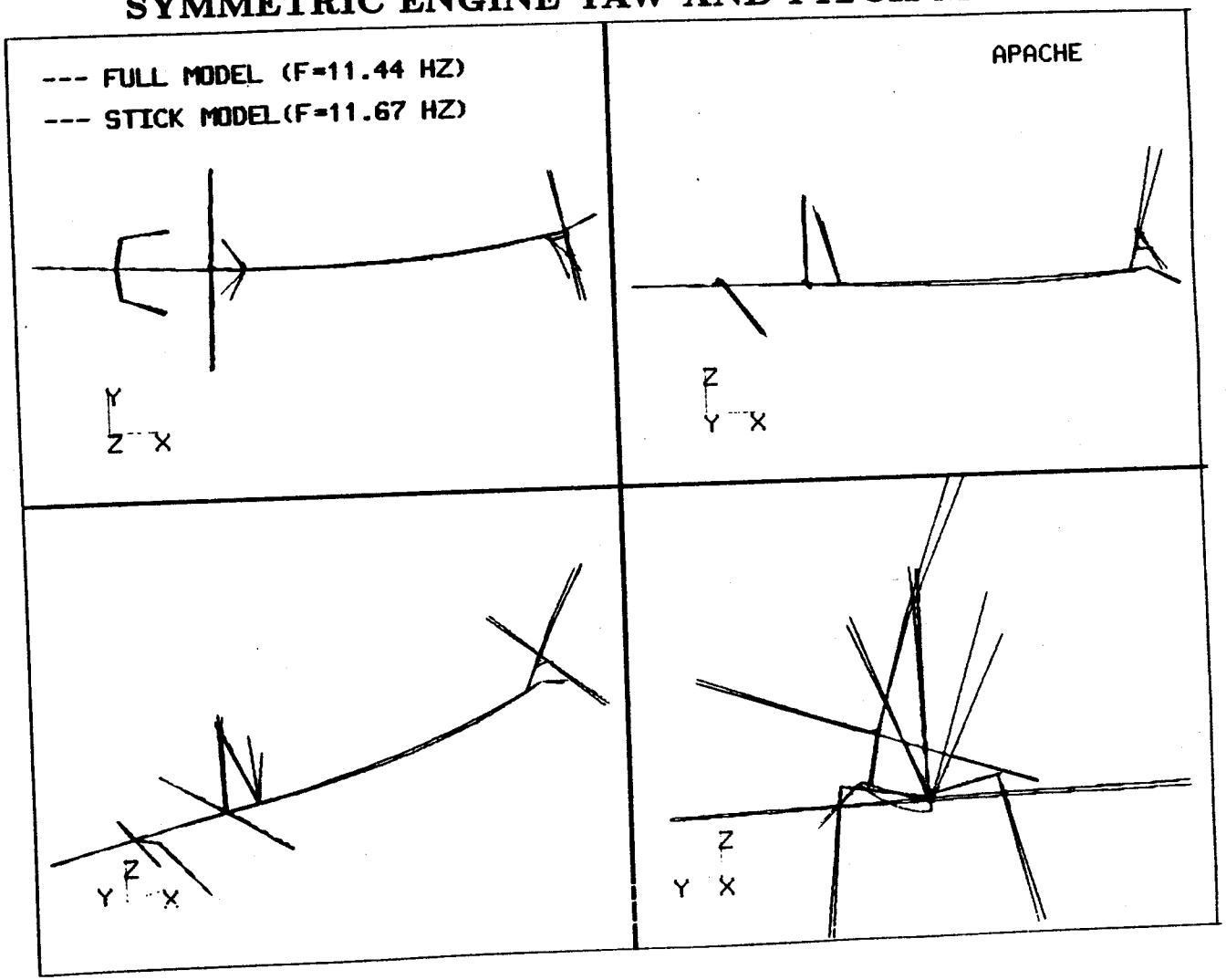

CORRELATION OF MODAL DATA

STICK VS. FULL MODEL

VERTICAL TAIL LONGITUDINAL BENDING MODE

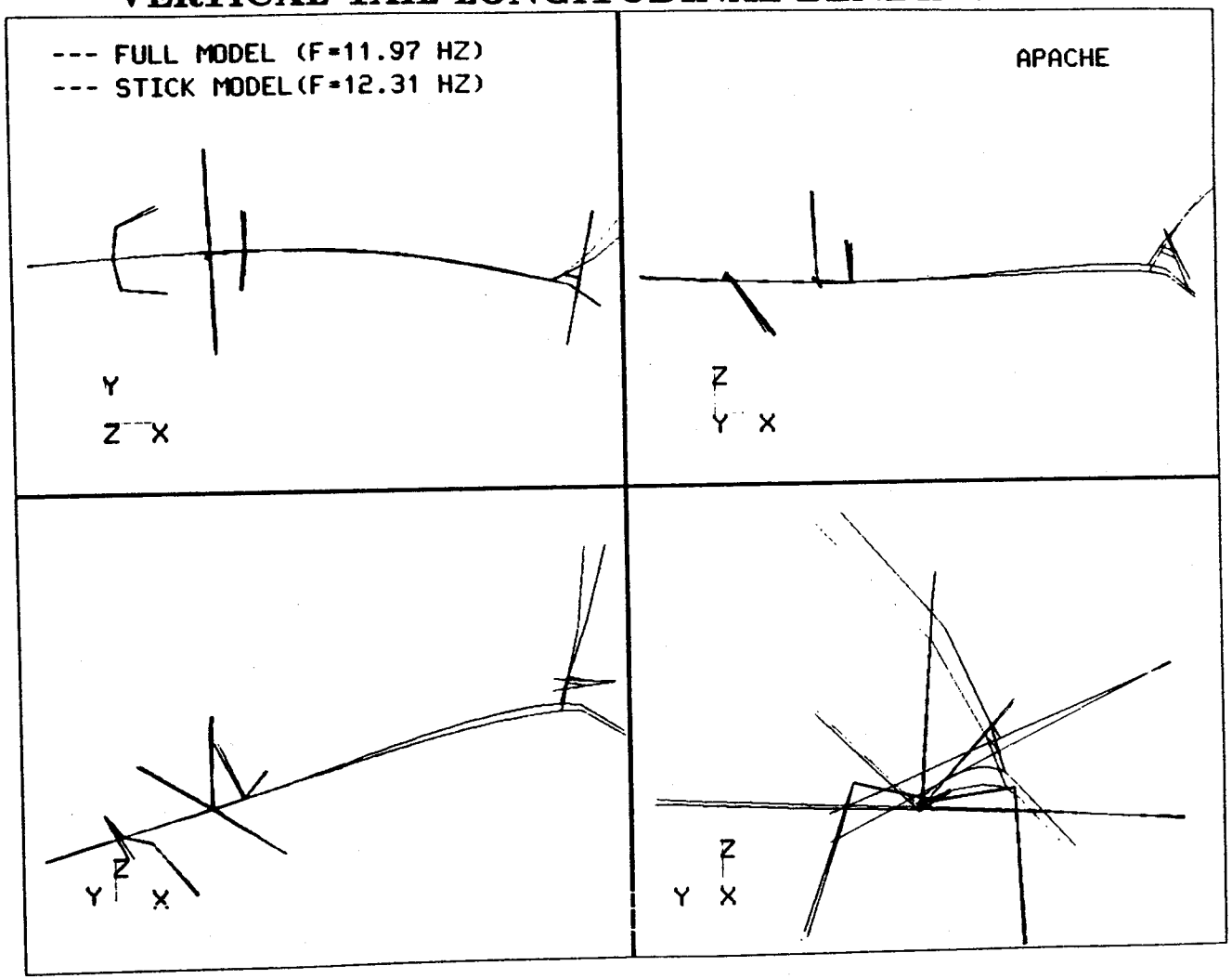

CORRELATION OF MODAL DATA

STICK VS. FULL MODEL

MAST LONGITUDINAL BENDING MODE

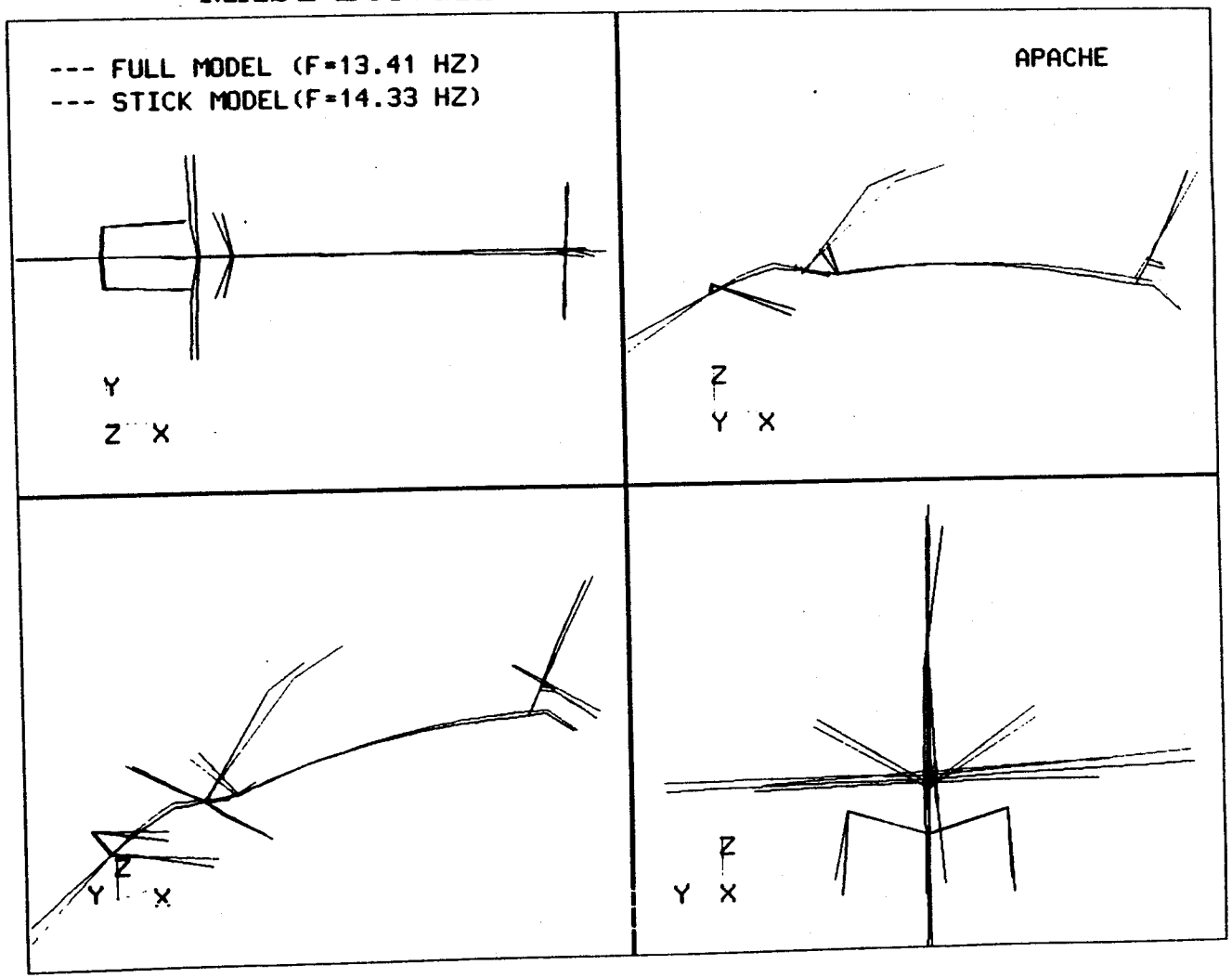

CORRELATION OF MODAL DATA

STICK VS. FULL MODEL

ANTISYMMETRIC ENGINE YAW MODE

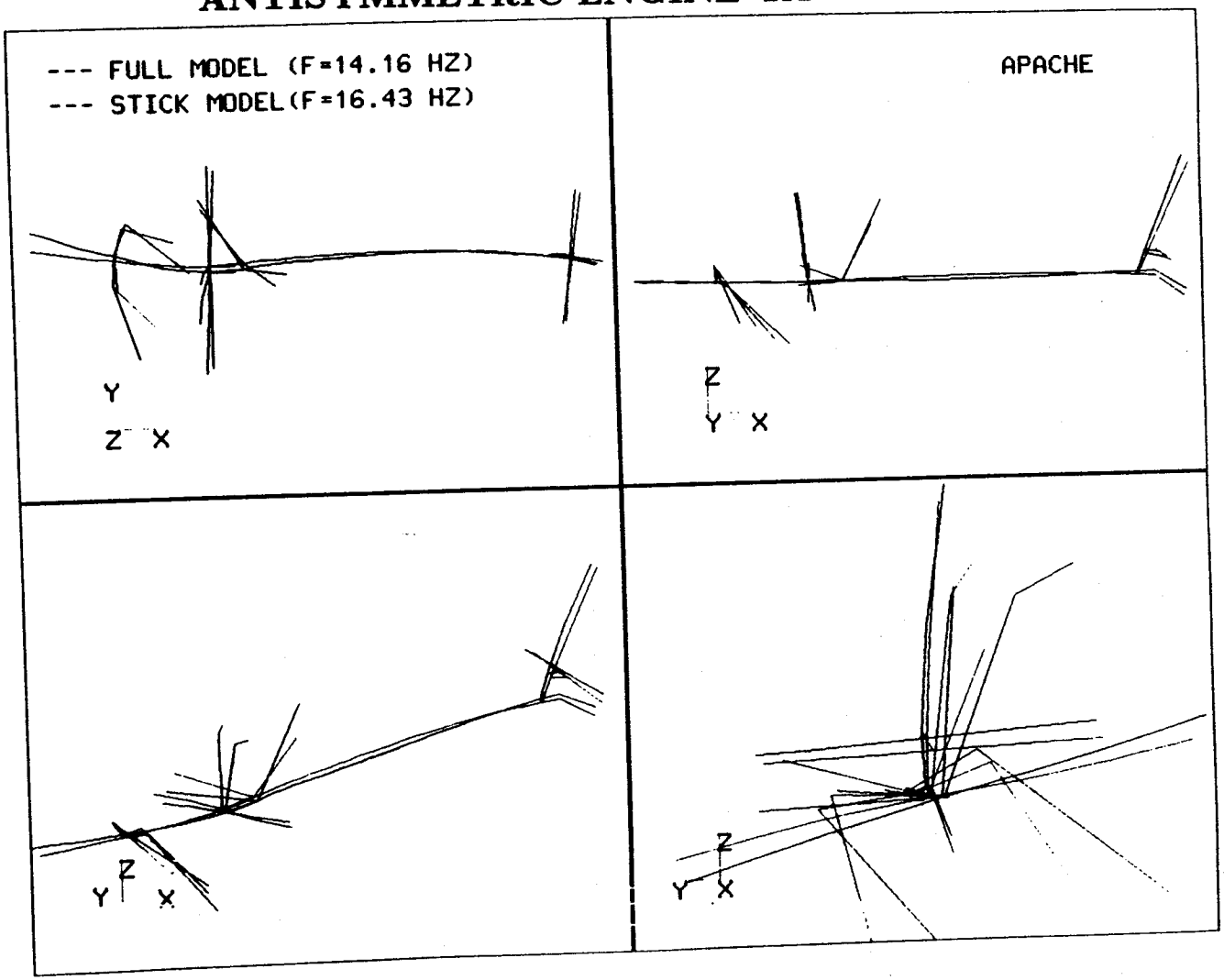

CORRELATION OF MODAL DATA

STICK VS. FULL MODEL

STABILATOR YAW MODE

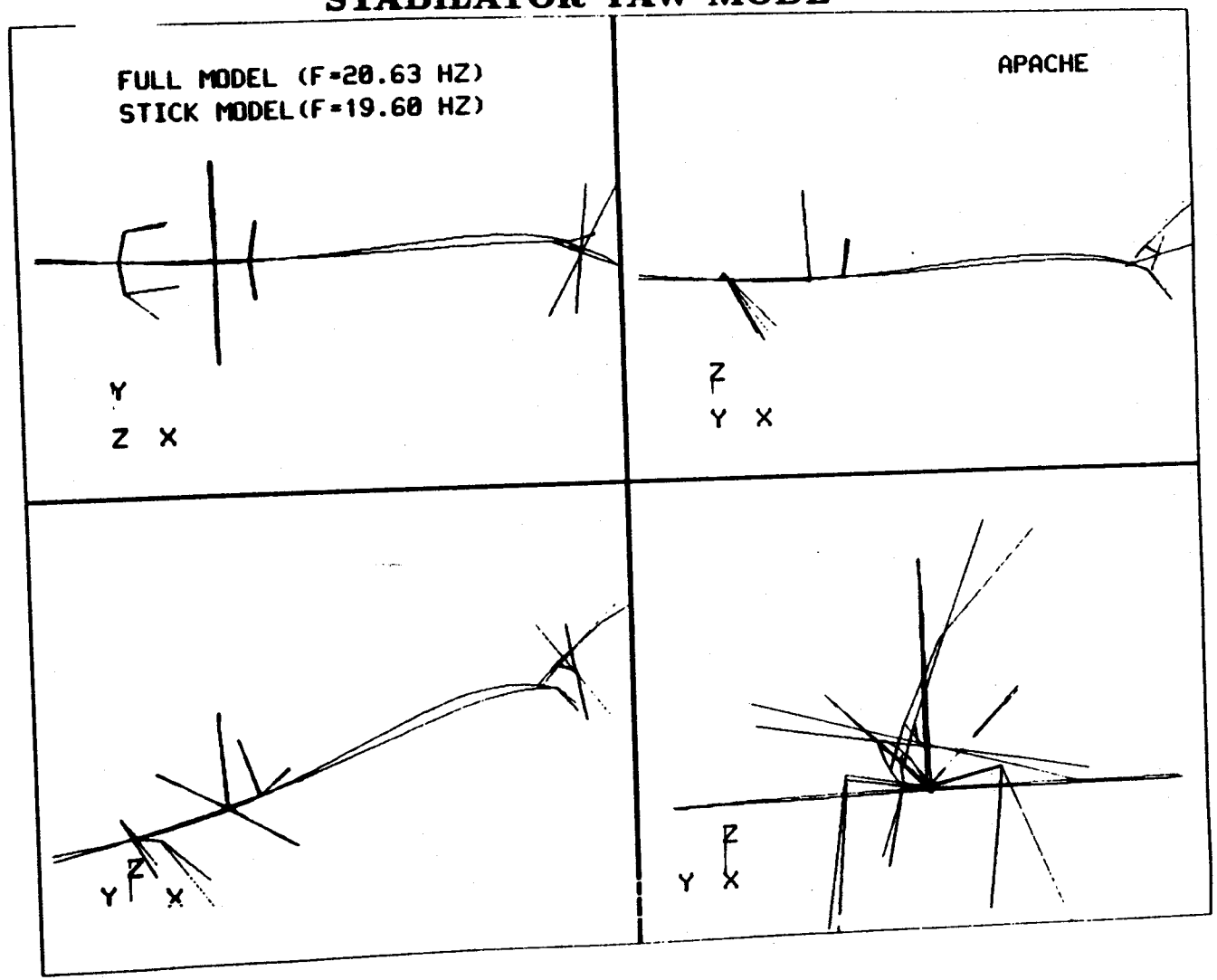

CORRELATION OF MODAL DATA

STICK VS. FULL, CORR=0.92

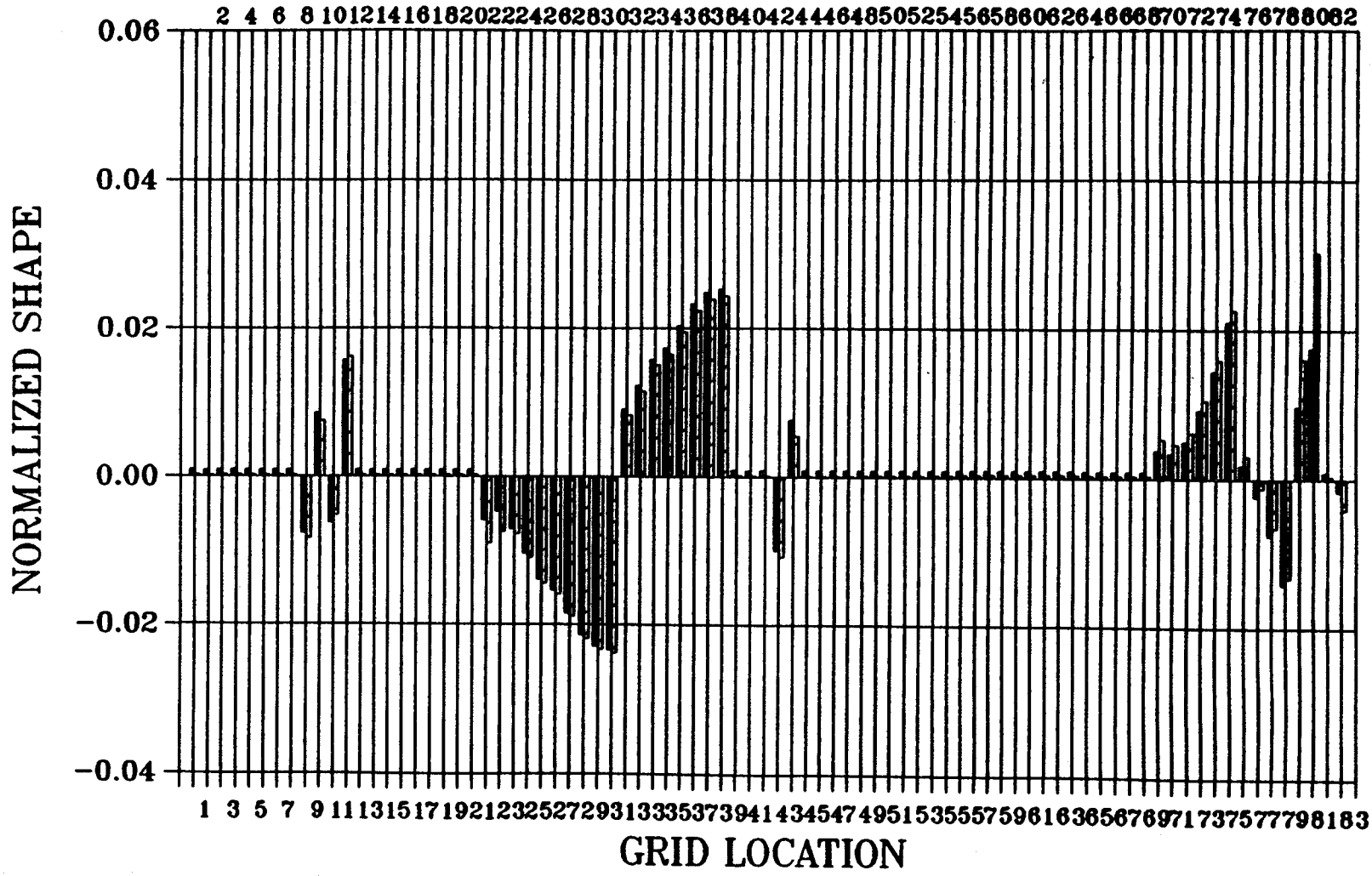

FULL MODEL, X-COMP. , NO. 13, 5.45 HZ

STICK MODEL, X-COMP. , NO. 7, 5.62 HZ

CORRELATION OF MODAL DATA

STICK VS. FULL, CORR=0.92

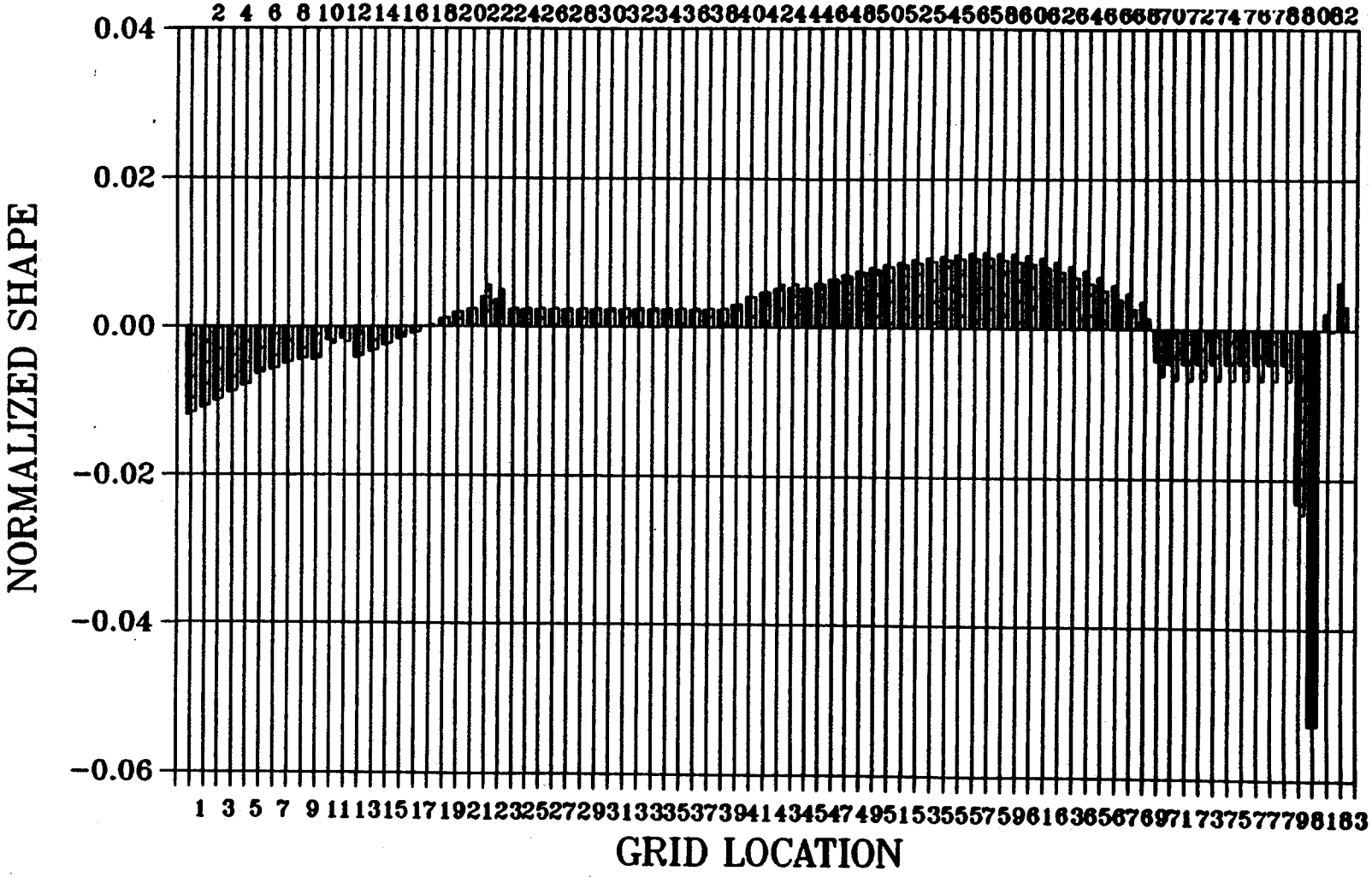

FULL MODEL, Y-COMP. , NO. 13, 5.45 HZ

STICK MODEL, Y-COMP. , NO. 7, 5.62 HZ

CORRELATION OF MODAL DATA

STICK VS. FULL, CORR=0.92

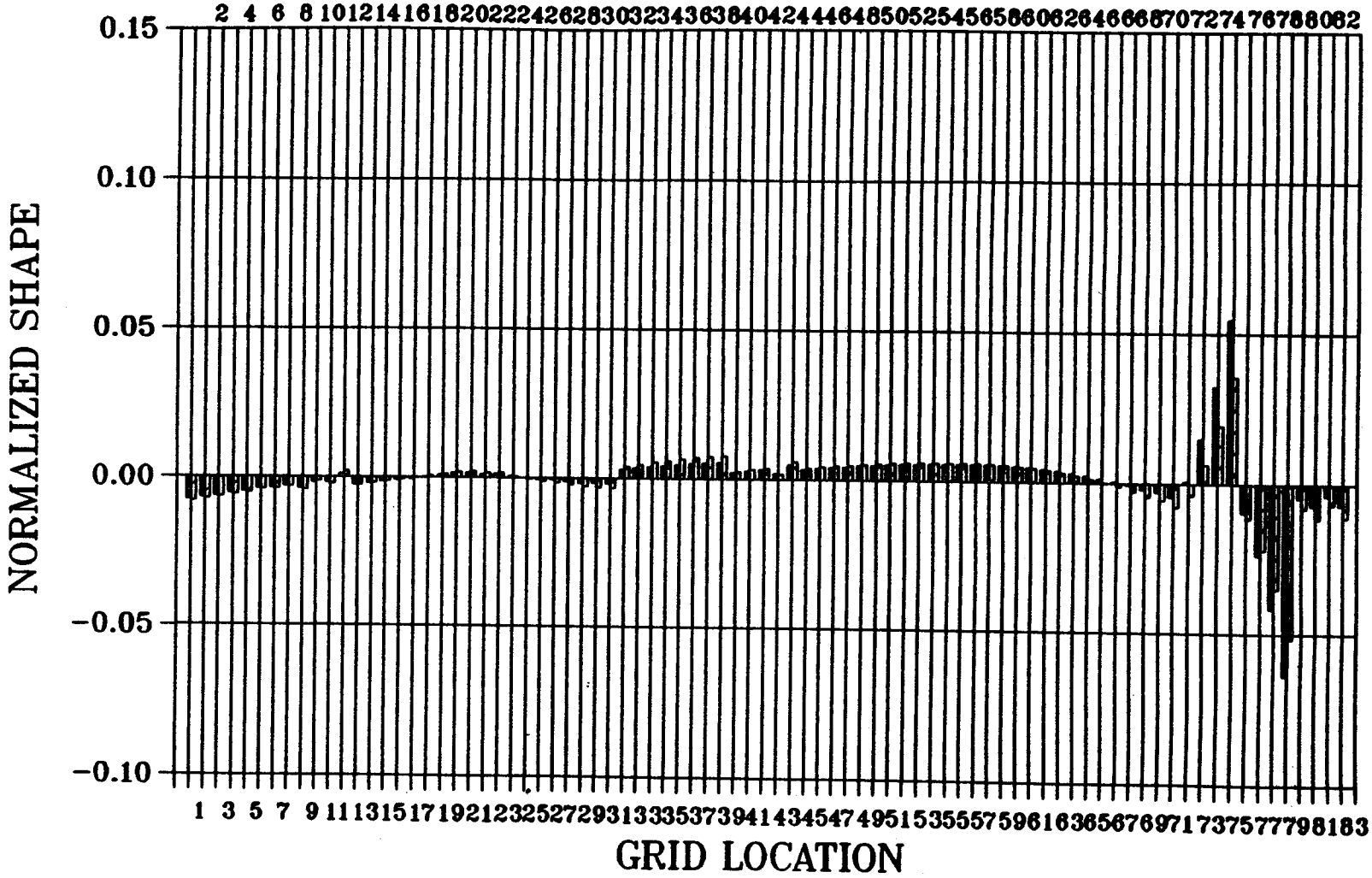

FULL MODEL, Z-COMP. , NO. 13, 5.45 HZ

STICK MODEL, Z-COMP. , NO. 7, 5.62 HZ

CORRELATION OF MODAL DATA

STICK VS. FULL, CORR=0.93

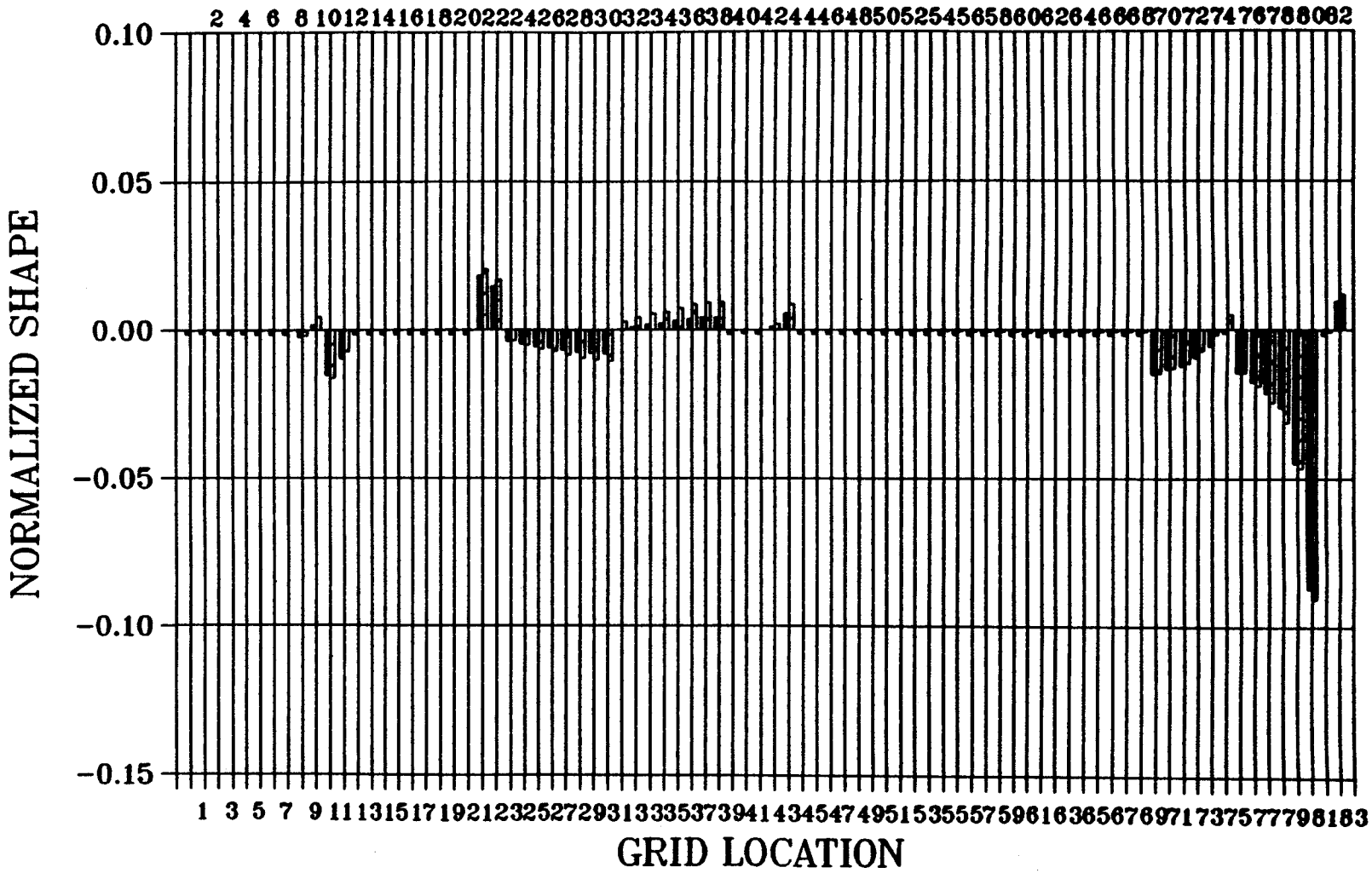

FULL MODEL, X-COMP. , NO. 14, 6.00 HZ

STICK MODEL, X-COMP. , NO. 8, 6.15 HZ

CORRELATION OF MODAL DATA

STICK VS. FULL, CORR=0.93

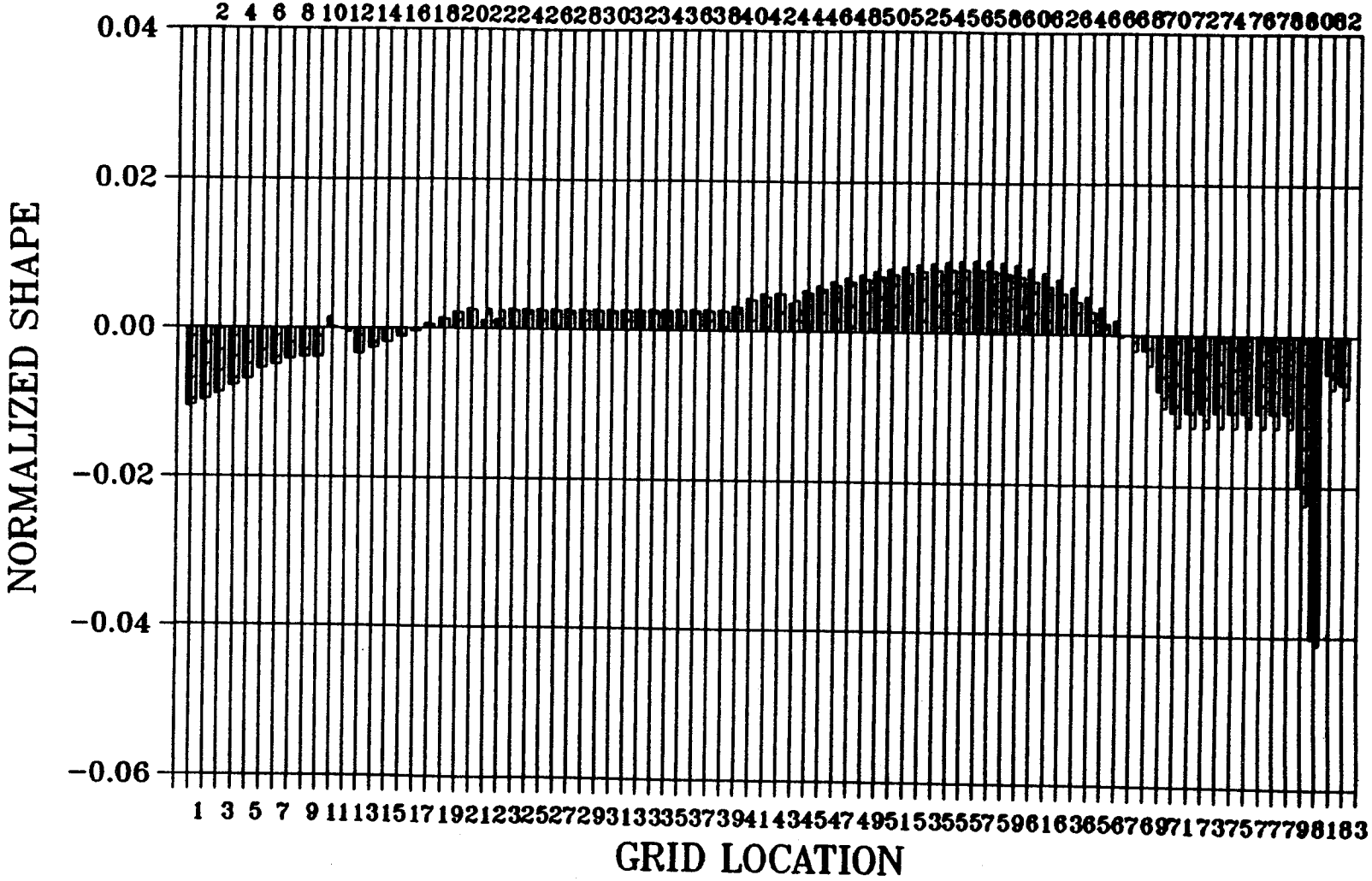

FULL MODEL, Y-COMP. , NO. 14, 6.00 HZ

STICK MODEL, Y-COMP. , NO. 8, 6.15 HZ

CORRELATION OF MODAL DATA

STICK VS. FULL, CORR=0.93

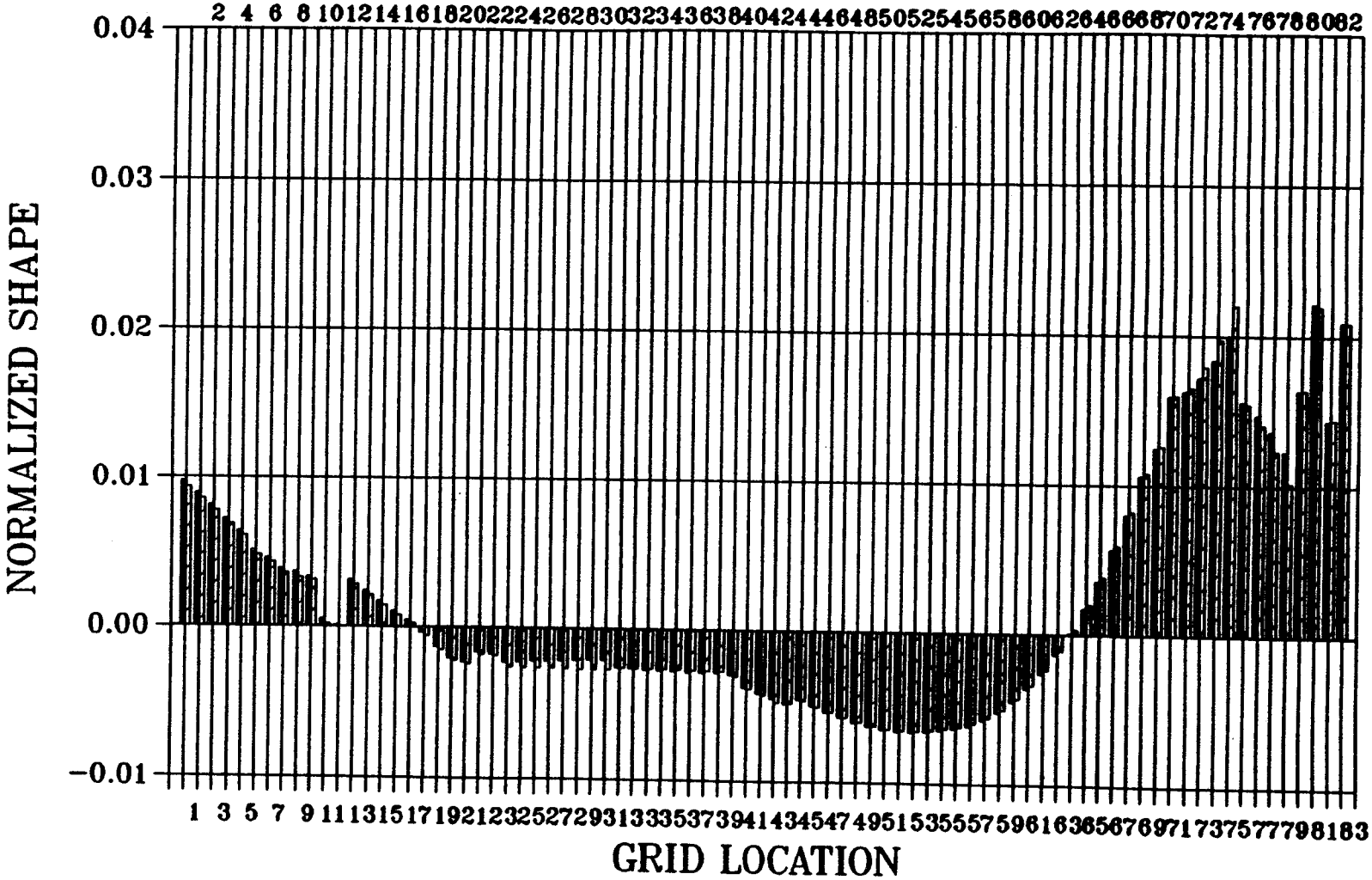

FULL MODEL, Z-COMP. , NO. 14, 6.00 HZ

STICK MODEL, Z-COMP. , NO. 8, 6.15 HZ

CORRELATION OF MODAL DATA

STICK VS. FULL, CORR=0.84

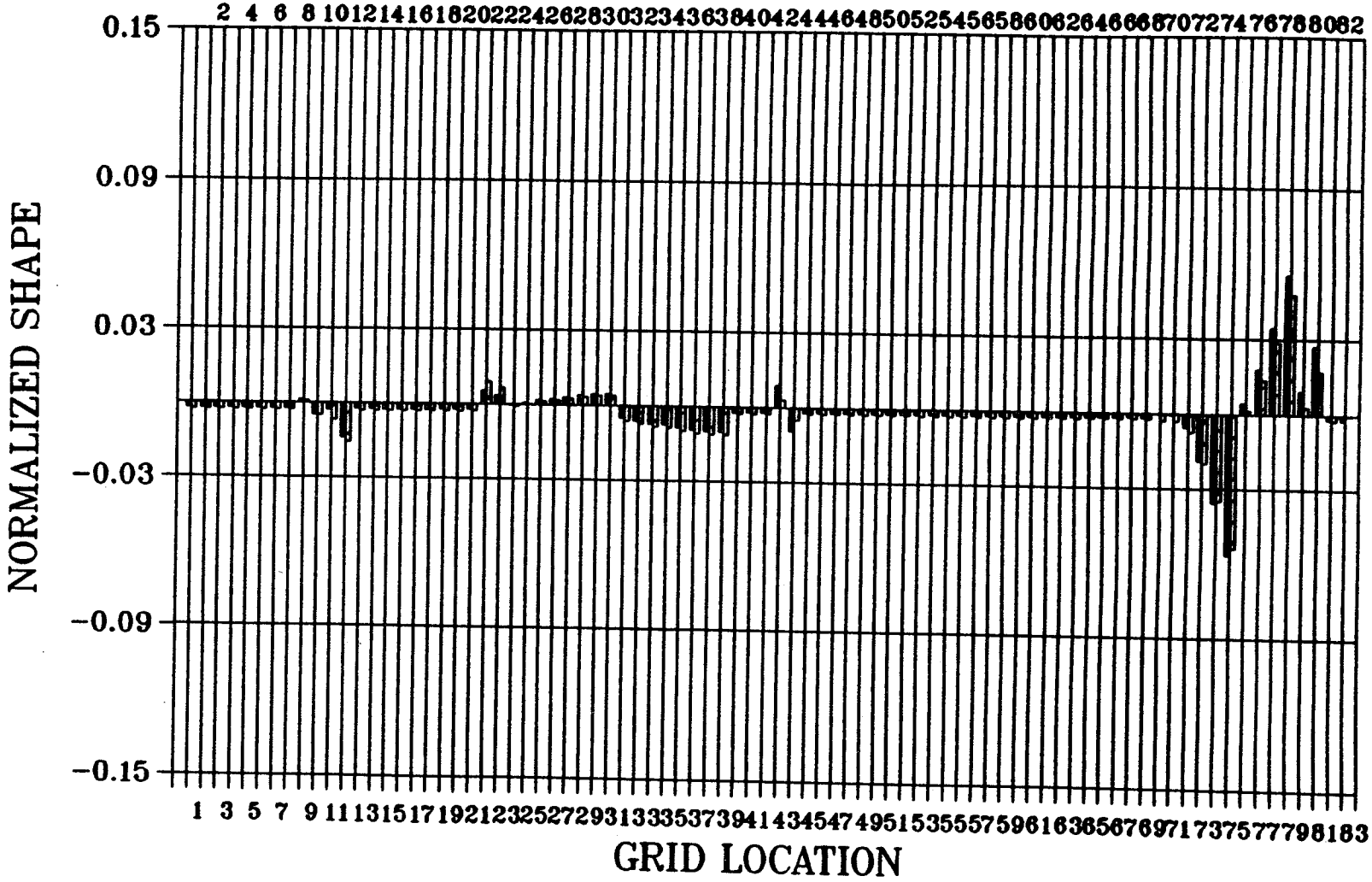

FULL MODEL, X-COMP. , NO. 16, 10.70 HZ

STICK MODEL, X-COMP. , NO. 9, 9.76 HZ

CORRELATION OF MODAL DATA

STICK VS. FULL, CORR=0.84

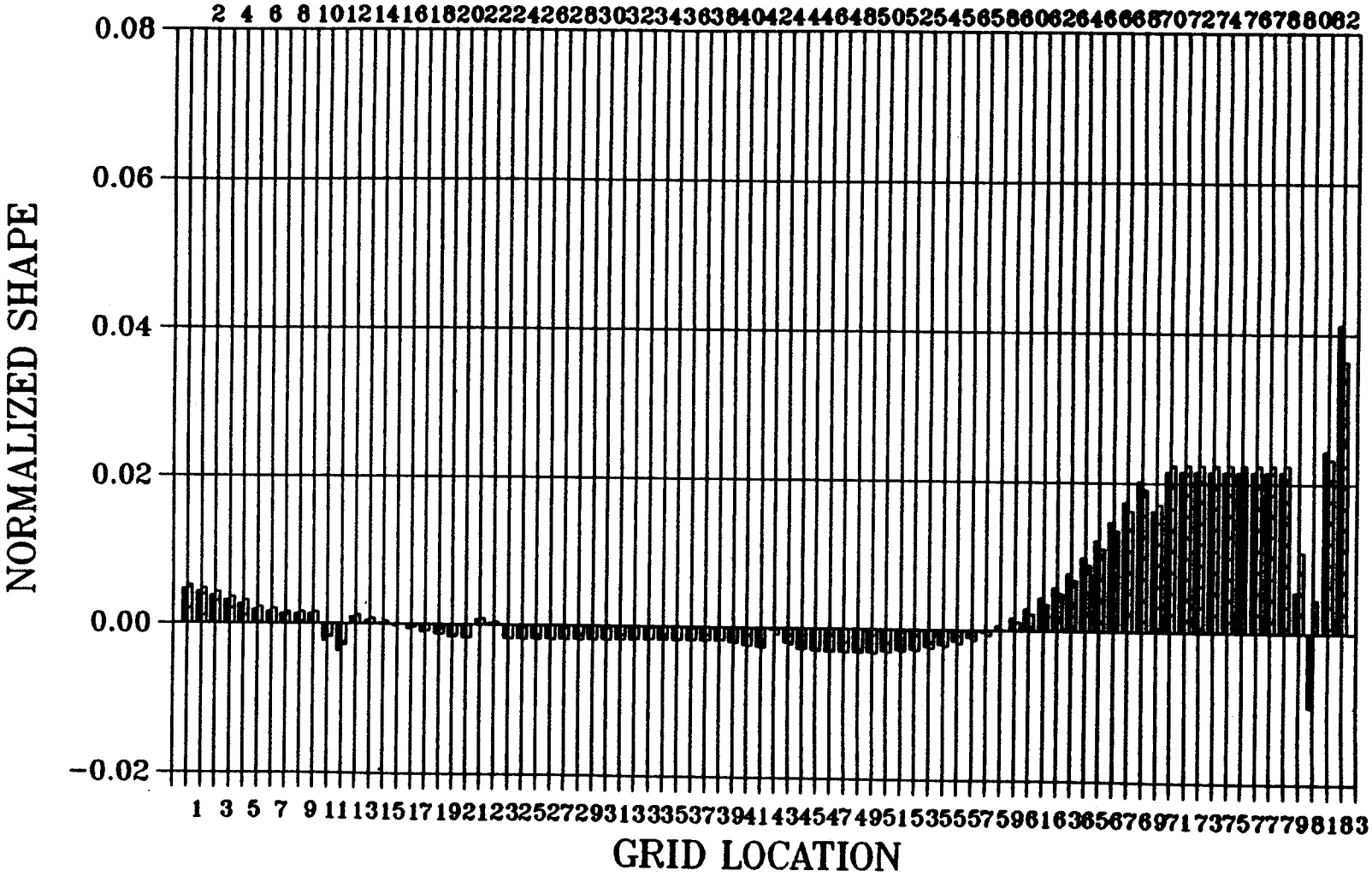

FULL MODEL, Y-COMP. , NO. 16, 10.70 HZ

STICK MODEL, Y-COMP. , NO. 9, 9.76 HZ

CORRELATION OF MODAL DATA

STICK VS. FULL, CORR=0.84

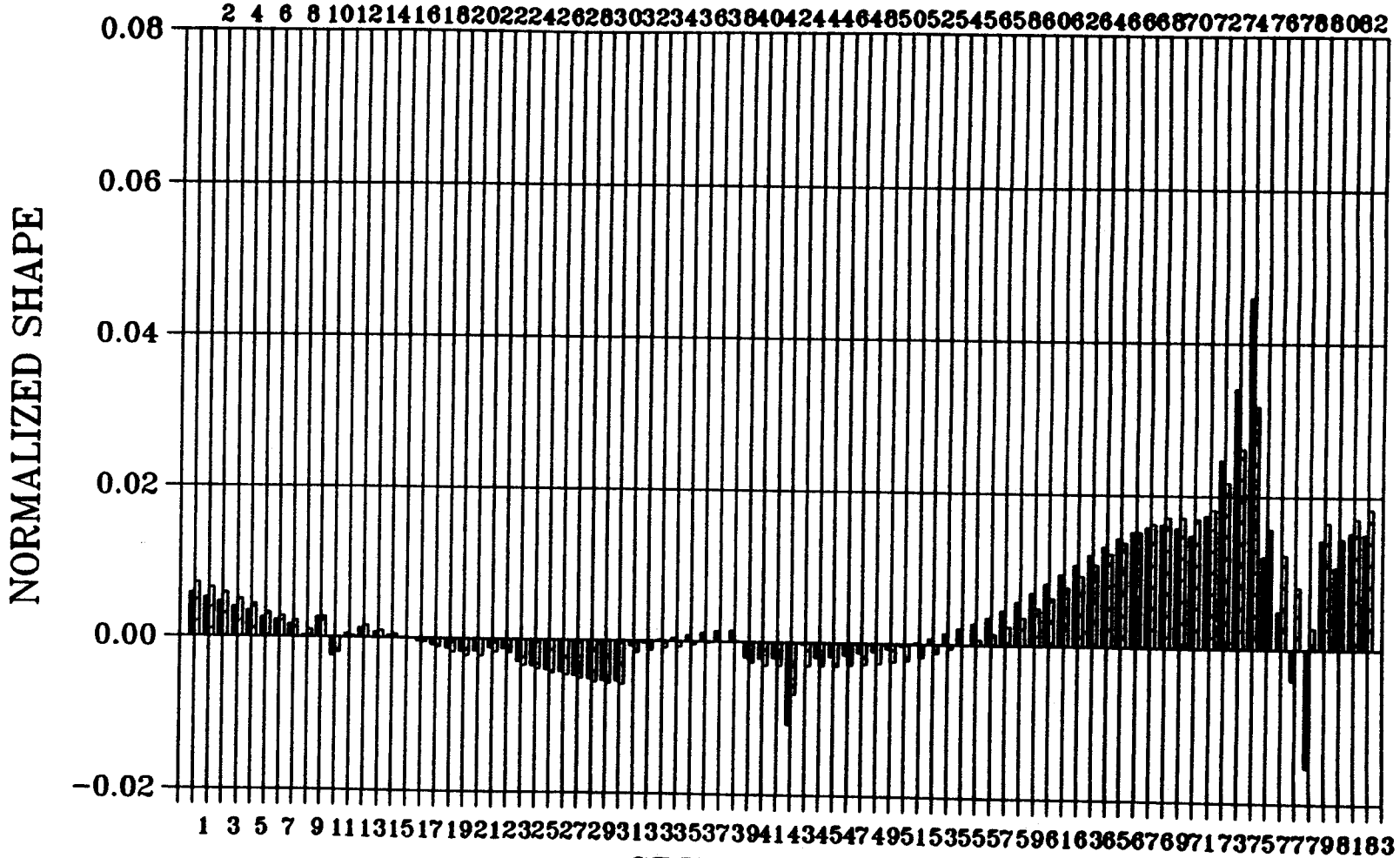

10.70 HZ

FULL MODEL, Z-COMP. , NO. 16, 10.70 HZ

STICK MODEL, Z-COMP. , NO. 9, 9.76 HZ

CORRELATION OF MODAL DATA

STICK VS. FULL, CORR=0.90

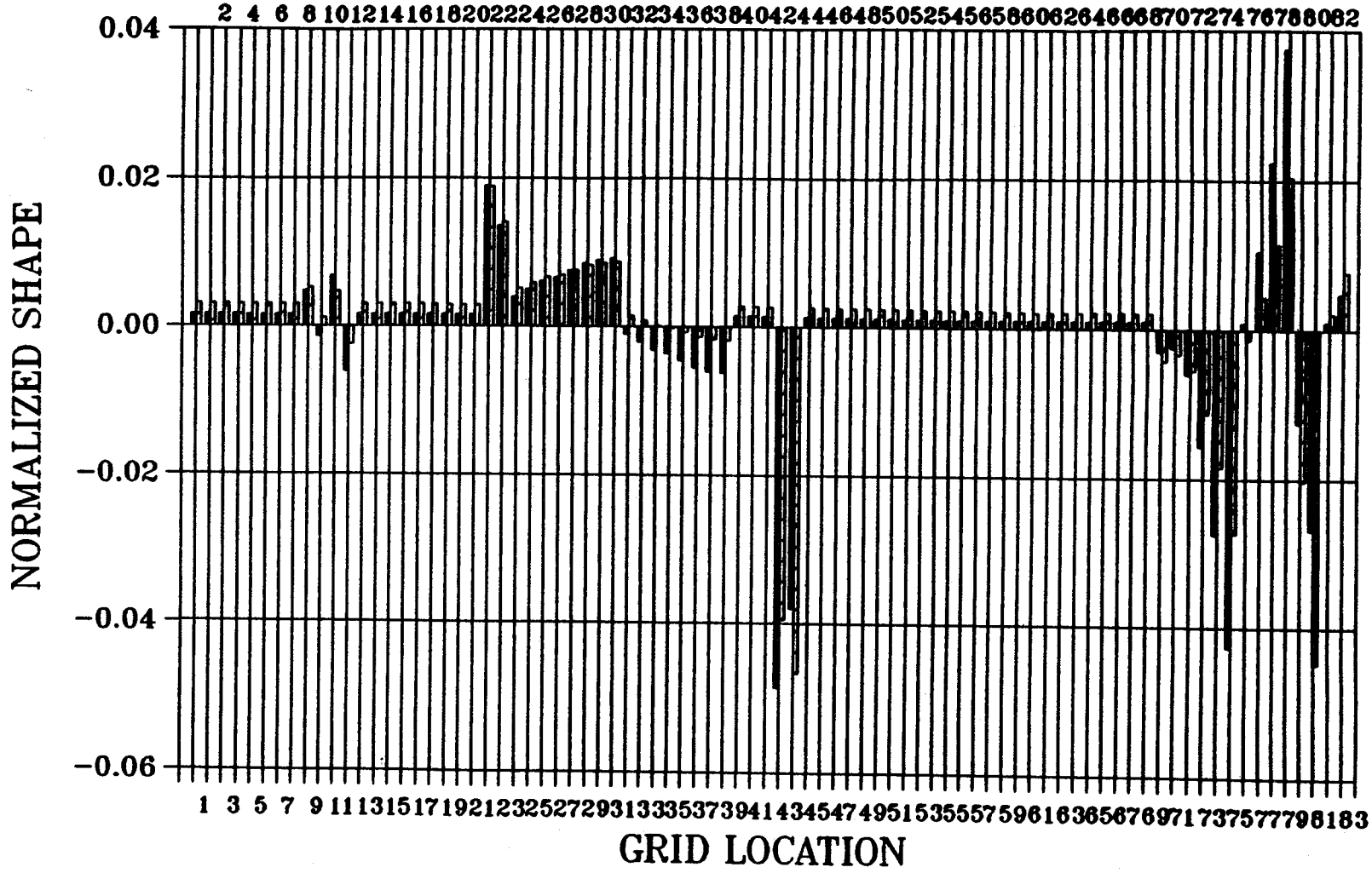

FULL MODEL, X-COMP. , NO. 18, 11.44 HZ

STICK MODEL, X-COMP. , NO. 11, 11.67 HZ

CORRELATION OF MODAL DATA

STICK VS. FULL, CORR=0.90

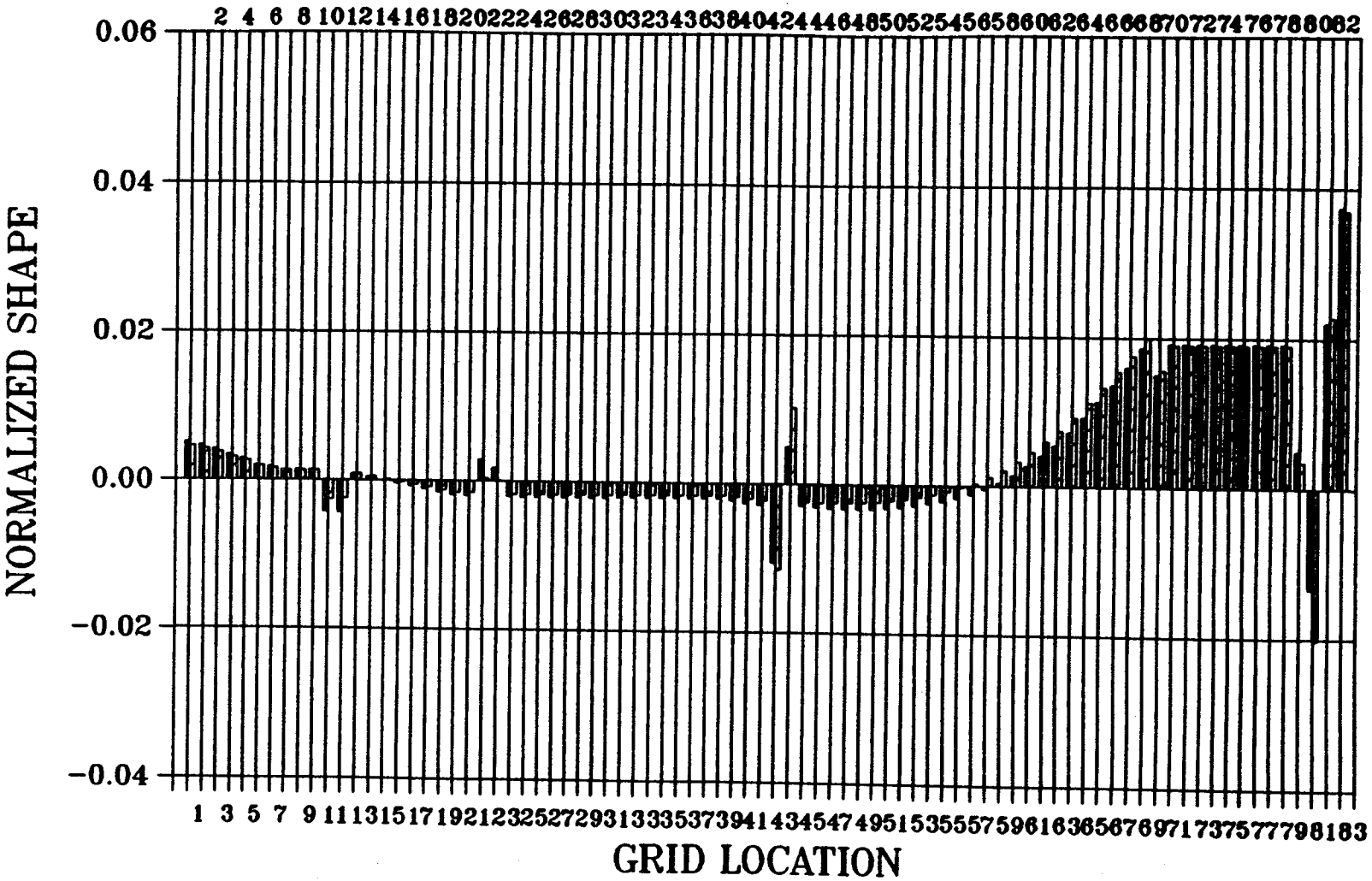

FULL MODEL, Y-COMP. , NO. 18, 11.44 HZ

STICK MODEL, Y-COMP. , NO. 11, 11.67 HZ

CORRELATION OF MODAL DATA

STICK VS. FULL, CORR=0.90

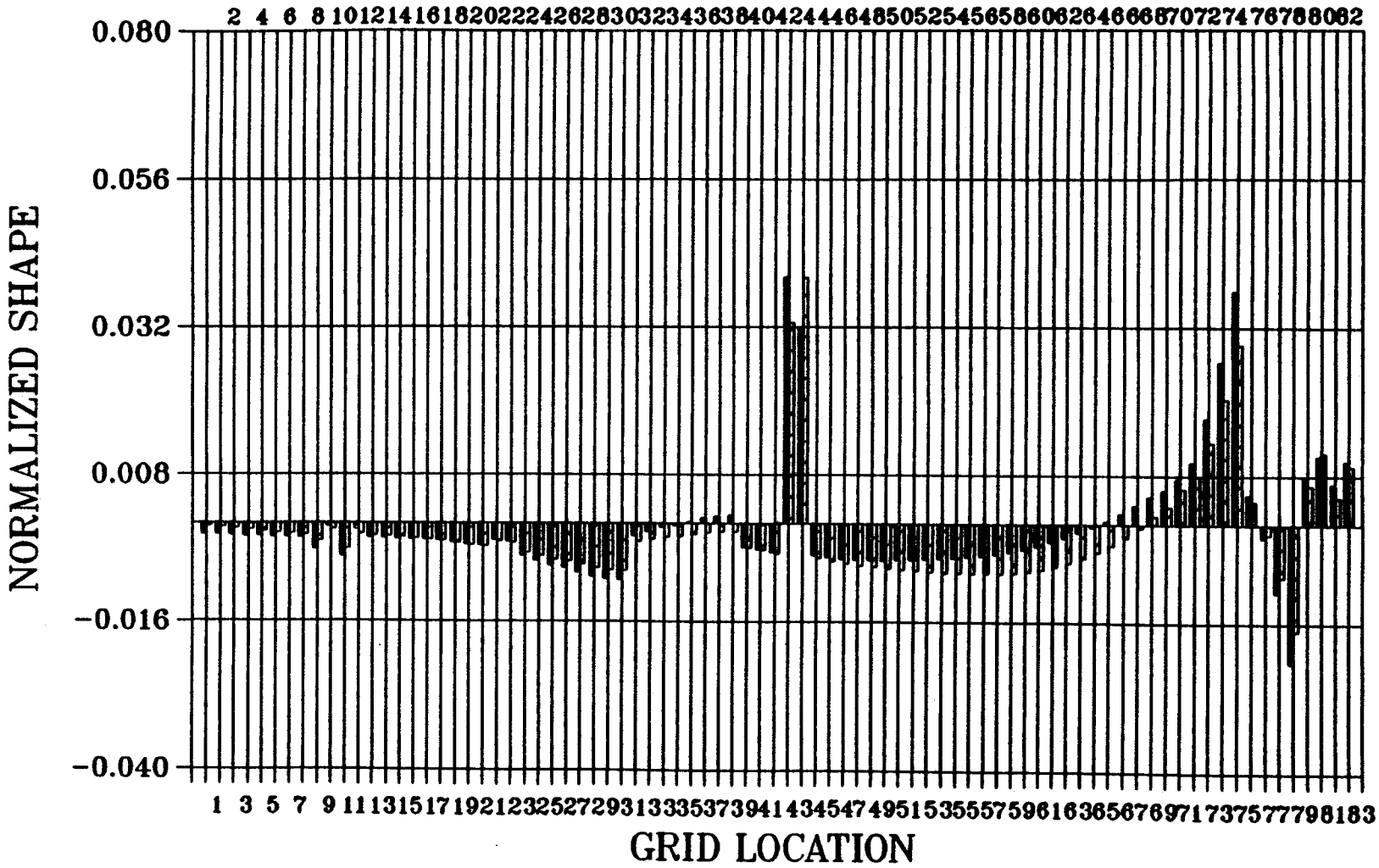

FULL MODEL, Z-COMP. , NO. 18, 11.44 HZ

STICK MODEL, Z-COMP. , NO. 11, 11.67 HZ

CORRELATION OF MODAL DATA

STICK VS. FULL, CORR=0.91

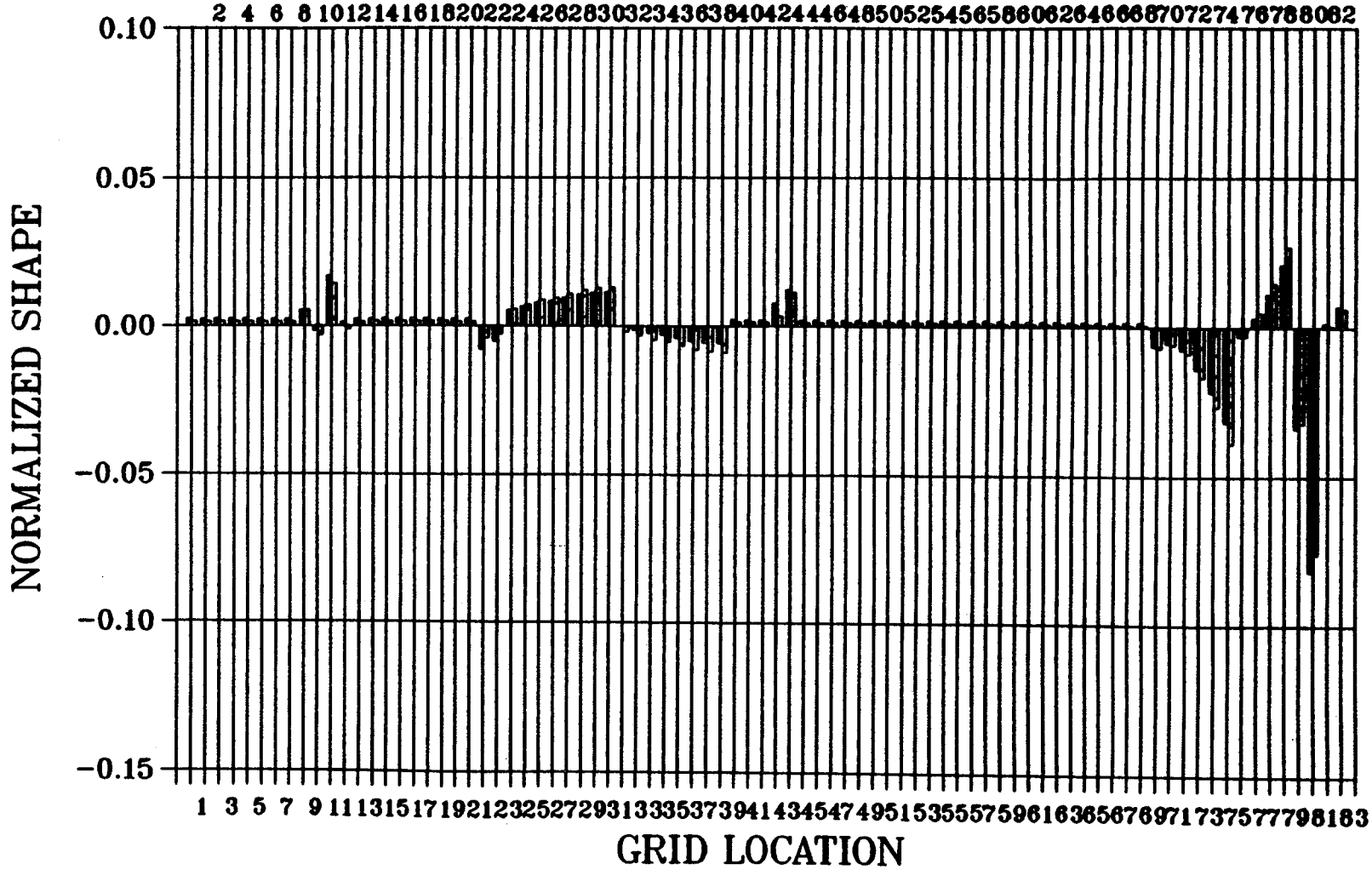

FULL MODEL, X-COMP. , NO. 19, 11.97 HZ

STICK MODEL, X-COMP. , NO. 12, 12.31 HZ

CORRELATION OF MODAL DATA

STICK VS. FULL, CORR=0.91

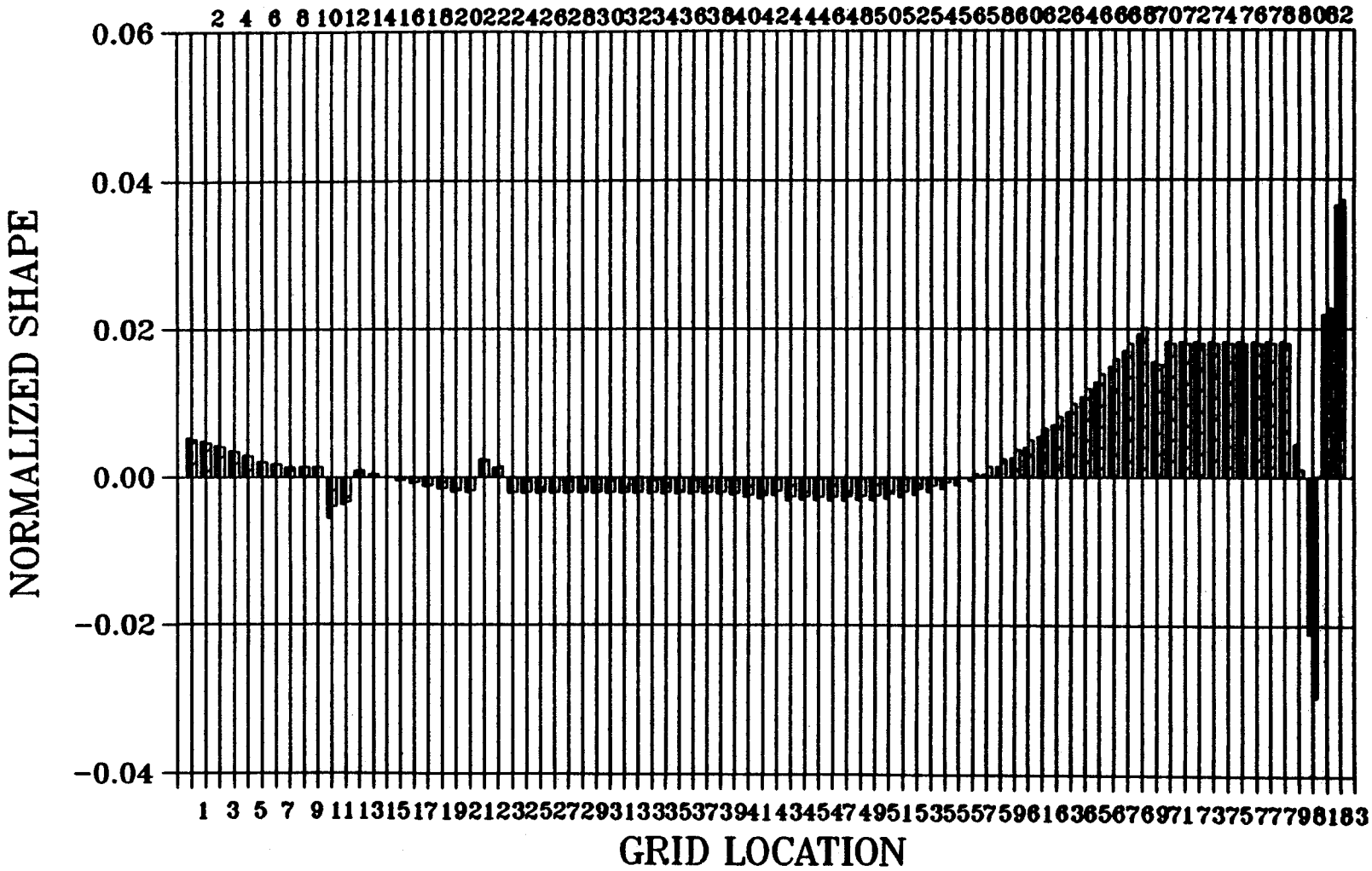

FULL MODEL, Y-COMP. , NO. 19, 11.97 HZ

STICK MODEL, Y-COMP. , NO. 12, 12.31 HZ

CORRELATION OF MODAL DATA

STICK VS. FULL, CORR=0.91

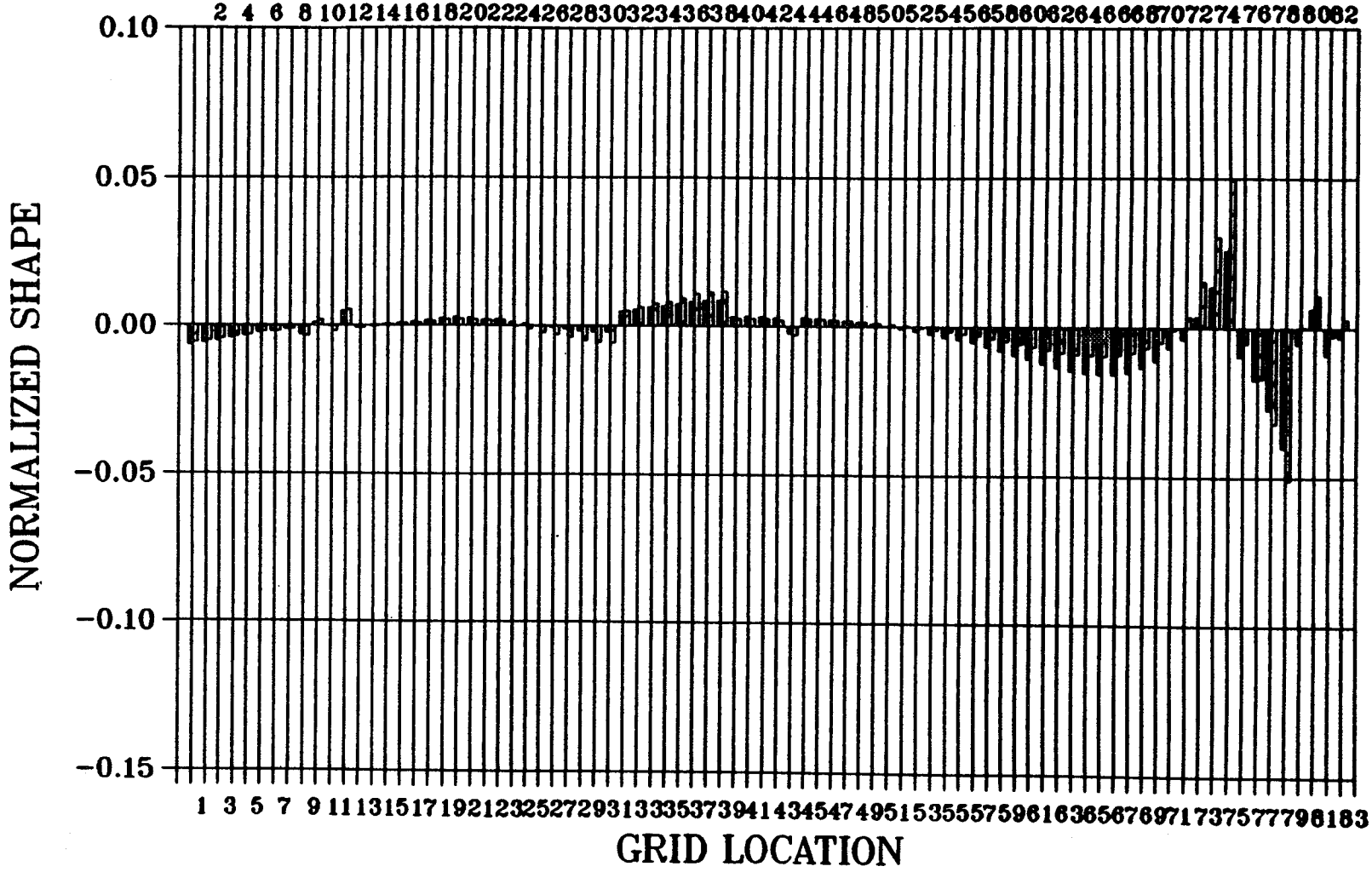

FULL MODEL, Z-COMP. , NO. 19, 11.97 HZ

STICK MODEL, Z-COMP. , NO. 12, 12.31 HZ

CORRELATION OF MODAL DATA

STICK VS. FULL, CORR=0.87

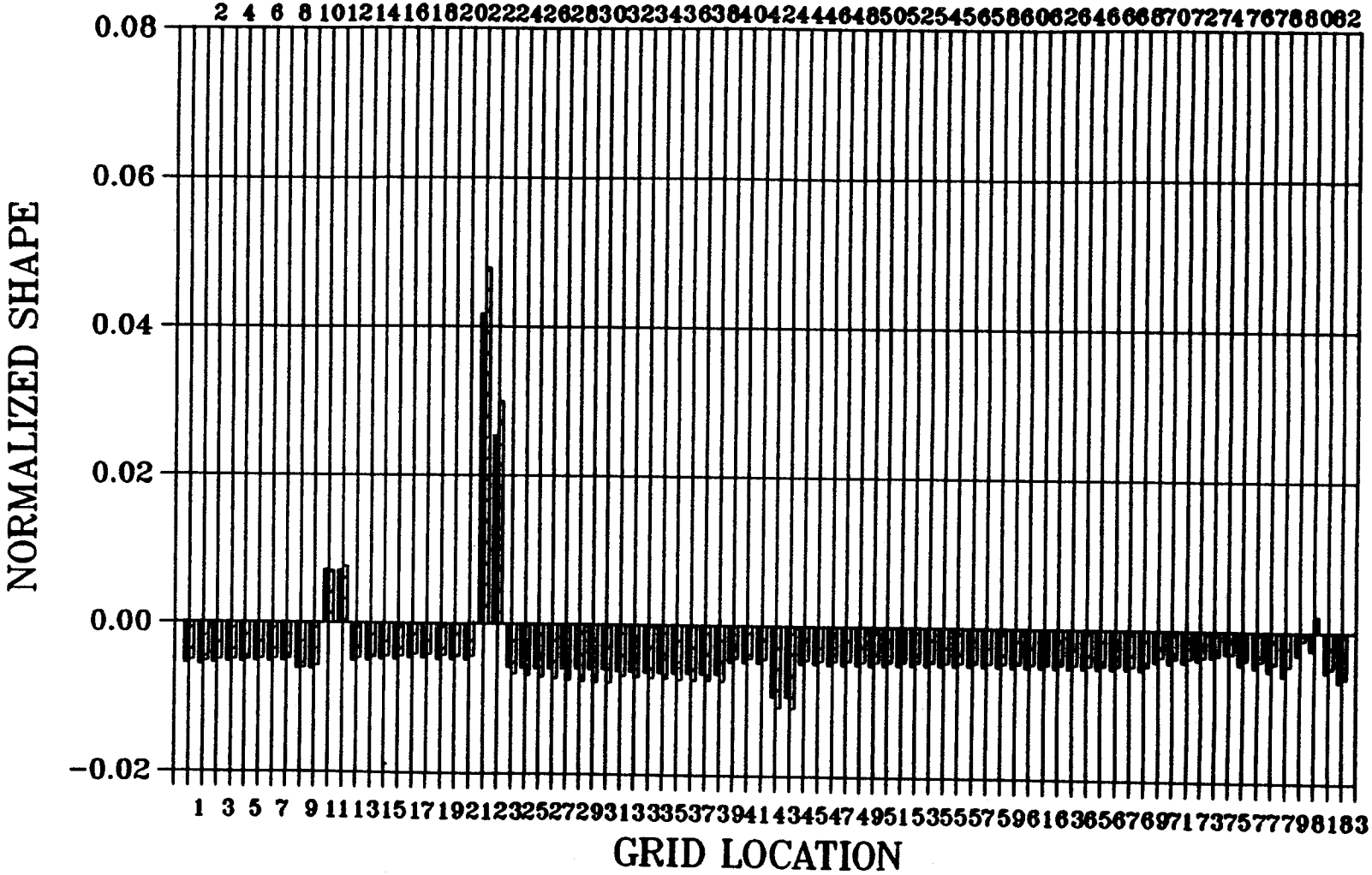

FULL MODEL, X-COMP. , NO. 20, 13.41 HZ

STICK MODEL, X-COMP. , NO. 13, 14.33 HZ

CORRELATION OF MODAL DATA

STICK VS. FULL, CORR=0.87

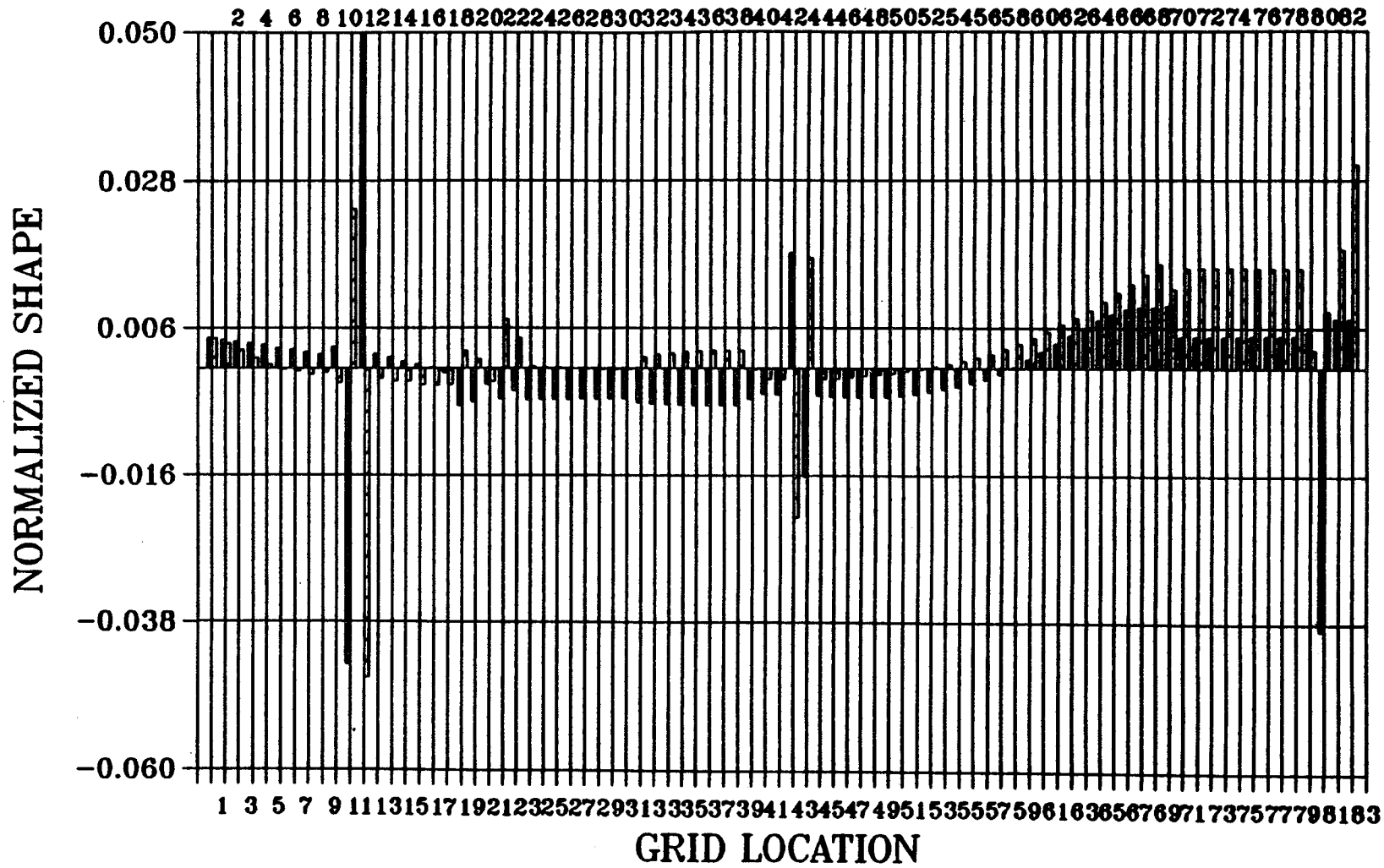

FULL MODEL, Y-COMP. , NO. 20, 13.41 HZ

STICK MODEL, Y-COMP. , NO. 13, 14.33 HZ

CORRELATION OF MODAL DATA

STICK VS. FULL, CORR=0.87

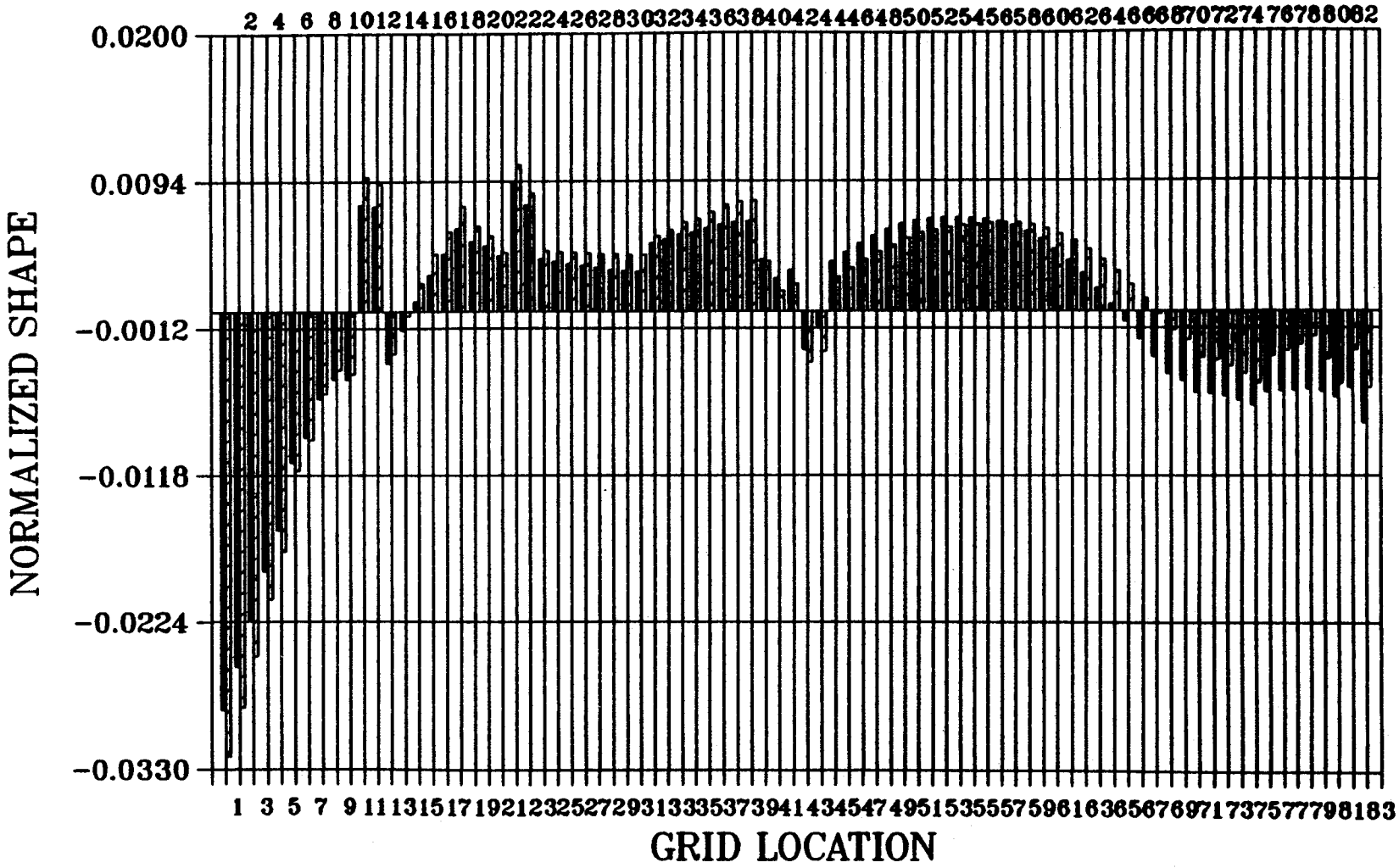

FULL MODEL, Z-COMP. , NO. 20, 13.41 HZ

STICK MODEL, Z-COMP. , NO. 13, 14.33 HZ

CORRELATION OF MODAL DATA

STICK VS. FULL, CORR=0.70

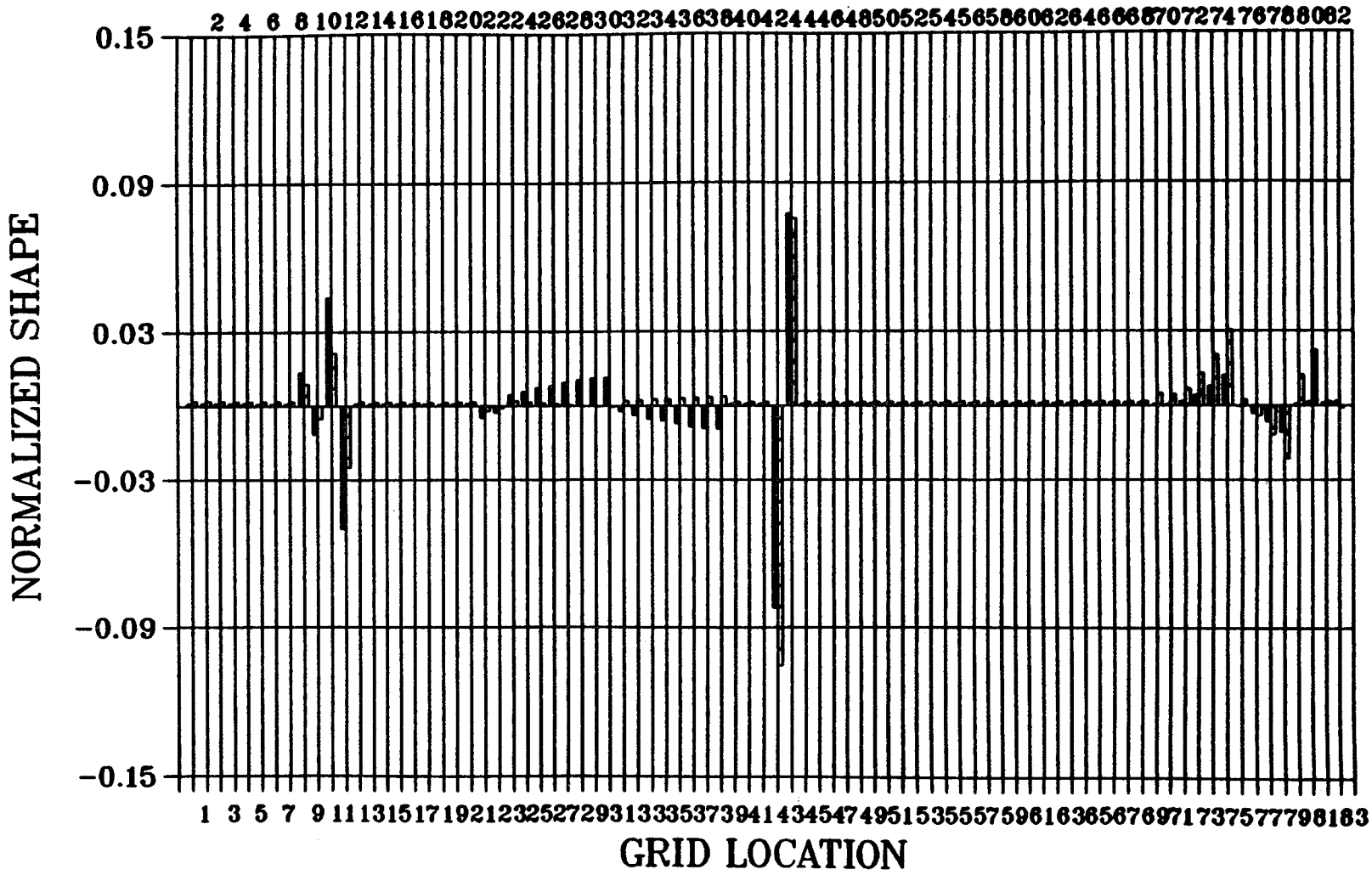

FULL MODEL, X-COMP. , NO. 21, 14.16 HZ

STICK MODEL, X-COMP. , NO. 14, 16.43 HZ

CORRELATION OF MODAL DATA

STICK VS. FULL, CORR=0.70

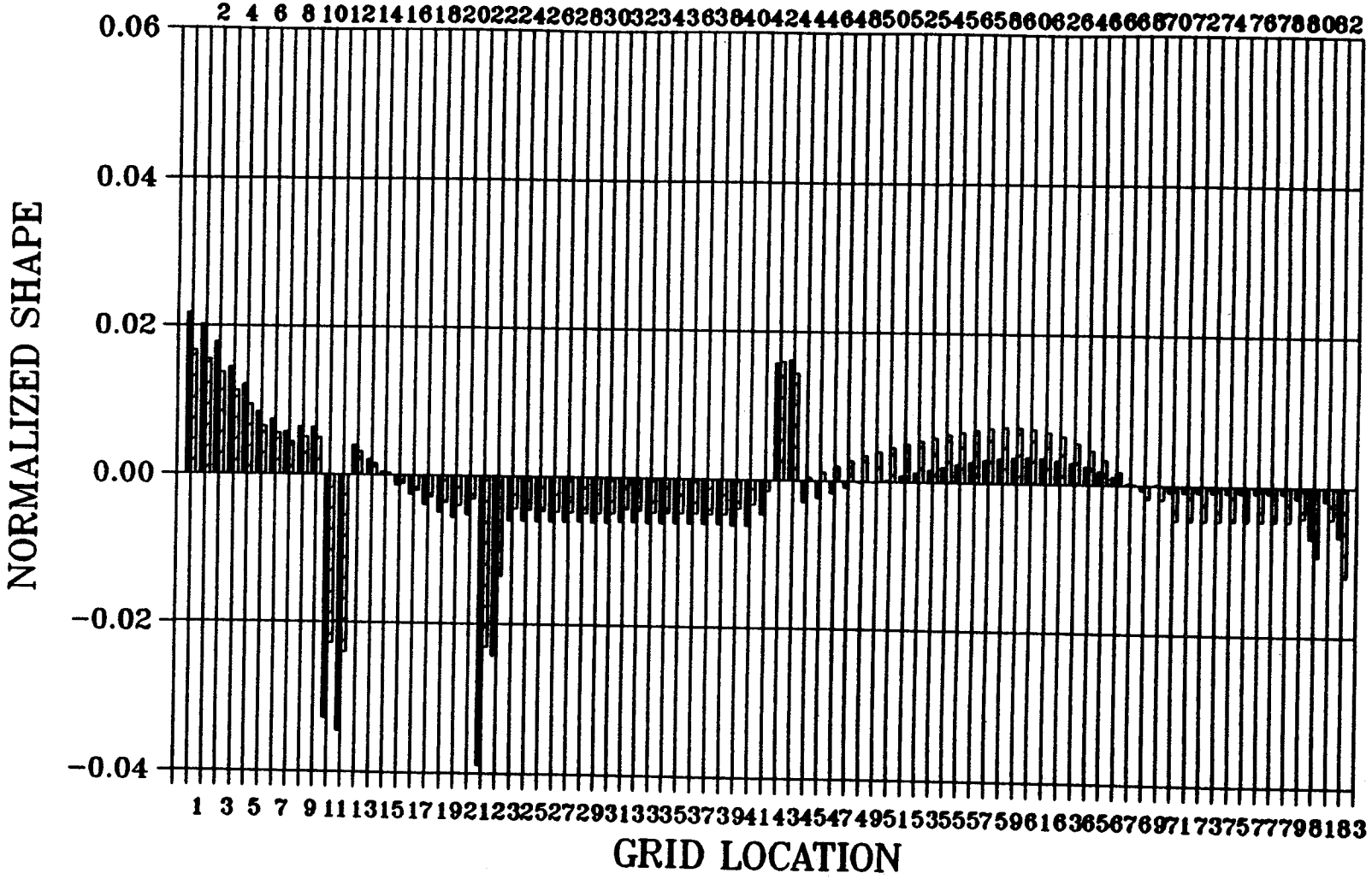

FULL MODEL, Y-COMP. , NO. 21, 14.16 HZ

STICK MODEL, Y-COMP. , NO. 14, 16.43 HZ

CORRELATION OF MODAL DATA

STICK VS. FULL, CORR=0.70

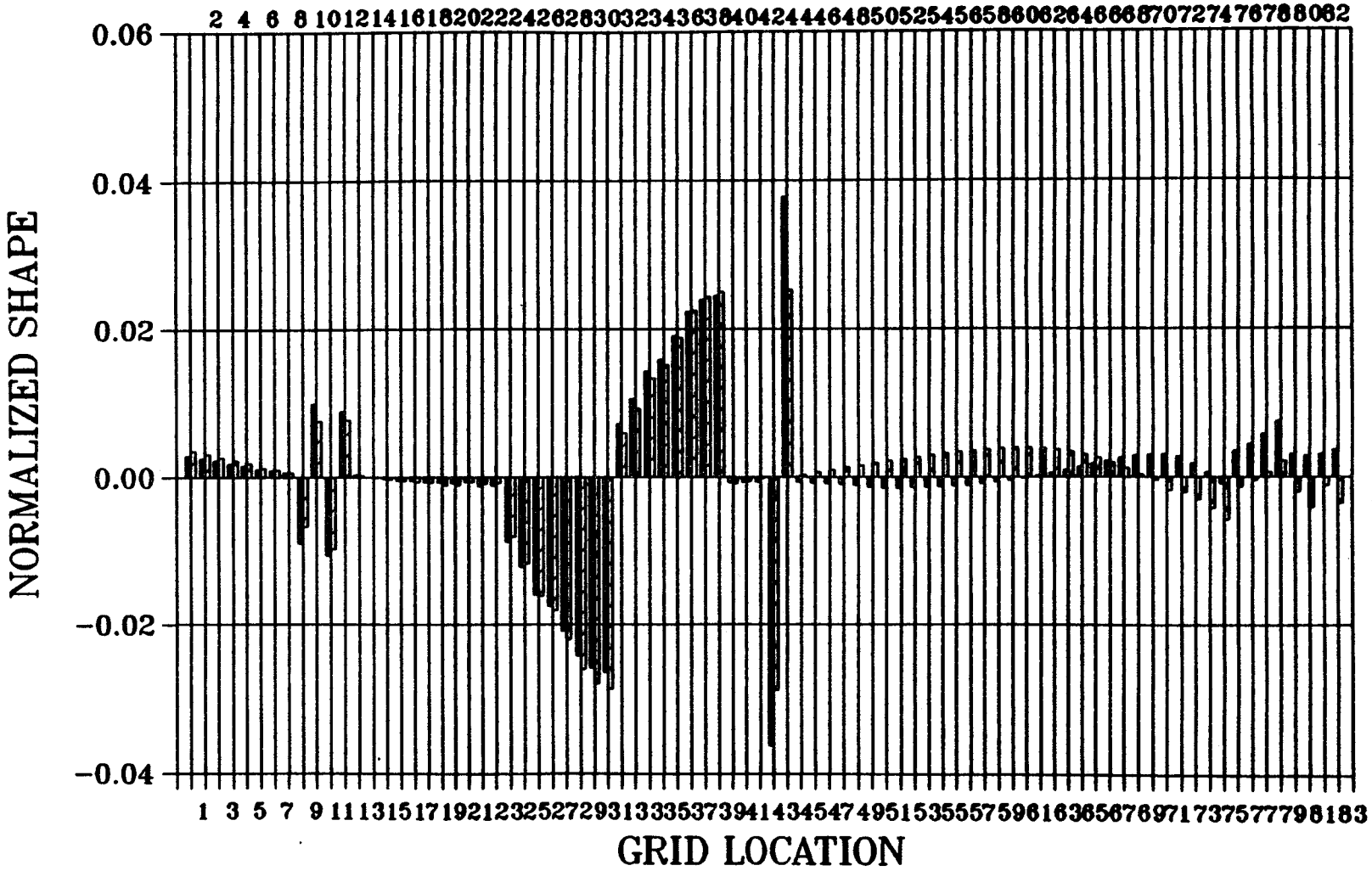

FULL MODEL, Z-COMP. , NO. 21, 14.16 HZ

STICK MODEL, Z-COMP. , NO. 14, 16.43 HZ

CORRELATION OF MODAL DATA

STICK VS. FULL, CORR=0.81

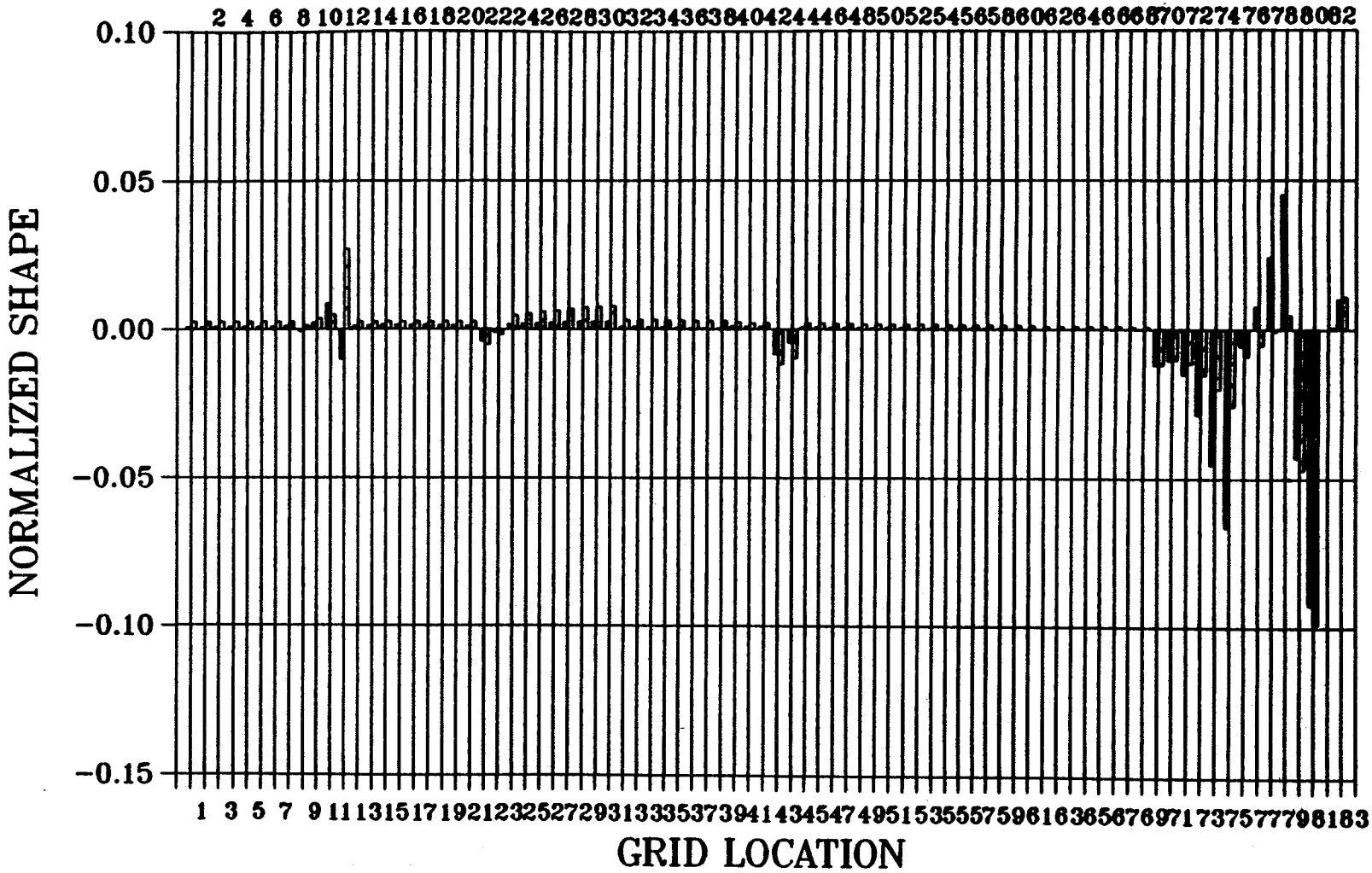

FULL MODEL, X-COMP. , NO. 30, 20.63 HZ

STICK MODEL, X-COMP. , NO. 17, 19.60 HZ

CORRELATION OF MODAL DATA

STICK VS. FULL, CORR=0.81

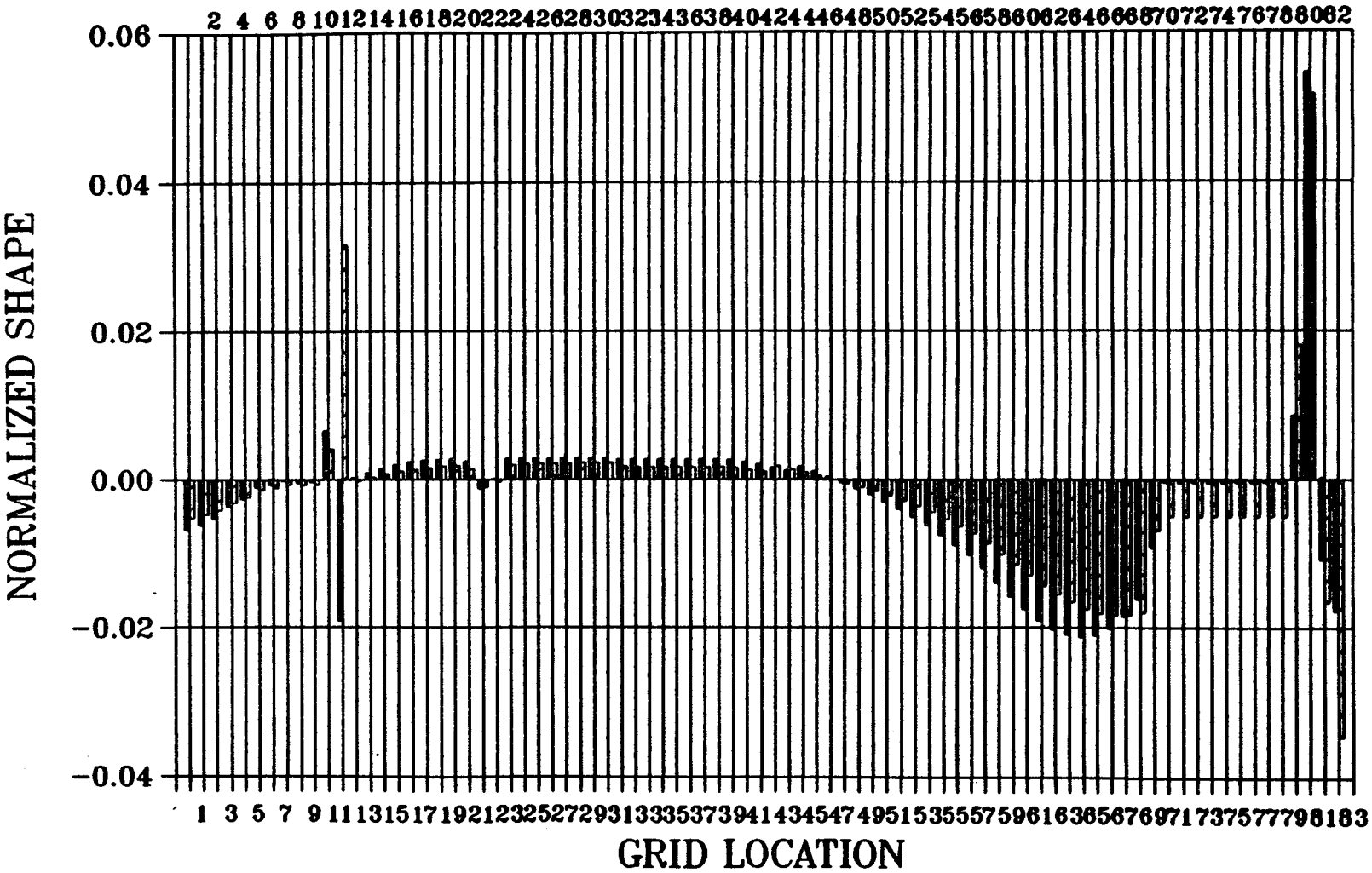

FULL MODEL, Y-COMP. , NO. 30, 20.63 HZ

STICK MODEL, Y-COMP. , NO. 17, 19.60 HZ

CORRELATION OF MODAL DATA

STICK VS. FULL, CORR=0.81

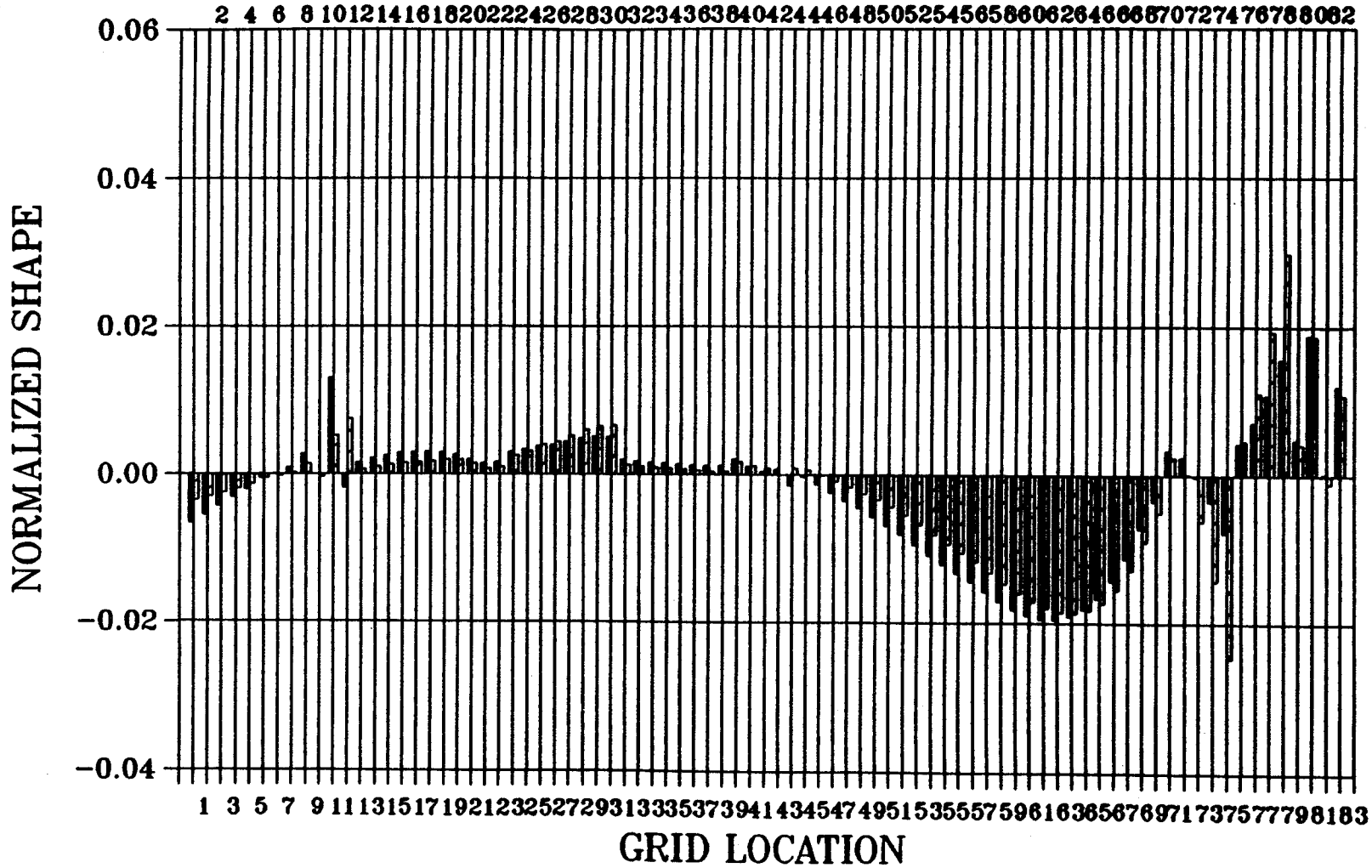

FULL MODEL, Z-COMP. , NO. 30, 20.63 HZ

STICK MODEL, Z-COMP. , NO. 17, 19.60 HZ

6.0 OTHER APPLICATIONS

VIBRATION REDUCTION STUDY

In addition to the development and application of the model reduction procedure, another study was made to examine the applicability of the reduced (stick) model to a vibration reduction study. For this purpose, the reduced model was subjected to different four-per-rev hub excitations and the modal frequency responses (SOL 30) of different locations of the structure, together with the contribution of each mode to the total response of each location, were calculated. Subsequent to the identification of the dominant modes, a design sensitivity analysis study (SOL 53) was performed to identify the pertinent model parameters (e.g., cross sectional area, area moment of inertia, etc.) which have the most effect on the vibrational response at the selected locations. Once these parameters were identified, certain incremental changes were made to each individually or a combination of these parameters (to be discussed later) to reduce the vibration at the selected locations.

VIBRATION REDUCTION STUDY

- TO EXAMINE THE APPLICABILITY OF REDUCED MODEL TO A VIBRATION REDUCTION STUDY

- USING THE REDUCED MODEL
  - CALCULATE CONTRIBUTION OF EACH MODE TO TOTAL FORCED RESPONSE
  - IDENTIFY THE STRUCTURAL PARAMETERS EFFECTING THE RESPONSE THROUGH DESIGN SENSITIVITY STUDIES
  - MODIFY STRUCTURE TO REDUCE VIBRATION

CALCULATION OF MODAL CONTRIBUTIONS TO TOTAL RESPONSE

In conjunction with the vibration reduction study, the first step was to determine the contribution of each mode to the total response of the selected portion of the structure, which for this case was the tip of the vertical tail of the AH-64A reduced model. For this purpose, an in-house DMAP program was used in conjunction with the MSC/NASTRAN modal frequency response solution sequence (SOL 30) to determine the contribution of each mode to the total displacement or acceleration response of the point of interest. The following figure shows the four modes with the largest contributions to the total response of the selected point, when the aircraft is subjected to a four-per-rev vertical hub excitation. As can be seen, mode 17 contributes the most to the total response. In addition, examination of other modes and the results obtained from the DMAP indicated that the fifteenth mode (i.e., 17.268 Hz) to be the next highest contributor to the response of the point of interest. Therefore, these two modes (i.e., modes 15 and 17) were selected to be used in the following design sensitivity analysis. This selection process was repeated for two other types of hub excitations (i.e., longitudinal and lateral excitations) and a similar pattern was obtained.

CALCULATION OF MODAL CONTRIBUTIONS TO TOTAL RESPONSE

(TIP OF VERTICAL TAIL)

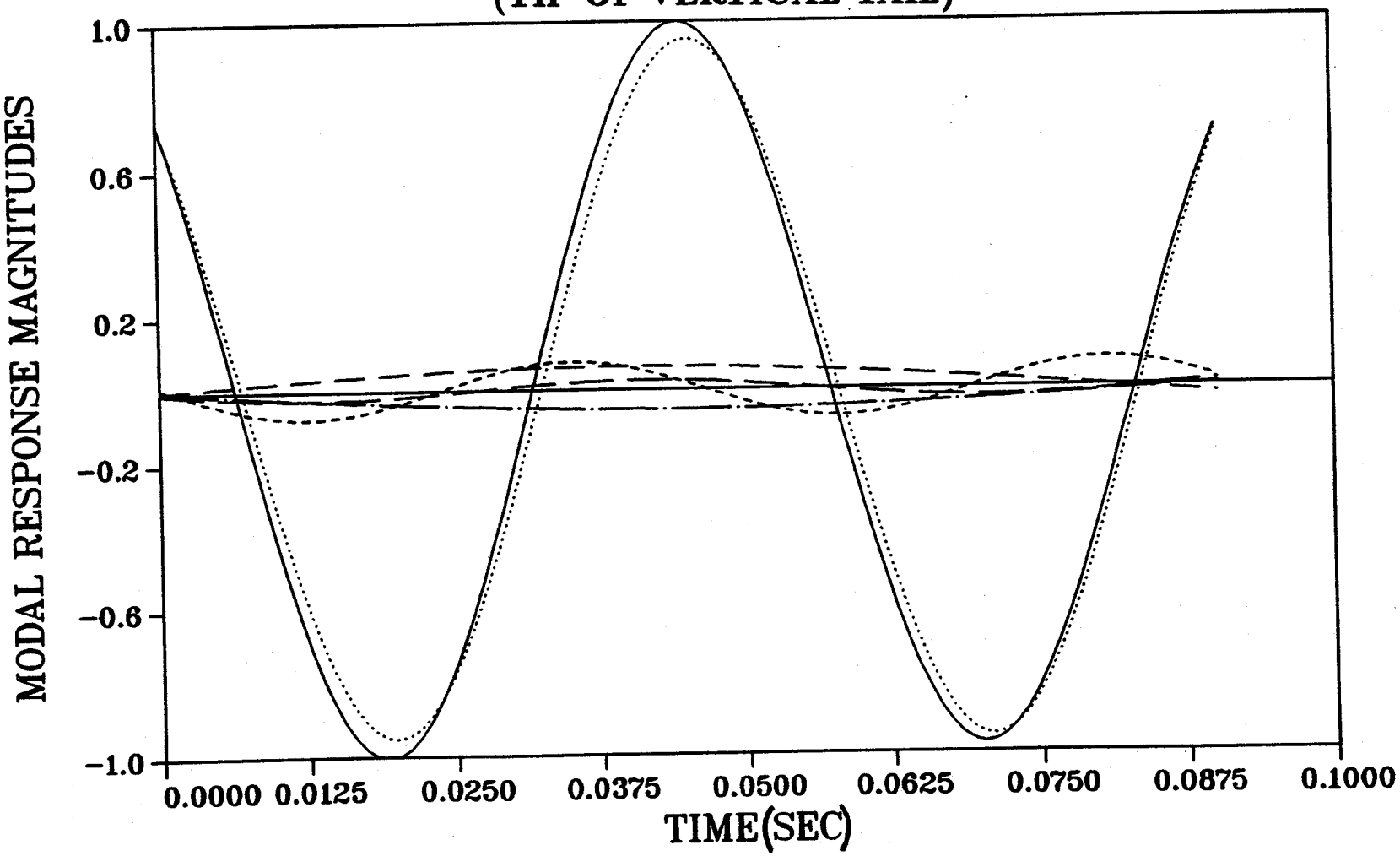

STICK MODEL

..... MODE-17, 19.603 HZ

------ MODE-20, 21.990 HZ

— — MODE- 8, 6.153 HZ

—·— MODE- 7, 5.623 HZ

— — MODE-15, 17.268 HZ

——— TOTAL RESPONSE

DESIGN SENSITIVITY ANALYSIS STUDIES

The purpose of this study was to identify those parameters which have the most effect on the response of selected normal modes in the area of interest of the structure. In relation to this effort, it was decided to use the design sensitivity analysis capabilities of MSC/NASTRAN. Prior to using SOL 53, it was necessary to introduce some MSC/NASTRAN element property cards without affecting its dynamic characteristics. This was due to the fact that the reduced model stiffness properties was represented only through a set of DMIG cards. For this purpose, a set of very soft CBARs was added between each pair of grid points of the reduced model. Another normal mode run was made to check the effects of the CBARs on the overall characteristics of the reduced model. Results indicated very little change.

Subsequent to the addition of CBAR elements, it was decided to study a section of the aircraft in close proximity to the point of interest (i.e., tip of the vertical tail). Based on the study of the mode shapes, the aircraft tailboom was selected for the following analysis. For this analysis, four structural parameters were selected as the design variables. These included: the cross-sectional area, the two area moments of inertia, and the torsional constant parameter. The two dominant stick model modes (i.e., modes 15 and 17) which represented mainly the tailboom vertical and lateral bendings, were selected as the "constraint" parameters.

Subsequent to selection of all design variables and "constraint" parameters, the design sensitivity analysis was run for all twelve tailboom frame segements and a set of sensitivity coefficients obtained. These are shown in the following figures. From these figures, it is apparent that the two area moments of inertia parameters have the most effect on the frequency placement of the two modes. Consequently, these parameters were altered which shifted the frequencies of these two modes away from the four-per-rev excitation frequenvy. The table following these figures represents the matrix of the changes which were made to the stick model. This process resulted in a fairly significant reduction of the vibration level at the tip of vertical tail. The calculated response for each of the three hub excitations are shown in the tables following the figures. As indicated in these tables, each response amplitude is normalized with respect to its corresponding stick model values. Similar changes were also made to the same locations of the full model and the response of the vertical tail was calculated. These results are tabulated in the following tables. In this case, the response amplitudes are normalized with respect to the baseline (i.e., prior to introducing any changes) full model.

DESIGN SENSITIVITY ANALYSIS STUDIES

- TO IDENTIFY THE PARAMETERS WHICH MOST EFFECT THE RESPONSE OF A SELECTED PORTION OF STRUCTURE THROUGH:
  - ADDITION OF ELEMENT PROPERTY CARDS TO THE REDUCED MODEL
  - SELECTION OF PERTINENT STRUCTURAL PARAMETERS AS DESIGN VARIABLES
  - APPLICATION OF NASTRAN DESIGN SENSITIVITY ANALYSIS
  - IDENTIFICATION OF IMPORTANT SENSITIVITY COEFFICIENTS
  - INTRODUCTION OF STRUCTURAL CHANGES FOR VIBRATION REDUCTION

DESIGN SENSITIVITY ANALYSIS STUDIES

(MODE-15, 17.26 Hz)

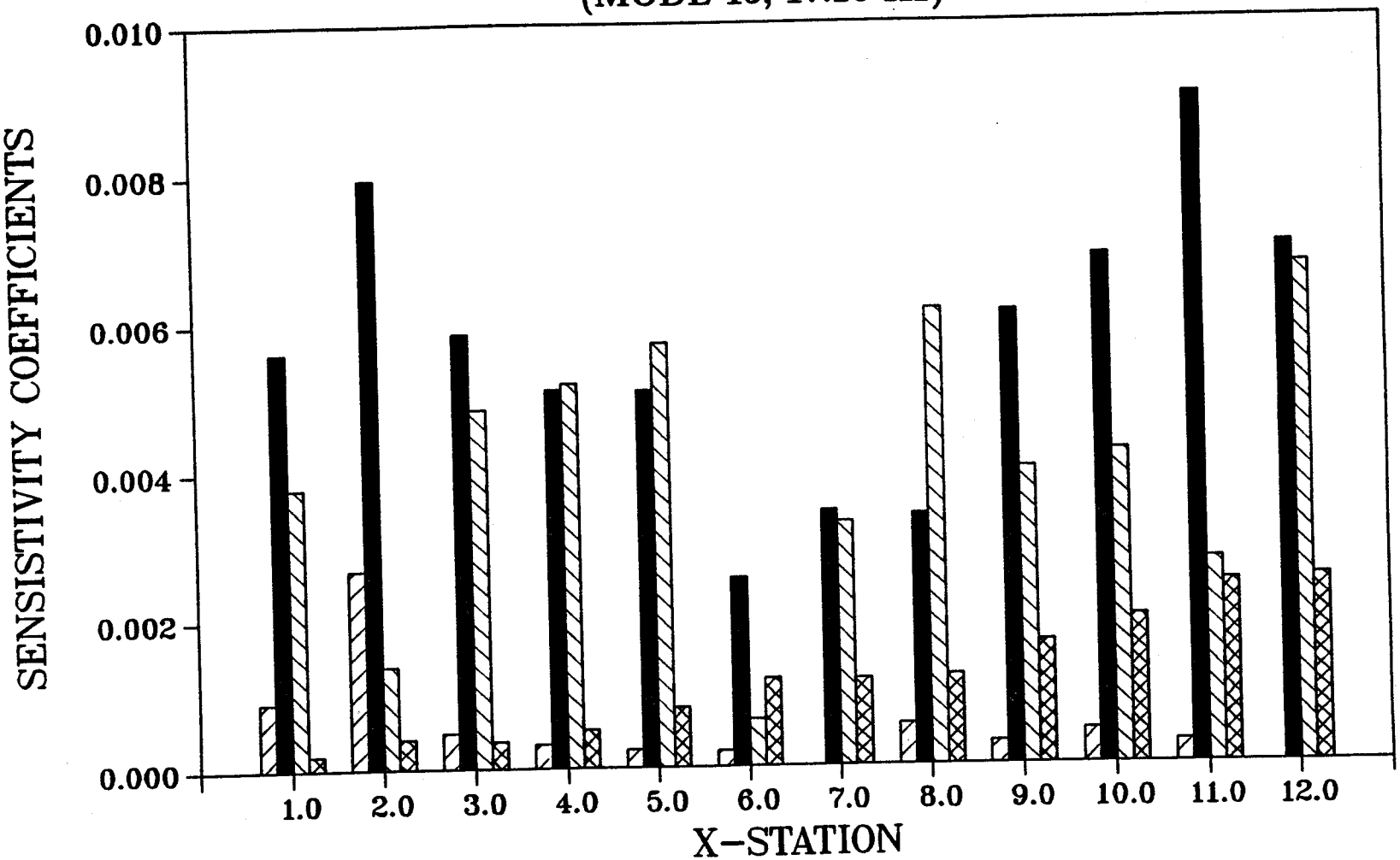

DESIGN SENSITIVITY ANALYSIS STUDIES

(MODE-17, 19.60 Hz)

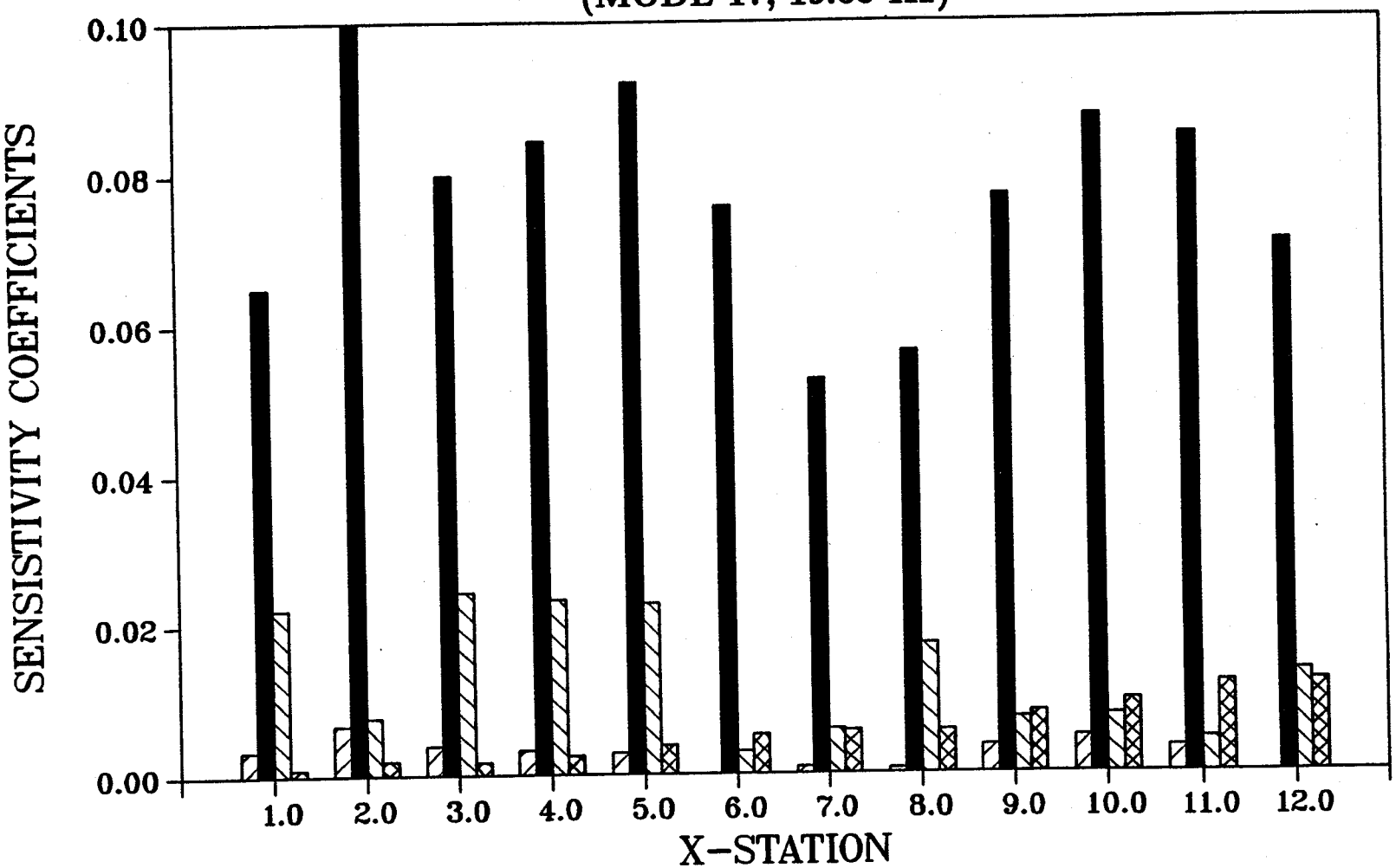

DESIGN SENSITIVITY ANALYSIS STUDIES

Model Changes	
Case No.	Changes
1	None (baseline stick model)
2	Baseline model with the soft CBAR elements
3	1 % increase in I_1 in sections located between stations 2 to 5.
4	1 % increase in I_1 and I_2 in sections located between stations 9 to 12
5	1 % increase in I_1 and I_2 in sections located between stations 2 to 5
6	5 % increase in I_1 in sections located between stations 2 to 5
7	5 % increase in I_1 in sections located between stations 2 to 5 and 9 to 12

DESIGN SENSITIVITY ANALYSIS STUDIES

STICK MODEL

Longitudinal Hub Excitation					
	Frequency(Hz)		Total Response (Normalized)		
Case No.	Mode-15	Mode-17	X-Comp.	Y-Comp.	Z-Comp.
1	17.268	19.603	1.000	1.000	1.000
2	17.269	19.604	0.998	0.998	0.998
3	17.271	19.629	0.971	0.973	0.969
4	17.273	19.636	0.963	1.006	0.964
5	17.272	19.633	0.966	0.968	0.963
6	17.275	19.652	0.945	0.949	0.943
7	17.288	19.770	0.828	0.842	0.827

DESIGN SENSITIVITY ANALYSIS STUDIES

STICK MODEL

Lateral Hub Excitation					
	Frequency(Hz)		Total Response (Normalized)		
Case No.	Mode-15	Mode-17	X-Comp.	Y-Comp.	Z-Comp.
1	17.268	19.603	1.000	1.000	1.000
2	17.269	19.604	0.989	0.991	0.989
3	17.271	19.629	0.961	0.989	0.963
4	17.273	19.636	0.950	0.993	0.956
5	17.272	19.633	0.951	0.986	0.954
6	17.275	19.652	0.935	0.985	0.941
7	17.288	19.770	0.811	0.969	0.833

DESIGN SENSITIVITY ANALYSIS STUDIES

STICK MODEL

Vertical Hub Excitation					
	Frequency(Hz)		Total Response (Normalized)		
Case No.	Mode-15	Mode-17	X-Comp.	Y-Comp.	Z-Comp.
1	17.268	19.603	1.000	1.000	1.000
2	17.269	19.604	0.998	0.999	0.998
3	17.271	19.629	0.968	0.972	0.970
4	17.273	19.636	0.967	0.973	0.973
5	17.272	19.633	0.963	0.970	0.966
6	17.275	19.652	0.940	0.946	0.943
7	17.288	19.770	0.827	0.846	0.847

DESIGN SENSITIVITY ANALYSIS STUDIES

FULL MODEL

	longitudinal excitation			lateral excitation			vertical excitation		
Case	response components								
No.	X	Y	Z	X	Y	Z	X	Y	Z
1	1.000	1.000	1.000	1.000	1.000	1.000	1.000	1.000	1.000
3	0.987	0.991	0.990	0.986	0.997	0.988	0.988	0.990	0.995
4	0.996	0.998	0.997	0.998	1.001	1.001	0.998	0.996	0.998
7	0.951	0.967	0.965	0.946	0.979	0.961	0.953	0.964	0.979

7.0 CONCLUDING REMARKS

CONCLUDING REMARKS

A computational procedure for the reduction of large airframe finite element models has been developed. This procedure, which has been implemented as a set of MSC/NASTRAN DMAP alters, is used to obtain a significantly reduced model while retaining the essential dynamic characteristics of the full-sized model. The procedure was applied to the airframe dynamic finite element model of AH-64A Attack Helicopter. As a result, a reduced model with significantly less DOFs was obtained. This reduced model, which is an adequately accurate representation of the global behavior of the full model, resulted in a substantial reduction in the computation time. An additional study was performed in order to examine the applicability of this reduced model to vibration reduction studies. In conjunction with this effort, the MSC/NASTRAN design sensitivity analysis was used to identify the pertinent structural parameters affecting the response of the aircraft's vertical tail area. Subsequent to the identification of these parameters, they were used in a vibration reduction study. As a result, a fairly significant reduction in vibration level at a selected location of the reduced model was demonstrated.

CONCLUDING REMARKS

- DEVELOPED A REDUCTION PROCEDURE WITH THE FOLLOWING CHARACTERISTICS:
  - PROVIDES A REDUCED MODEL WHILE RETAINING THE ESSENTIAL DYNAMIC CHARACTERISTICS OF THE FULL MODEL
  - REDUCTION PROCEDURE WAS IMPLEMENTED IN TERMS OF NASTRAN DMAP ALTERS
- APPLIED THE REDUCTION PROCEDURE TO AH-64A DYNAMIC FEM MODEL
- VALIDATED THE REDUCTION PROCEDURE
- EXAMINED THE APPLICABILITY OF THE REDUCED MODEL TO A VIBRATION REDUCTION PROBLEM

8.0 REFERENCES

References

[1] Guyan, R. J., "Reduction of Stiffness and Mass Matrices," AIAA Journal, Vol. 13, No. 2, Feb., 1965, P. 380.

[2] Kidder, R. L., "Reduction of Structural Frequency Equations, "AIAA Journal, Vol. 13, No. 5, 1975, P. 892.

[3] Miller, C. A., "Dynamic Reduction of Structural Models, " Journal of Structural Division, ASCE, 1980, pp. 2097-2108.

[4] Paz Mario, "Dynamic Condensation, " AIAA Journal, Vol. 23, No. 5, May 1985, pp. 724-727.

[5] MSC/NASTRAN Application's Manual, Volume-I, The MacNeal-Schwendler Corporation, California, 1984.

NASA

Report Documentation Page

1. Report No.	2. Government Accession No.	3. Recipient's Catalog No
NASA CR-187448		

4. Title and Subtitle
Development and Application of a Technique for Reducing Airframe Finite Element Models Dynamics Analysis

5. Report Date
October 1990

6. Performing Organization Code

7. Author(s)
M. Hashemi-Kia and M. Toossi

8. Performing Organization Report No

10. Work Unit No.
505-63-36-01

9. Performing Organization Name and Address
McDonnell Douglas Helicopter Company
5000 E. McDowell Road
Mesa, AZ 85205

11. Contract or Grant No.
NAS1-17498

13. Type of Report and Period Covered
Contractor report

12. Sponsoring Agency Name and Address
National Aeronautics and Space Administration
Langley Research Center
Hampton, VA 23665-5225

14. Sponsoring Agency Code

15. Supplementary Notes
Langley Technical Monitor: Dr. Raymond G. Kvaternik

16. Abstract

A computational procedure for the reduction of large finite element models has been developed. This procedure, which has been implemented as a set of MSC/NASTRAN DMAP alters is used to obtain a significantly reduced model while retaining the essential global dynamic characteristics of the full-size model. This reduction procedure is applied to the airframe finite element model of AH-64A Attack Helicopter. The resulting reduced model is then validated by application to a vibration reduction study.

17. Key Words (Suggested by Author(s))	18. Distribution Statement		
Finite Element, AH-64A, Model Reduction, Airframe, NASTRAN, Vibration Reduction	Unclassified - Unlimited Subject Category 39		
19. Security Classif. (of this report)	**20. Security Classif. (of this page)**	**21. No. of pages**	**22. Price**
Unclassified	Unclassified	139	A07